Studies on Preparation and Application of Microcapsules(Dissertation_全文)

AUTHOR(S):

Iso, Mamoru

STUDIES ON PREPARATION AND APPLICATION OF MICROCAPSULES

MAMORU ISO

STUDIES ON PREPARATION AND APPLICATION OF MICROCAPSULES

MAMORU ISO

Contents

Preface

Introduction

Microcapsules are minute containers made of natural or synthetic polymers called as "wall material", with diameters of 1 to 1000 μm. Microencapsulation is a process by which small solid particles or small liquid droplets are completely surrounded and enclosed by the wall materials.

Microcapsules have two major functions in practical use. First, they can prolong the release rate of core substances into the external environments in a sustained manner. In this case, the thickness, chemical property and physical structure of the wall materials may be designed to release the core substances at specific rate and/or under a specific set of conditions.

Second, microcapsules are containers of core substances against the environmental conditions. For example, microcapsules can be used to separate reactive substances, to mask taste and odor, and to reduce toxicity of a substance. These functions have been applied commercially for some years. The initial example in utilization of microcapsules is carbonless copy papers using the aqueous coacervation method developed by Green and coworkers[1-3] of The National Cash Register Co. Dayton, Ohio.

Thereafter, the techniques used to prepare microcapsules for practical use have been refined and detailed over the last decades. The wide application of microcapsules has become a potential reality. Especially in pharmaceutical and medical use, many coating materials and processes of application have been de-

veloped.

Microcapsules may be prepared by different methods, and the methods may be generally divided into the next categories[4].

(a) Coacervation method

(b) Interfacial polymerization method

(c) Mechanical method

(d) Solvent evaporation method

According to the objectives and conditions of the application, the most suitable method should be selected out of these.

Significance of this thesis

Many applications of microcapsules to practical use have been particularly developed in pharmaceutical industry. Besides this pharmaceutical use, the unique functions of microcapsules promise commercial possibility in other industries, such as food, cosmetic, paint, print, adhesive, photographic, fertilizer industries in the near future. This work intends to evaluate quantitatively two important functions of microcapsules for the sake of wide practical application.

As described above, the controlled-release function of microcapsules is to maintain desirable concentration of core substances in a certain region. In pharmaceutical examples, the sustained release can maintain the therapeutic range of the drug over an extended period without undesirable side effects. In most examples investigated so far, the water solubility of core sub-

stances encapsulated was rather low. Since such core substances have inherent sustained release properties, further reduction in their rates of release can be easily attained by microencapsulation procedures. On the other hand, core substances with high water solubility are difficult to formulate into sustained-release microencapsulation. Therefore, few instances have been reported about microencapsulation of water-soluble core substances.

In Part 1 of this thesis, microencapsulation of core substances having high water solubility was investigated for the sake of extensive application in new field. Nonaqueous coacervation, spray drying and (W/O)/W multiple phase emulsion methods were tried. Since no method is available that is suitable in all cases, several methods of microencapsulation must be examined according to the states of core substances and the usage of encapsulated products. Anhydrous sodium sulphate (ASS), nicotinic acid and Vitamin B_6, all of which can be easily analyzed, were chosen as model compounds though they may not be a favored substance as a commercial product. In this Part 1, microencapsulation of pheromone-analog was also carried out by using a new method. Because elucidating the release behavior of vaporizable core substances to atmospheric environment is particularly interesting as a new application in controlled release.

Release behavior is a mass transport phenomenon involving diffusion of core substances from a region of high concentration

in the capsules to low concentration in the surrounding environment. Several release models of core substances have been proposed[5,6], however, no models have enjoyed a reputation of universal applicability. This is due to the great diversity in the physical form of microcapsules with respect to shape, size, combination of core substances and wall materials, and that in the chemical properties. No single approach to quantify the release of core substance from microcapsules are universally accepted. However, from the standpoint of engineering it is desirable to establish a model applicable to microcapsules prepared by different methods.

In Part 2, release of core substances from microcapsules prepared by several methods stated above was measured, and attempts to model the release behavior were carried out. The model that agreed fairly well with the observed values could be proposed. Furthermore, in order to understand universally the release phenomenon, the relationship between the individual models was revealed in relation to the structure of microcapsules. These results are significant in understanding the factors to control release behavior.

In Part 3, an application of microcapsules as a minute container of sensitive substances, immobilization of enzyme by microencapsulation, was studied, and the performance of the encapsulated enzyme was evaluated through the reaction with the particular substrate. Commercial application of bioreactors

employing immobilized enzyme has drawn a wide attention in recent years. Extensive researches on immobilized enzymes have been carried out for these two decades. Needless to say, there is a vast potential for using immobilized enzymes as recoverable, stable and specific industrial catalysts.

The immobilization of the enzyme may be achieved by various means[7-9]. Enzymes can be covalently bonded to, and physically entrapped in or on a suitable carrier. However, immobilization by covalent bonding method has a defect that the immobilization reagent will often preferentially attack to the active site of the enzyme, thus rendering it inactive. Physical adsorption method on the carrier has also disadvantage of weak bonding of enzymes that may lead to desorption during the catalysis.

On the other hand, the enzyme immobilization by microencapsulation is advantageous, because it is free from steric defects associated with covalent bonding method, or desorption problems encountered in physical adsorption method. However, though fundamental researches have been carried out on the potential application of microencapsulated enzymes, they have not been employed commercially. The main reason is that microcapsules are too fragile to cope with the mechanical shear or vigorous agitation in a practical use.

In this thesis, the wall material that has mechanical durability superior to those reported in past investigations was obtained as a result of extensive research in polymeric materi-

als. This wall material, a mixture of polystyrene (PS) and styrene butadiene rubber (SBR), is recommended for the industrial processes.

Furthermore, attempts to model the catalysis by the microencapsulated enzyme were investigated. In addition to mass transfer phenomenon of the substrate molecules through the capsule wall, the catalysis in microcapsules should be considered. As has been developed in the case of chemical reactions involving inorganic catalysts or carriers, the concept of the catalyst effectiveness factor can be also applied to the encapsulated enzyme for the successful modeling. The results obtained from this mathematical modeling will support the designing of large-scale industrial processes using the encapsulated enzymes.

Content of this thesis

The thesis consists of four parts. The Part 1 consists of four chapters, and is related to the preparation method of microcapsules.

In Chapter 1, the microencapsulation was carried out by the nonaqueous coacervation method. The term "coacervation" has been used to describe the phase separation into polymer-rich phase "coacervate" and lean phase. This step is rather stable but essentially a transient process observed just before the formation of polymer precipitation[10,11]. Aqueous coacervation method involves the dissolution of polymeric wall materials in water,

therefore the core substances must either be immiscible with or insoluble in water[12]. However, there are many cases where microencapsulation of water soluble substances is desirable, and the aqueous coacervation method is not available.

For nonaqueous method, a suitable combination of organic solvents and polymers is used. While the wall material used in the aqueous coacervation method is limited to a few kinds of water-soluble polymers, the nonaqueous method has an advantage that suitable wall materials can be selected from varieties of polymers. This chapter dealt with the nonaqueous coacervation method consisting of two-component system[13] (polymer-solvent) and three-component system[14] (polymer-solvent-nonsolvent), and elucidated the relation between the properties of microcapsules formed and the preparation conditions. The phase separation in this system was carried out either by the temperature change or by the addition of poor solvent to the polymer solution.

For explaining the behavior of nonaqueous coacervation , the theoretical thermodynamic approach on polymer chemistry can be used to describe the behavior of phase separation[15]. This theoretical calculation of phase separation is able to predict the wall thickness of microcapsules to some quantitative extent that is an important factor in the controlled release of core substances.

In Chapter 2, the microencapsulation of water soluble substances by the spray drying method[16,17] was dealt with as one of

the mechanical methods. The dispersion of core substance in the solution dissolving wall material was sprayed into a hot gas chamber. Being rapid, single-stage operation suitable for continuous production in large scale, this method can be used for the encapsulation or granulation of a wide range of drugs and flavors. Even a heat sensitive substance can be encapsulated by spray drying because the exposure to elevated temperature is so short. In this chapter, microencapsulation of nicotinic acid mainly coated with bees wax white was reported. A handmade spray drying tower equipped with a two-fluid nozzle was employed as an apparatus. The effect of operational conditions, e.g. nozzle diameter, gas flow rate, drying temperature and the component of the wall materials on the properties of microcapsules were discussed[18].

In Chapter 3, multiple phase emulsion methods[19-22], classified as one of the solvent evaporation method, was used to produce microcapsules having thicker wall. A water-in-oil-in-water (W/O)/W multiple phase emulsion was prepared. The W/O emulsion was prepared by dispersing the aqueous solution of core substance in the polymer solution using a low boiling point solvent. This mixture was dispersed in the aqueous solution of stabilizing agent to form stable (W/O)/W emulsion. The solvent was evaporated under the reduced pressure and/or mild heating, and the capsules formed were collected by filtration or centrifugation.

The advantage of this method is that one can select suitable

wall materials, and the combination of several kinds of polymers can be also used if they are miscible. Additionally, it should be also emphasized that the heat sensitive or reactive core substance can be successfully encapsulated without damage because of a mild condition of preparation. In this chapter, several kinds of wall materials were used to prepare the microcapsules, and the advantage and disadvantage as the wall material were compared[23,24].

In Chapter 4, a novel method of multiple phase suspension was proposed for the purpose of long term controlled release[25]. Generally, the release behavior of the core substance from the microcapsules is the order of hours or utmost days. In the application to the sustained release of insecticides and pesticides, it is preferable to maintain the release effect over a long period of time for saving the man-power. The study in this chapter was conducted to establish the feasible production and application of concerned microcapsules with a duration at least half a year.

In Part 2, controlled release of the core substance from the microcapsules prepared in Part 1 was discussed. This part consists of four chapters.

In Chapter 1, release behavior from the microcapsules prepared by nonaqueous coacervation method of the binary and ternary systems was discussed. Anhydrous sodium sulfate (ASS) crystal as a model core substance was employed for the measurement of con-

trolled release. In either case, Higuchi model[26,27] was most suitable to explain the release behavior of ASS through the capsule wall. The values of diffusion coefficient estimated by this model was correlated to the operational conditions[13,14].

In Chapter 2, controlled release of encapsulated nicotinic acid by the spray drying method was investigated. The operational conditions, gas flow rate, inner diameter of two-fluid nozzle, drying temperature and the component of the wall material, contributed to the release behavior[18]. Higuchi model was effective to correlate the release behavior over the wide range of those parameters as well as in Chapter 1.

In Chapter 3, as a core substance, Vitamin B_6 was encapsulated by multiple phase emulsion technique, and release behavior was observed. Polystyrene (PS), copolymers of styrene with acrylates, and styrene-butadiene rubber (SBR) were employed as wall materials together with natural waxes to change the mode of release and the rate. In this case, two-parameter masstransfer model was proposed to simulate the release behavior[24].

In Chapter 4, as an application for long term release, the release behavior of encapsulated pheromone-analog, 2-ethylhexyl acetate, to the atmosphere was investigated. Pheromones have been used to obstruct insect mating by communication disruption in a particular field. Controlled release is therefore essential for efficient and economical dose because pheromones are expensive, volatile and in some cases labile compounds. As a release model,

two-step process of masstransfer was proposed, and the related parameters in terms of the capacity coefficient and effective diffusion coefficient were estimated[25].

In Part 3, immobilization of enzyme by microencapsulation was studied. This Part 3 consists of four chapters.

In Chapter 1, lipase (Pseudomonas fluorescens) was encapsulated by (W/O)/W multiple phase emulsion method. Mixed composition of PS and SBR yielded a tough structure as wall material[28]. The morphology of the wall structure was studied in detail by a scanning electron microscope (SEM) and a transmission electron microscope (TEM).

In Chapter 2, performance of the encapsulated enzyme was examined employing hydrolysis of short-chain lipid in a well-stirred batch reactor. A mathematical model was derived under the assumption that the diffusion of substrate molecules through the wall of capsules plays a dominant role to the overall reaction rate. The calculated values agreed quite well with the observed data[28].

In Chapter 3, the microencapsulated lipase were applied to a continuous packed-column reactor, and longevity and mechanical strength of the microcapsules were fully confirmed. The reaction model derived in the stirred batch reactor was also applicable to simulate the behavior in the packed column reactor as it was proved that there is no mass transfer resistance between the reactant stream and the surface of microcapsules[29].

In Chapter 4, an application of encapsulated lipase to the hydrolysis of lipid was carried out with a continuous stirred tank reactor (CSTR) in which the encapsulated enzyme was dispersed under the shear-stress. An automatic control device to adjust pH of the reaction mixture at a desired level was designed and installed in the reactor system. Conversion of substrate at the steady state operation with pH control became significantly higher than that without pH control. A reaction model proposed in the preceding chapters was also applicable to simulate the behavior of CSTR system[30].

References

1) B.K.Green and L.Schleicher, U.S.Patent 2,730,456 (1956)

2) B.K.Green and L.Schleicher, U.S.Patent 2,730,457 (1956)

3) B.K.Green and L.Schleicher, U.S.Patent 2,800,457 (1957)

4) T.Kondo and M.Koishi, Maikurokapuseru(microcapsules), Sankyo Shuppan (1977)

5) J.R.Nixon and S.E.Walker, J. Pharm. Pharmacol., 23, 147, (1971)

6) P.L.Madan, J. Pharm. Sci., 70, 430 (1981)

7) Z.Bohak and N.Sharon, Biotechnological Applications of Proteins and Enzymes, Academic Press (1977)

8) A.D.McLaren and L.Packer, Advs. in Enzymology, 33, 245 (1970)

9) E.Katchalski and I.Silman, Advs. in Enzymology, 34, 445 (1971)

10) H.G.Bungenberg de Jong and H.R.Kruyt, Proc. Kon. Ned. Wetensch., 32, 849 (1929)

11) H.G.Bungenberg de Jong, in Colloid Science, Vol.2 (H.R.Kruyt, ed.), Elsevier, Amsterdam, p.248 (1949)

12) J.E.Vandegaer, Encapsulation by coacervation, in Microencapsulation - Process and Application (J.E.Vandegaer, ed.), Plenum, New York, p.21 (1974)

13) M.Iso, T.Kando and S.Omi, J. Microencapsulation, 2, 275 (1985)

14) M.Iso, I.Suzuki and S.Omi, Zairyo Gijutsu, 3, 287 (1985)

15) P.J.Flory, Principles of Polymer Chemistry, Cornell University Press, Ithaca, New York, p.554 (1953)

16) H.A.Lieberman and A.Rankell, Drying, in The Theory and Practice of Industrial Pharmacy (L.Lachman, H.A.Lieberman and J.L.Kanig, eds.), Lea & Febiger, Philadelphia, p.22 (1970)

17) F.Nielsen, Spray Drying Pharmaceuticals, Manuf. Chem. 53, 38 (1982)

18) N.Umeki, K.Terauchi, M.Iso and S.Omi, Zairyo Gijutsu, 5, 133 (1987)

19) M.N.Vrancken and D.A.Claeys, U.S.Patent 3,523,906 (1970)

20) H.Takenaka, Y.Kawashima, Y.Chikamatsu and Y.Ando, Chem. Pharm. Bull., 30, 695 (1982)

21) A.Mac, D.Negi and D.Friend, J. Microencapsulation, 6, 361 (1989)

22) R.Alex and R.Bodmeier, J. Microencapsulation, 7, 347 (1990)

23) T.Furuno, A.Ikeda, M.Iso, S.Omi and H.Yokota, Zairyo Gijutsu, 5, 141 (1987)

24) S.Omi, T.Furuno, A.Ikeda and M.Iso, "Drug Targeting and Delivery" ed. A.T.Florence and G.Gregoriadis., in press

25) S.Omi, N.Umeki, H.Mohri and M.Iso, J.Microencapsulation, 8, 465 (1991)

26) T.Higuchi, J. Pharm. Sci., 50, 874 (1961)

27) T.Higuchi, J. Pharm. Sci., 52, 1145 (1963)

28) M.Iso, T.Shirahase, S.Hanamura, S.Urushiyama and S.Omi, J. Microencapsulation, 6, 165 (1989)

29) M.Iso, T.Shirahase, S.Hanamura, S.Urushiyama and S.Omi, J. Microencapsulation, 6, 285 (1989)

30) M.Iso, H.Masumoto, S.Urushiyama and S.Omi, J. Microencapsulation, 7, 167 (1990)

Part 1

Preparation of Microcapsules

Chapter 1

Microencapsulation by nonaqueous coacervation method

Abstract

Nonaqueous coacervation in polystyrene (PS)-cyclohexane solution induced by the lowering of temperature (binary system) and the addition of nonsolvent (ternary system), n-hexane, was utilized to investigate the fundamental problems involved in the microencapsulation procedure. In either case, the phase equilibrium diagrams that gave basic knowledge on practicing coacervation method were prepared prior to the encapsulation. The appearance temperature of coacervate droplets in the binary system was accurately measured by a specially designed device. In the microencapsulation, percentage of encapsulated PS by the addition of n-hexane remarkably increased as compared with the result where coacervation was induced by temperature lowing of PS-cyclohexane solution. Though the addition of talcum powder was unavoidable to prevent microcapsules from adhering each other, controlling of PS wall thickness was quite successfully performed by adjusting PS concentration in cyclohexane solution, encapsulated temperature and amount of n-hexane.

Introduction

Coacervation, phenomenologically generation of droplets of a dense polymer concentration from a homogeneous polymer solution[1,2], has been extensively studied as a potential physicochemical technique to obtain microcapsules utilized in various field such as pharmacy, foods, cosmetics and agricultural chemicals.

Water-soluble polymers of natural origin, such as gelatin, gum arabic, carboxymethyl cellulose, pectin, polyvinyl alcohol and mixtures of these have been accepted as suitable wall materials due mainly to their non-toxic natures, a great advantage when utilized in the fields mentioned above. Physicochemical aspects of coacervation, especially the choice of reagents or operational temperature to induce coacervation and wall-hardening reagents for wall materials have been thoroughly studied and well established as practical procedures[3-9].

From the literature, it may seem that coacervation involving polymers which are only soluble in nonaqueous solvents has been paid less attention due to the rather restricted applications in the fields where toxicity and in vivo acceptability become important issues. Rowe[10] and Powell[11,12] et al. have given a number of synthesized polymers together with solvents and non-solvents applicable for use in the encapsulation process classified as phase separation technique.

In this chapter, the coacervation induced from a binary system of polystyrene(PS)-cyclohexane and a ternary system of PS-cyclohexane-n-hexane is discussed from the engineering view point and its possible applications to microencapsulation is demonstrated experimentally.

Experimental

Reagents

Polystyrene as a wall material was synthesized by employing a conventional suspension polymerization technique. Styrene monomer (ST) 100ml was dispersed in 900ml of an aqueous phase containing 0.2g sodium lauryl sulphate, 2.0g anhydrous sodium sulphate (ASS) and 15ml 10wt percent calcium phosphate slurry, which plays the role of a stabilizing agent for viscous PS-ST droplets. Polymerization was carried out at 363K under nitrogen for 5hr. The molecular weight of PS was controlled by changing the amount of benzoyl peroxide, an initiator, from 1.25 to 10.0g. PS samples used in the following experiments are listed in Table 1-1 with their molecular weights and polydispersities.

In binary system, cyclohexane, n-butyl ether, tributyl phosphate, cyclohexanone and dioxane were found capable of generating phase separation in PS solution by adjusting the equilibrium temperature. Cyclohexane was more suitable than the others, since the coacervation takes place at room temperature. In ter-

nary system, n-hexane was used as an agent inducing phase separation in PS-cyclohexane solution.

n-Hexane and ethyl alcohol were selected as wall-hardening agents of PS. Methyl alcohol was used as a solvent for washing the hardened microcapsules.

Spherical glass beads of a mean diameter 59.5μm were used as a core substance when the encapsulation was intended to investigate basic problems such as the performance of encapsulation, the utilized amount of wall materials, the desired amount of talcum powder etc. Talcum powder ($H_2Mg_3(SiO_3)_4$) was used as a stabilizing agent to prevent encapsulated particles, covered with a viscous PS layer, from sticking to each other. From 20 to 40wt percent of the powder based on the amount of core substance was added.

All these reagents were used without further purification.

Measurement of phase equilibrium

Temperature at phase separation

The onset of phase separation in binary system, which can be detected by the appearance or disappearance of coacervate droplets, was observed by a specially designed device as shown in Figure 1-1. Small amounts of PS-cyclohexane solution where placed on the shallow cavity of a haemocytometer slide, whilst the temperature was controlled by recirculation cooling water. The apparatus was set on the objective stage of a microscope and the

Table 1-1. Molecular weights of polystyrene samples employed as wall material.

Sample Number	Molecular weight		Dispersion index($\bar{M}_n/\bar{M}_w$)
	Number average ($\bar{M}_n \times 10^{-4}$)	Weight average ($\bar{M}_w \times 10^{-4}$)	
PS-1	0.89	1.69	1.90
PS-2	2.24	3.73	1.67
PS-3	1.35	2.62	1.94
PS-4	0.80	1.58	1.98
PS-5	2.32	5.09	2.19

Measured with GPC, solvent dimethyl formamide.

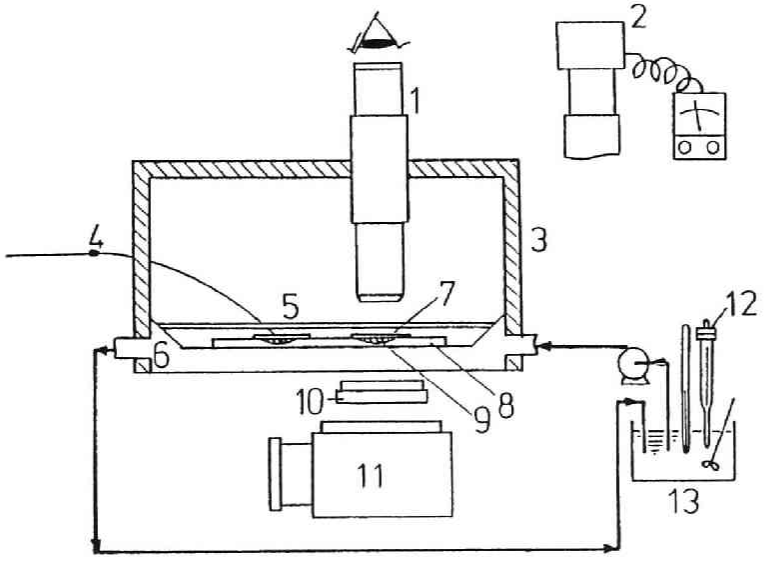

Figure 1-1. *Apparatus for measurement of phase separation point. Key: [1] microscope, [2] exposure meter, [3] dark chamber,[4] thermocouple, [5] shield glass, [6] measurement cell, [7] cover glass,[8] slide glass, [9] test solutions, [10] condenser lens, [11] lamp, [12] thermoregulater, [13] temperature control circuit.*

separation point was detected through the ocular lens either by a naked eye or photographically using an exposure meter which latter is very sensitive to slight changes in the intensity of transmitted light, due to the light scattered from surface of the coacervate droplets. The temperature at phase separation was accurately measured by a thermocouple placed in the other cavity.

Equilibrium composition of coacervate

In the binary system, 150ml of cyclohexane solution containing 7-8 vol percent of PS was introduced into a 300ml flask, stirred for a certain period with a magnetic stirrer, and allowed to stand for 6 to 7hr so that coacervate droplets would settle. Samples were withdrawn from the dilute (continuous) and dense (coacervate) phases in order to determine the equilibrium compositions. A gas chromatograph having thermal conductivity detector (TCD)(MODEL-802T, Okura Riken Co. Ltd.) and a UV spectrophotometer (UVIDEC-320, Japan Spectroscopic Co. Ltd) were employed for analyses of the samples (λ = 252.5nm).

In the ternary system, 20g of 1wt percent cyclohexane solution of PS was added in a 50ml centrifuging cell, held for 15min at constant temperature, and then prearranged amount of n-hexane was added in the cell with agitation. After droplets of coacervate were generated, it was allowed to stand still for 3hr to make the floating droplets settle. After centrifuged for 5 to 10min, dilute and dense phases were analyzed by the similar methods.

Preparation of Microcapsules

Microencapsulation using the binary system was carried out as follows. 30ml of PS-cyclohexane solution containing 1 to 4wt percent of PS was mixed with 2g of core substance and stirred with a magnetic stirrer. The dispersion was subsequently to a desired temperature to allow the generation of coacervate droplets and 0.4 or 0.8g talcum powder was added to prevent the coagulation of the encapsulated particles. The procedure in the ternary system was essentially regarded as same as in the case of binary system except the addition of n-hexane after mixing with core substance.

In either case, after the particles surrounded with coacervate phase settled down under intermittent agitation, the dilute phase was removed from the system. Approximately 50ml of a precooled non-solvent for PS (ethyl alcohol or n-hexane) was extract cyclohexane and harden the PS wall. After the upper layer was removed by decantation, the microcapsules were rinsed with methyl alcohol and dried under the vacuum at room temperature, or at 333K in a dryer.

Characterization of microcapsules

The average thickness of microcapsules was calculated as half of the diameter difference between the two samples. In the gravimetric analysis, 0.5g of dried microcapsules was added in 30mL of cyclohexane and PS wall was completely dissolved under the influence of ultrasonic oscillation. The average wall thickness was routinely determined by the following equation.

$$\delta = \frac{\bar{d}_{pm}}{6}\left(\frac{\rho_c}{\rho_w}\right)\left(\frac{W_w}{W_c - W_w}\right) \qquad (1\text{-}1)$$

where ρ_c and ρ_w denote the densities of core and wall materials, W_c and W_w denote their respective weights per capsule, and $\bar{d}_{pm}$ denotes the average diameter of the microcapsules.

Results and Discussion

Combination of polymer and solvent to induce the coacervation

Coacervation is phenomenologically located between dissolution and solid precipitation of polymer, and can be induced in the case where the appropriate combination of polymer and solvent is obtained. However, the selection of solvents inducing coacervation cost a great deal to trouble because of widely researching range of solvents. Classification of solvents, either good or poor solvent of PS, was given by Kurata and Stockmeyer[13], and the results are illustrated in Figure 1-2. In figure, solubility parameter[14] and hydrogen bonding index[15] are chosen as coordinates. Among the good solvents, the experiment revealed that those capable to induce the coacervation are unanimously located near the boundary separating good and poor solvents. In the case of ternary system by adding nonsolvent, selection of nonsolvent (poor solvent) is not so strict, in fact any nonsolvent can be

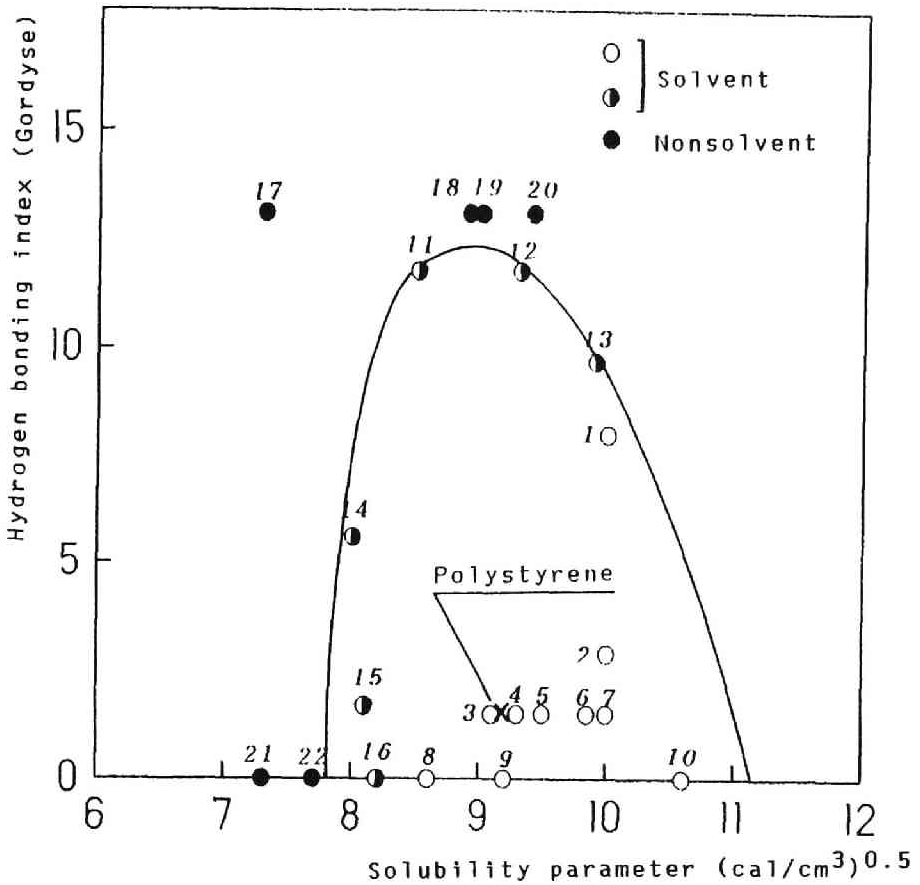

Figure 1-2. Soluble boundary of polystyrene as a function of hydrogen bonding index and solubility parameter.

1. Ethyl chloroformate
2. Nitrobenzene
3. Tetrachloroethylene
4. Styrene
5. Trichloroethane
6. Methylene dichloride
7. Chlorobromoethane
8. Tetrachloromethane
9. Benzene
10. Biphenyl
11. Tributyl phosphate
12. Cyclohexanone
13. Dioxane
14. n-butyl ether
15. Turpentine
16. Cyclohexane
17. Ethyl ether
18. Butyl cellosolve
19. Phenyl cellosolve
20. Diacetone alcohol
21. n-Hexane
22. Isooctane

paired with the good one as far as it is capable to produce the coacervates. This fact is quite understandable, if one considers that the coacervation is regarded to be in-between of the soluble and insoluble states.

In this work, cyclohexane and n-hexane was selected as a good and poor solvent.

Phase diagram of coacervation

In Figure 1-3, the phase diagram for the PS-cyclohexane binary system was obtained by interconnecting the temperatures of phase separation points observed for PS solutions of different compositions as shown by the appearance of coacervate droplets. Two broken lines are also shown in the figure, which were obtained from the measurement of the equilibrium compositions in the coacervate and dilute phases. Initial concentrations were selected as 7.7 vol percent for PS-1, and 7.0 vol percent for PS-2, respectively.

Comparisons between phase diagrams obtained from two different runs showed that the polydispersity of PS (shown in the Table 1-1 in terms of the dispersion index) is mainly for the wide discrepancy between the two diagrams. The two curves would be expected to coincide with each other if monodispersed PS was used. In the present case, fractionation of PS inevitably takes place during the prolonged period required to reach the equilibrium state, whereas the appearance of coacervate droplets occurs

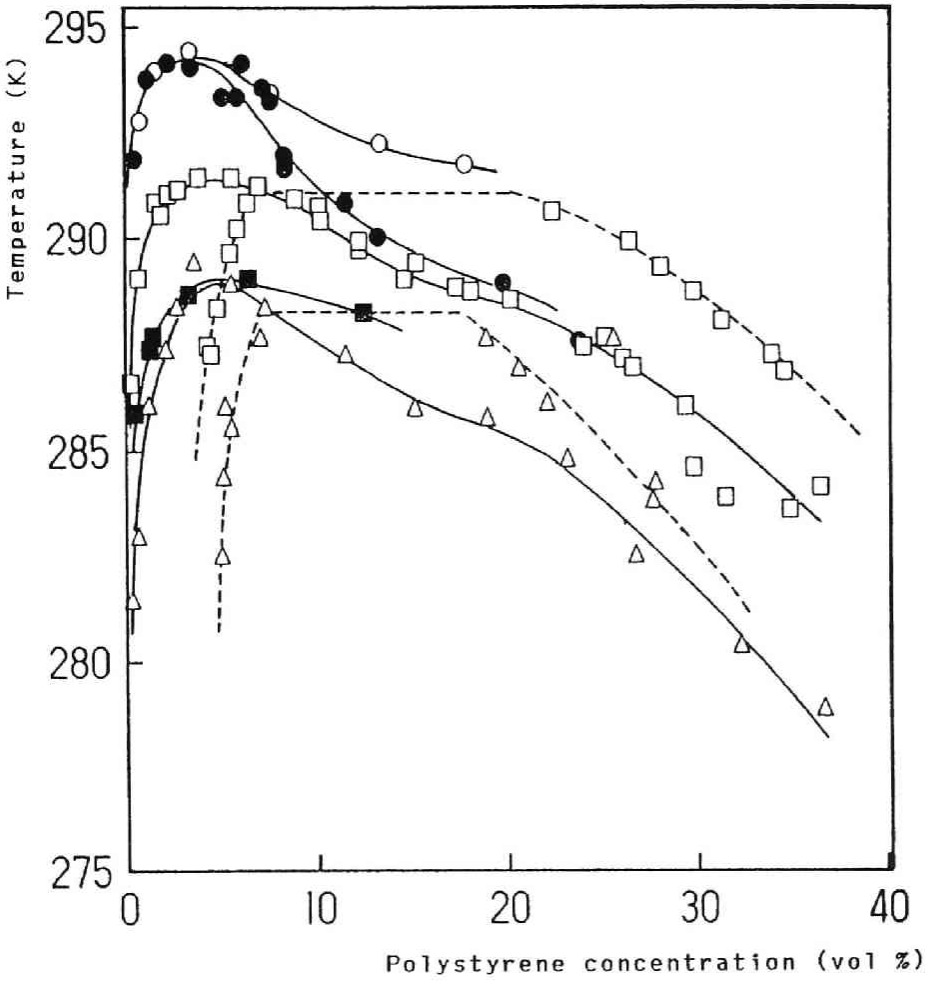

Figure 1-3. Phase diagram between coacervate (dense) and lean phase induced from PS-cyclohexane system.
○, *PS-5*; ●, *PS-3*; □, *PS-2*; △, *PS-1*; ■, *PS-4*.
——, *Determined by measurement of phase separation temperature*; - - - - -, *determined by measurement of equilibrium composition.*

instantaneously. Since polydisperse polymers are utilized commercially, these different determinations will offer substantial information about the actual encapsulation conditions, such as maximum allowable temperature and polymer concentration of the original solution.

The evidence for the dominant role of polydispersity can be found from comparison between the two sets of samples PS-2 & PS-3 and PS-1 & PS-4. As shown in the table, PS-3 and PS-4 have lower average molecular weights, but have more enhanced polydispersities than their respective counterparts. The reason why those PS samples, which have lower molecular weights, showed higher or equivalent values of the critical temperature for phase separation can only be ascribed to their higher polydispersities.

The three-phase diagram for the PS-cyclohexane-n-hexane ternary system which were obtained from the equilibrium compositions using PS-5 is shown in Figure 1-4. Theoretical curves calculated from Flory-Huggins theory[16,17] are also shown in figure as compared with experimental values. PS was assumed to be monodispersed with molecular weight of 50,000, while parameters were calculated by setting the values of solubility parameter as 9.1, 8.2 and 7.3[14] for PS, cyclohexane and n-hexane, respectively. Tie lines in the both figures are drawn for the equilibrium at 303K. The agreement between calculated and observed values are not good, especially those for the coacervate phase, due to the polydispersity of PS used for the measurement. The other

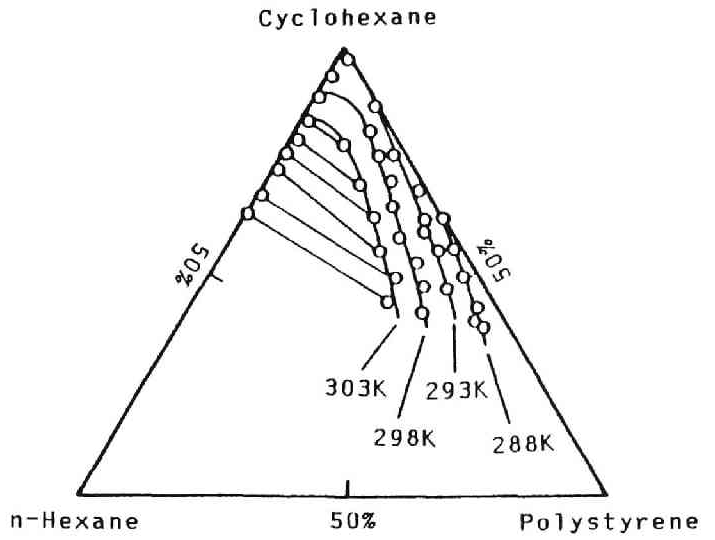

(a) *Observed diagram.*

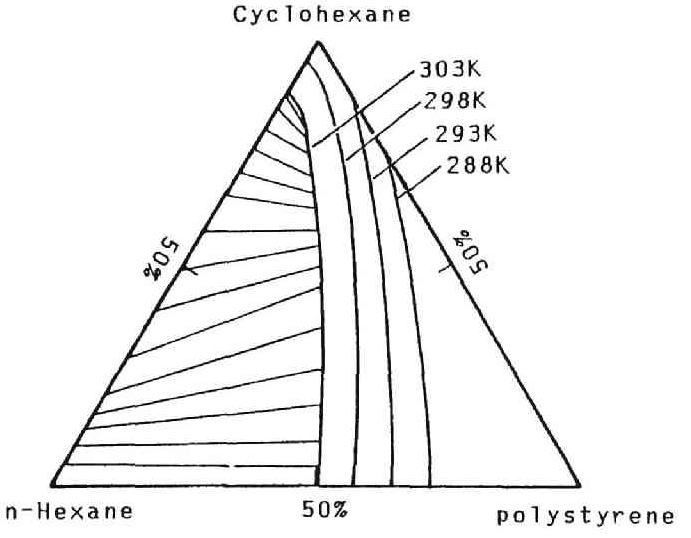

(b) *Calculated diagram.*

Figure 1-4. *Phase diagram between coacervate and lean phase induced from PS-cyclohexane-n-hexane system.*

Tie lines are drawn for 303K.

reason to be considered is an inadequate presumption to derive the entropy term in the theory which regards each segment in a polymer chain as completely flexible, leading to the over-esti mation of conformational entropy.

Amount of PS utilized in microcapsules

In the binary system, the wall thicknesses calculated from the amount of encapsulated PS (PS-5) are shown in Figure 1-5 as a function of the encapsulation temperature. Two grams of glass beads with smooth surfaces (d=59.5μm) were used as model core particles. The amount of encapsulated PS was determined by UV spectrophotometer after the dissolution of PS by cyclohexane. The contribution from the talcum powder attached to the wall was not considered in this figure. From the observation by scanning electron microscope (SEM) as shown in Photo. 1-1, the wall structure of microcapsules indicated that a thin film of PS covers the surface of glass beads, and flat talcum powder attaches onto the PS film. When the glass beads were encapsulated at 293.9K, using a PS solution of 4wt percent, the thickness of PS film is approximately 0.3μm. Supposing all PS in the coacervate phase is included in the microcapsule, the thickness of PS film should be 16.7μm, but the PS utilized in practice in calculated to be only 3.0 percent; an indication of very poor utilization of PS. This result means that a large number of coacervate droplets are wasted or lost in the effluent. The main reason, which in fact

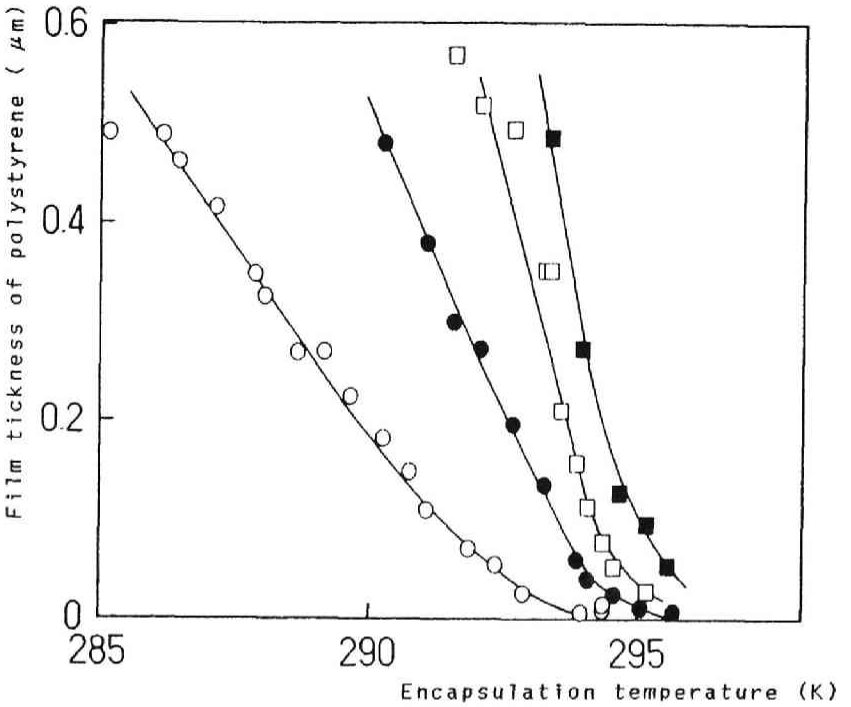

Figure 1-5. Film thickness of PS on encapsulated glass beads in binary system. Effect of polymer concentration: ○, 1wt % ; ●, 2wt %; □, 3wt %; ■, 4wt %. PS-5 was used.

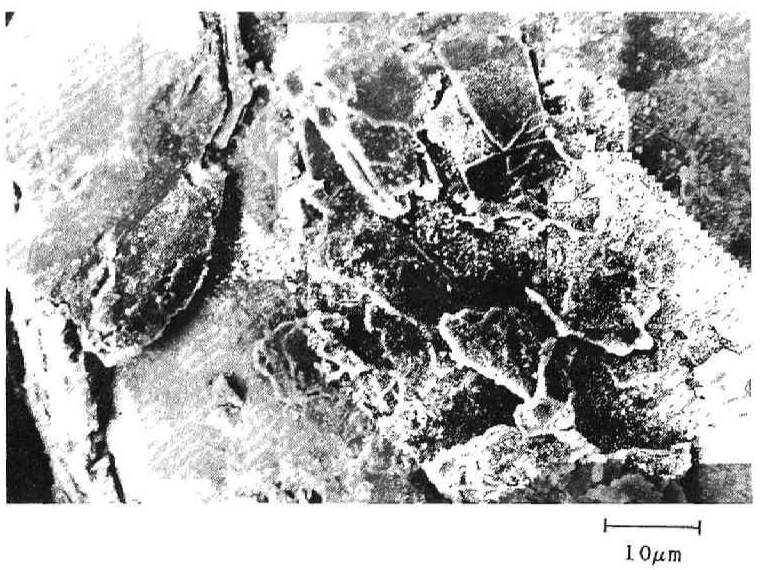

Photo. 1-1. Surface of glass bead microcapsules.

was observed by microscope, may be by the adhesion of free coacervate droplets with talcum powder. Poor utilization of PS may limit the use of this binary system for practical purposes.

The wall thicknesses of PS in the ternary coacervation system are shown in Figure 1-6 as a weight ratio of n-hexane. As the amount of added n-hexane increases, the wall thickness differences became enhanced. When the concentration of PS exceeds 3.0wt percent, encapsulation became different due to the too much generation of coacervate droplets. Conversion of PS utilized for the encapsulation based on the total amount of PS in coacervate phase gradually increased from 20 to 40 percent as the added amount of n-hexane increases, a remarkable improvement compared with the values obtained in the binary system. Effect of encapsulation temperature on the wall thickness is shown in Figure 1-7. This result indicates that temperature can also play a role as effective operating factor. Difference of 5K in the temperature results in the change of wall thickness from 0.2 to 0.4μm.

From these results of encapsulation procedures, it is concluded that the controlling of wall thickness is quite possible by changing the amount of added n-hexane, encapsulation temperature and PS concentration in the original solution.

Conclusion

Fundamental problems involved in a microencapsulation proce-

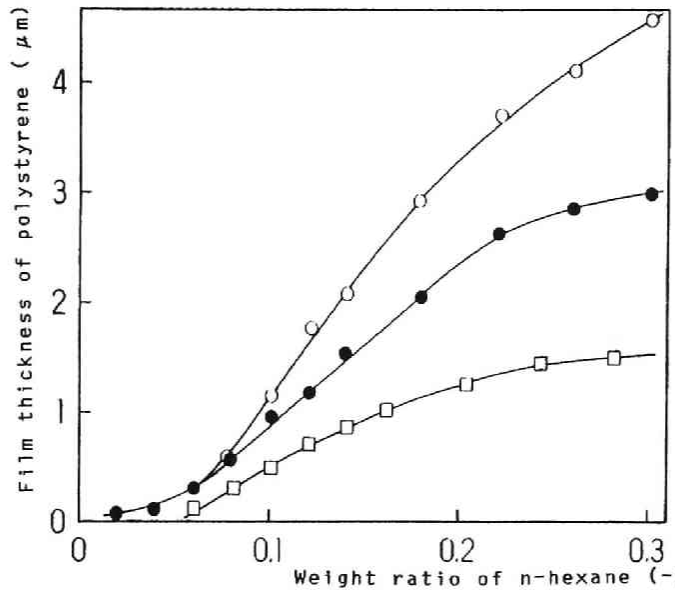

Figure 1-6. Film thickness of PS on encapsulated glass beads in ternary system. Effect of initial PS concentration: ○, 3wt %; ●, 2wt %; □, 1wt %. Encapsulation temperature was 298K.

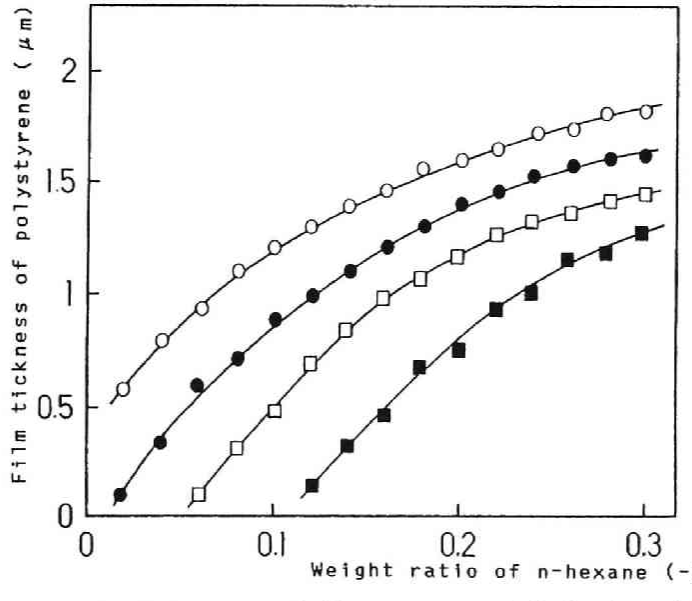

Figure 1-7. Film thickness of PS on encapsulated glass beads in ternary system. Effect of encapsulation temperature: ○, 288K; ●, 293K; □, 298K; ■, 303K. Initial PS concentration was 1wt percent.

dure in which coacervate droplets generated in a PS-cyclohexane binary system and a PS-cyclohexane-n-hexane ternary system plays a vital part were investigated. Low efficiency of PS in the binary system is, to a great extent, improved by introducing the third component in this system, n-hexane. In this ternary system microencapsulation is efficiently performed by the addition of n-hexane into PS-cyclohexane solutions coupled with temperature lowering.

References

1) H.G.Bungenberg de Jong and H.R.Kruyt, Proc. Kon. Ned. Akad. Wetensch., 32, 849 (1929)

2) H.G.Bungenberg de Jong, in Colloid Science, Vol. 2, Elsevier, Amsterdam, p.248 (1949)

3) J.E.Vandegear, ed., Microencapsulation Processes and Applications, Plenum, New York,(1974)

4) J.R.Nixon, ed., Microencapsulation, Dekker, New York, (1976)

5) T.Kondo, ed., Microencapsulation: New Techniques and Applications Techno, Tokyo,(1979)

6) M.W.Ranney, Microencapsulation Technology, Noyes Development Corporation, Park Ridge, New Jersey,(1969)

7) M.H.Gutcho, Microcapsules and Microencapsulation Techniques, Noyes Data Corporation, Park Ridge, New Jersey,(1976)

8) A. Kondo, Microcapsule Processing and Technology, Dekker, New York (1979)

9) P.B.Deasy, Microencapsulation and Related Drug Processes, Dekker, New York,(1984)

10) E.L.Rowe, U.S.Patent 3,336,155 (1967)

11) T.C.Powell, M.E.Steinle and R.A.Yoncoskie, U.S.Patent, 3,415,758 (1968)

12) T.C.Powell, U.S.Patent , 3,623,997 (1971)

13) M.Kurata and W.H.Stockmayer, Advance in Polymer Sci., 3, 196 (1963)

14) A.Beerbower, L.A.Kaye and D.A.Pattison, Chem. Eng., 118, Dec. 18 (1967)

15) H.Burrell, Interchem.Rev., 14 (1), 3 (1955)

16) P.J.Flory, Principles of Polymer Chemistry, p.554, Cornell University Press, Ithaca, New York (1953)

17) H.Tompa, Polymer Solutions, p.198, Butterworth Scientific Publications, London (1956)

Chapter 2

Microencapsulation by spray drying method

Abstract

Microcapsule of volatilizable nicotinic acid crystal was prepared using a spray drying tower equipped with a two-fluid nozzle. Crystals of nicotinic acid were suspended in hot chloroform containing beeswax white and n-praffin, and then introduced to the two-fluid nozzle for spraying.

Nozzle diameter, gas flow rate of the nozzle and the drying temperature were changed as well as the composition of the suspension. The observation of prepared microcapsules by the scanning electron microscope (SEM) showed that the crystal was uniformly coated with the wall material. Agglomerated microcapsules and smaller particles of the wall material not utilized for the encapsulation were also observed as the encapsulation condition became less favorable.

Introduction

Spray drying tower is normally regarded as an efficient instrument for commercial scale granulation with which solutions, suspensions and emulsions were sprayed from a two-fluid nozzle or a rotating disc, the latter being more suited to the large scale production. If a polymeric material, easy to form film or skin, is dissolved in the solvent, microcapsules or spherical matrices are formed depending on the affinity of the polymer with core substance. Two kinds of spray granulation method have been employed so far; one is a spray drying in which solvent is volatilized to yield solidified product, and the other is a spray congealing in which ingredients were sprayed into the cooled atmosphere. Kawashima published an informative review concerning to the recent development of spray granulation employed in the fields of foodstuffs, medicine and so forth[1].

Generally speaking, microencapsulation by the spray drying technique is favored for a large scale commercial process, but its applicability is rather limited when uniformly coated microcapsules are requested. Choice of solvent may also be a problem because of the inflammability of organic solvents which will demand additional cost to protect from a probable fire[2].

In this chapter, water soluble substance, nicotinic acid, was encapsulated with beeswax white and n-praffin by using nonaqueous system. The nonaqueous systems were only reported in some pat-

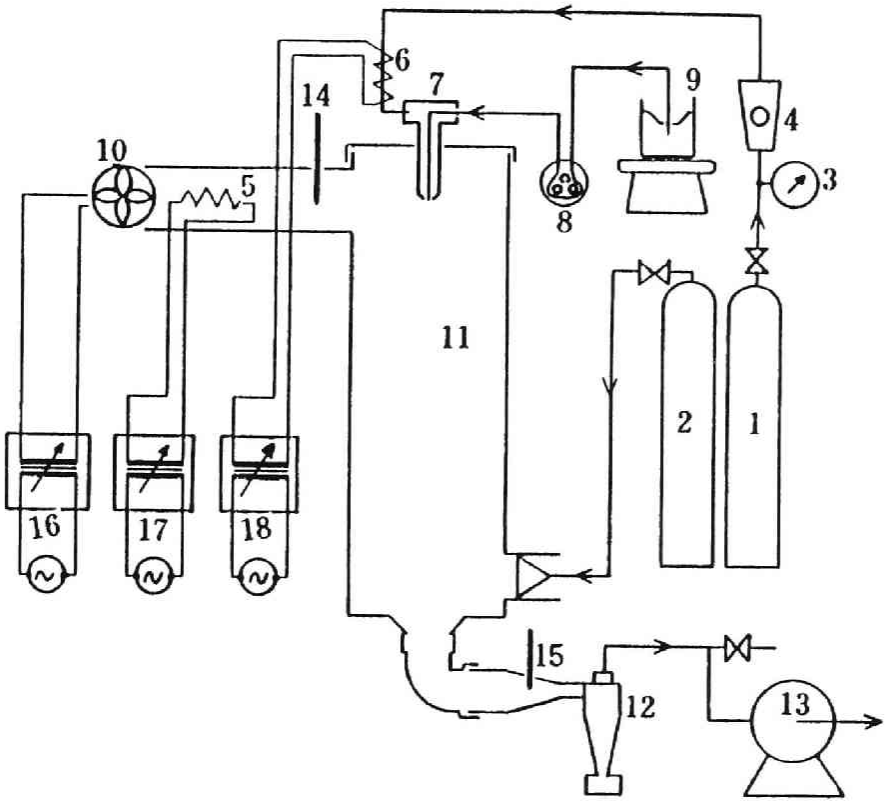

Figure 2-1. Schematic diagram of spray drying tower.

Key: [1] N_2 cylinder 1, [2] N_2 cylinder 2, [3] pressure gauge, [4] flowmeter, [5] heater 1, [6] heater 2, [7] spray nozzle, [8] slurry pump, [9] slurry tank, [10] fan, [11] spray tower, [12] cyclone, [13] air blower, [14] thermometer, [15] thermometer, [16] voltage controller 1, [17] voltage controller 2, [18] voltage controller 3.

ents[3,4]. A handmade spray drying tower equipped with a two-fluid nozzle was employed as an apparatus. Encapsulated nicotinic acid crystals were quite stable even though they were exposed under a high vacuum condition.

Experimental

Apparatus

A schematic diagram of handmade spray drying tower was shown in Figure 2-1. Drying chamber [11] is cylindrical shape, 30cm in diameter, and 100cm in height. Drying gas was introduced from the upper wall preheated by a 2kW heater [5] on the way to the chamber. Two-fluid nozzle (Yamato Kagaku Co. Ltd.) [7] was used for spraying slurries. Inner diameter of the nozzle was selected from 508, 711, and 1100μm. Outer diameter of the annular nozzle was fixed at 1778μm for spraying gas. Cooling gas was introduced from the lower wall of the tower. Nitrogen gas from the cylinders [1],[2] was used for spraying and cooling. Gas-solid mixture in the chamber was withdrawn and introduced to the cyclone [12] by an air blower [13], the capacity of which was 12m^3/min at 135mmH_2O, and the rate being adjustable.

Reagent

Reagent grades of nicotinic acid ($\bar{d}_{pc}$=50.3μm, volume aver-

age), beeswax white (m.p. 335-339K), n-paraffin (m.p. 341-343K) and chloroform were used as served. Beeswax white, a mixture of long chain esters, was selected for its better affinity with nicotinic acid than n-paraffins. Chloroform is among all things nonflammable, and suited for the spray drying. Hot chloroform dissolves these waxes, but nonsolvent for nicotinic acid.

Preparation of microcapsules

Nicotinic acid crystal was added in hot chloroform solution of the wall material [9], and then exposed under the ultrasonic wave to ensure a fine dispersion. Meanwhile the temperature in the drying chamber was controlled at the desired level introducing hot air from a fan blower [11], and small flow of nitrogen from the two-fluid nozzle. Then the flow rate of nozzle gas was adjusted to the desired level [4], and the slurry was fed through a slurry pump [8]. The flow rate was fixed at 10ml/min, and the slurry hold tank was kept warm to prevent the precipitation of the wall material [9]. Cooling gas was also introduced [2], and the air blower was on during the spraying [13].

After the spraying was over, dried particles were collected from the cyclone, and also from the chamber wall at which quite a few amount of microcapsules were attached.

Analysis

General features of microcapsules, in particular condition

of coated wall, attachment of smaller particles of the wall material on the surface, and degree of agglomeration, were observed from SEM. Mono-nucleus microcapsules coexisting with agglomerated ones were picked up from the photographs to measure the average diameter, $\bar{d}_{pm}$. They were assumed to be a group of ellipsoids. Average diameter was regarded to be equal to that of a sphere having an identical volume with that averaged for the ellipsoids. In actual practice longer and shorter axis of microcapsules were measured, and after a mathematical treatment, the diameter of equivalent sphere was obtained.

Percent drug content in microcapsules was determined by melting the wall with hot water, and measuring dissolved amount of nicotinic acid in water by a UV spectrophotometer (λ=261nm).

Average wall thickness of microcapsules, δ, can be evaluated using the percent drug content, m, and either $\bar{d}_{pm}$ or $\bar{d}_{pc}$.

$$\delta = \frac{\bar{d}_{pm}}{2}\left[1 - \left[1 + \left(\frac{100}{m} - 1\right)\frac{\rho_c}{\rho_w}\right]^{-1/3}\right] \qquad (2\text{-}1)$$

$$\delta = \frac{\bar{d}_{pc}}{2}\left[\left[1 + \left(\frac{100}{m} - 1\right)\frac{\rho_c}{\rho_w}\right]^{1/3} - 1\right] \qquad (2\text{-}2)$$

While there exists uncertainties with the values of $\bar{d}_{pm}$, m may be regarded as most accurate. Then the following relationship will be useful to judge the accuracy of measurement and to evaluate percent utilization of the wall material with respect to the core substance.

Table 2-I. Effect of operational condition on the characteristics of microcapsule

Changed condition	Percent drug content (%)	$\bar{d}_{pm}$(obs) (μm)	$\bar{d}_{pm}$(calc) (μm)	δ (calc)*1 (μm)	δ (calc)*2 (μm)	(Ww/Wc) (-)
(A) Gas flow rate (l/min)						
10.6	71.9	56.0	58.9	4.07	4.28	0.391
13.8	68.1	57.6	60.3	4.77	5.00	0.468
17.5	75.3	59.9	57.7	3.82	3.68	0.328
20.0	71.3	58.8	59.1	4.37	4.39	0.403
25.6	66.7	65.4	60.8	5.67	5.27	0.499
30.9	67.7	68.7	60.5	5.77	5.08	0.477
(B) Drying temp. (K)						
313	81.1	59.0	55.7	2.87	2.71	0.233
333	69.1	61.2	59.9	4.91	4.81	0.447
353	71.3	58.8	59.1	4.37	4.39	0.403
373	77.1	55.7	57.0	3.29	3.37	0.297
393	71.7	57.6	58.9	4.22	4.32	0.395
(C) Nozzle diameter(μm)						
508	83.7	59.1	54.9	2.48	2.30	0.195
711	71.3	58.8	59.1	4.37	4.39	0.403
1000	71.5	69.3	59.0	5.12	4.36	0.379
(D) Bees wax white(g)						
3	80.1	56.2	56.0	2.88	2.87	0.248
5	71.3	58.8	59.1	4.37	4.39	0.403
7	60.8	--	63.3	--	6.51	0.645
10	40.0	62.8	75.0	10.3	12.3	1.500
(E) Fraction of n-paraffin (-)						
0	71.3	58.8	59.1	4.37	4.39	0.403
0.2	69.7	67.4	59.8	5.34	4.74	0.435
0.5	63.8	66.3	62.3	6.39	6.01	0.567
0.8	63.8	64.4	62.5	6.28	6.09	0.567
1.0	61.5	59.5	63.6	6.23	6.67	0.626

**1 Calculated from Equation (2-1).*
**2 Calculated from Equation (2-2).*
Standard operational condition: Chloroform 50ml, Nicotinic acid 5g, Beeswax white 5g, Gas flow rate 20l/min, Drying temperature 353K, Nozzle diameter 711μm, No n-paraffin.

$$\left(\frac{\bar{d}_{pm}}{\bar{d}_{pc}}\right)_{obs.} = \left[1 + \left(\frac{100}{m} - 1\right)\frac{\rho_c}{\rho_w}\right]^{1/3} \qquad (2\text{-}3)$$

$$\left(\frac{W_w}{W_c}\right)_{obs.} = \frac{100}{m} - 1 \qquad (2\text{-}4)$$

Result and Discussion

Effect of the operation conditions

Percent drug content and average diameter of mono-nucleus microcapsules were listed in Table 2-1 as one of the operational conditions were changed. Average wall thickness, δ, calculated from Equation (2-1) and Equation (2-2), ratio of wall material and core substance calculated from Equation (2-4), and $\bar{d}_{pm}$ calculated from Equation (2-3) were also included in the table. Gas flow rate (A) and nozzle diameter (C) of two fluid nozzle, temperature in the drying chamber (B), amount of the wall material (D), and composition of the wall material (E) were selected as principal conditions.

Unanimously higher drug content than that predicted from assuming 100 percent utilization for the wall and core substance indicates that the considerable amount of the wall material is wasted uncapsulated. This is reflected in the column of W_w/W_c in the table. In fact uncapsulated wall material was collected at the filter of the blower as well as in the cyclone. It is quite probable that a few amount of nicotinic acid was accompanied with the wasted wall material, and to obtain accurate material balance

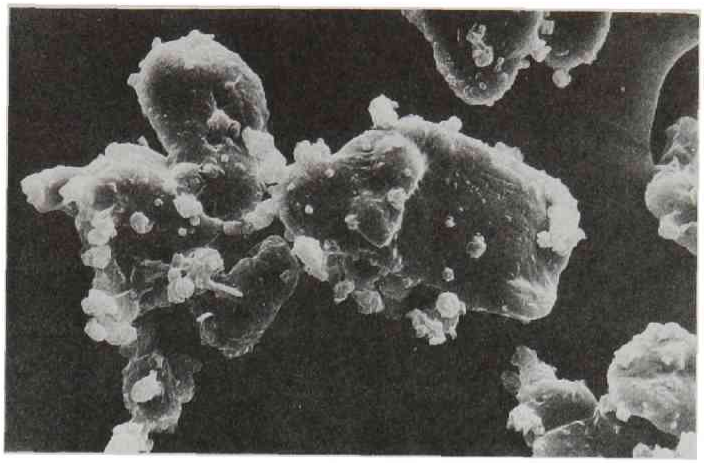

10μm

Photo. 2-1. SEM photograph of nicotinic acid microcapsule.

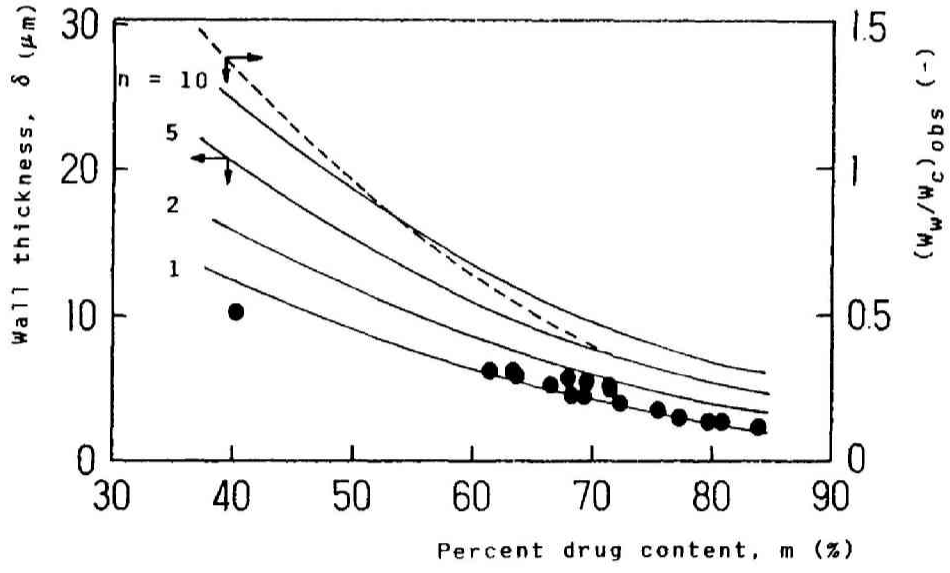

Figure 2-2. Effect of agglomeration on the wall thickness as a function of percent drug content. ●, *δ(calc)*1 in table 2-1;* ———, *calculated curve by Equation (2-5);* – – – –, *calculated curve by Equation (2-4).* $\bar{d}_{pc}$ = *50.3 μm.*

becomes difficult.

Greater difference between observed and calculated value of the average diameter anticipates a less favored encapsulation condition indicating enhanced agglomeration of microcapsules and/or increase in the amount of uncapsulated wall material.

General features of nicotinic acid microcapsule

SEM photographs of nicotinic acid microcapsules prepared by the standard operational conditions were shown in Photo. 2-1. Nicotinic acid was encapsulated with its crystal shape retained. Inspection of the surface revealed that the wall was smooth with no cracks and pinholes. Small particles of beeswax white were also observed attached on the surface. Since the diameter of these particles is an order of micron, no nicotinic acid crystals are included. Amount of these particles increased as gas flow rate of the two-fluid nozzle increased. Multi-nucleus microcapsules due to the agglomeration of mono-nucleus ones were observed in Photo. 2-1. The portion of agglomeration increased as W_w/W_c or percentage of n-paraffin in the wall increased.

Equation (2-1) and (2-2) estimating the wall thickness were obtained on the assumption of mono-nucleus microcapsules. In case of agglomeration, however, the wall thickness that was an important property of microcapsules might be erroneously estimated. The agglomeration between microcapsules or core crystals will result in the thicker wall as a schematic diagram in Figure 2-2

indicates. The concept drawing the figure is an introduction of the degree of agglomeration, n, average number of core crystals included in agglomerated capsules. Theoretically wall thickness of agglomerated capsules can be written as follows.

$$\delta = \frac{n^{1/3}\bar{d}_{pc}}{2}\left[\left[1 + \left(\frac{100}{m} - 1\right)\frac{\rho_c}{\rho_w}\right]^{1/3} - 1\right] \qquad (2\text{-}5)$$

Strictly speaking, δ in the lefthanded vertical axis shows merely a conceptual value because Equation (2-5) is derived assuming that all the wall material is present on the surface of agglomerated microcapsules, neglecting the possible presence in-between the core crystals.

Conclusion

Microencapsulation employing the spray drying method was discussed. Nicotinic acid microcapsules coated with beeswax white and n-paraffin were prepared with a handmade spray drying tower with a variety of operational conditions. It was confirmed by the observation with SEM that nicotinic acid crystal were uniformly coated with the wall material. Detailed descriptions of the effect of operational conditions on the release behavior will be given in Chapter 2 of Part 2.

References

1) Y.Kawashima, Huntai to Kogyo, 4, 32, 50 (1972)

2) K.Masters, Spray Drying Handbook, 3rd ed., George Godwin, London, (1979)

3) M.J.Robinson and E.V.Svedres, U.S.Patent 2,805,977 (1957)

4) A.P.Granatek, B.C.Nunning, N.G.Athanas, R.L.Dana, E.S.Granatek and R.G.Daoust, U.S.Patent 3,549,746 (1970)
U.S.Patent 3,626,056 (1971)

Chapter 3

Microencapsulation by (W/O)/W multiple phase emulsion method

Abstract

Aqueous solution of Vitamin B_6 (5-hydroxy-6-methyl-3,4-pyridinedimethanol hydrochloride) was encapsulated with the (W/O)/W multiple phase emulsion method. Natural waxes, polystyrene (PS) and styrene (ST) copolymers were employed as wall materials. Particular attentions were focussed on how the physical properties of polymers such as molecular weight, composition, glass transition temperature (T_g), miscibility with solvent and possible blending with others affected the general features and performances of microcapsules. SEM photographs and measurement of drug content were quite informative to judge applicability of products.

ST-acrylic copolymers and the blends of ST-butadiene rubber (SBR) and PS gave tough wall structures, while PS gave a homogeneous but fragile wall structure.

Introduction

In previous chapters, water soluble solids were encapsulated by two different methods. However, these methods are not applicable to the encapsulation of aqueous liquids.

Two conventional methods may be employed to encapsulate liquids as core substance; one is interfacial polycondensation method[1], and the other is multiple phase emulsion method[2-4] classified as a modified solvent evaporation method[5]. Normally the former is more frequently employed than the latter, because the latter has been less employed for commercial purposes mainly due to the smaller drug content per capsule.

However, the advantage of multiple phase emulsion method is that almost any kind of polymeric materials can be utilized as wall material, if only suitable solvent is found. One of the most effective ways to carry out the feasibility study, in which a particular substance is to be employed in encapsulated form, may be achieved by adopting the multiple phase emulsion method.

In this chapter, it will be found that the general feature of microcapsules changed dramatically depending on the wall materials employed for the multiple phase emulsion method[6]. They also intend to collect as much information how the properties of polymeric materials such as molecular weight, composition of copolymer, glass transition temperature (T_g), and probable blending between them will affect the overall features of capsules.

Experimental

Reagents

Wall materials. n-praffin (m.p. 341-343K) and beeswax white (m.p. 335-339K) were used as served. SBR (Solprene T-414: copolymer containing 33wt. percent of styrene by solution polymerization) was from Asahi Chemicals Co. Ltd. PS and copolymers of styrene with acrylic esters were polymerized in the laboratory employing either the suspension or emulsion polymerization technique. Physical properties of the synthesized polymers were listed in Table 3-1.

Solvents. Chloroform, methylene chloride and benzene used as solvents were reagent grade.

Other materials. Vitamin B_6 and polyvinyl alcohol (PVA, $\bar{P}_n$=500, 97 percent hydrolyzed), each being reagent grade, were from Wako Pure Chemical Industries.

Preparation of microcapsules

In standard recipe, 1.3g of Vitamin B_6 was dissolved in 5g of 2wt percent PVA aqueous solution. 3g of wall materials were dissolved in 27g of chloroform. (W/O) emulsion was prepared with a conventional homogenizer operated at 5000rpm for 3min, the temperature being controlled at 313 to 318K. This emulsion was then poured into 250ml of 1wt. percent PVA aqueous solution in a 500ml round-bottomed flask, and stirred at 250rpm to form (W/O)/W emulsion. The system was kept at 328K for 2hr under the slightly

reduced pressure to remove chloroform. After 2hr elapsed, the ingredient was cooled with ice water, microcapsules being filtered, and stored in a desiccator.

Quantitative measurement of Vitamin B_6

Quantitative measurement of Vitamin B_6 in the aqueous solution was carried out employing a UV spectrophotometer (λ=244nm). 2ml of sample solution was dissolved in 8ml of 0.125N NaOH aqueous solution.

Vitamin B_6 content in microcapsules was determined in a same procedure after the wall of microcapsules was broken in a ceramic mortar with a pestle, and all the drug was leached out with water.

Characterization of microcapsules

General feature of microcapsules was observed with a SEM including measurement of average wall thickness. Average diameter of microcapsules was determined from photographs obtained with an optical microscope. For rough estimation of the average wall thickness the following equation was derived assuming the additivity of volume for each component.

$$\delta = \frac{\bar{d}_{pm}}{2}\left[1 - \left[1 + \frac{\frac{W_W}{\rho_W}}{\frac{W_C}{\rho_C}\left[1 + \rho_C\left(\frac{100}{m} - 1 - \frac{W_W}{W_C}\right)\right]}\right]^{-1/3}\right] \quad (3\text{-}1)$$

where, δ, $\bar{d}_{pm}$ = average wall and diameter of microcapsules, W_W, W_C = weight of wall material and drug encapsulated, ρ_W, ρ_C = density of wall and drug, and m = drug content, respectively.

Table 3-1. Polymers employed as wall material.

Wall material	Copolymer composition (mol. ratio)	Molecular weight		Dispersion index ($\bar{M}_w/\bar{M}_n$)	Glass transition temp. (K)
		Number average ($\bar{M}_n \times 10^{-4}$)	Weight average ($\bar{M}w \times 10^{-4}$)		
PS	--	0.70	1.10	1.56	363
P(ST-co-BA)					
B-4	71.6/28.4	1.34	2.95	2.20	315
B-5	74.3/25.7	3.89	8.71	2.24	315
B-6	74.7/25.3	8.58	19.25	2.24	315
B-7	74.5/25.5	12.6	30.6	2.43	315
P(ST-co-MA)					
M-1	68.2/31.8	6.91	19.68	2.85	338
M-2	56.3/43.7	7.20	15.93	2.22	321
M-3	35.4/74.6	6.38	15.45	2.42	313
M-4	69.3/30.7	0.97	2.75	2.83	338
P(ST-co-EA)					
E-1	64.7/35.3	9.61	21.22	2.21	325
E-2	50.7/49.3	6.44	15.04	2.34	301
E-3	33.9/66.1	4.46	13.40	3.01	279
E-4	70.6/29.4	1.13	3.24	2.87	325
P(MMA-co-BA)	77.4/22.6	4.07	12.40	3.05	325
P(MMA-co-EA)	72.5/27.5	2.14	10.50	4.91	335
SBR(Solprene T-414)	33/67	7.40	10.74	1.45	209-214
Natural wax					
n-Paraffin	--	--	--	--	m.p.341-343
Beeswax white	--	--	--	--	m.p.335-339

ST = styrene, BA = n-butyl acrylate, EA = ethyl acrylate, MA = methyl acrylate, SBR = styrene-butadiene rubber.

Results and discussion

Vitamin B_6 containing microcapsules were prepared employing various polymers (shown in Table 3-1) as wall materials. Average diameter, $\bar{d}_{pm}$, average wall thickness, δ, and the drug content for each preparation were listed in Table 3-2.

Attempts to prepare microcapsules employing natural waxes as sole wall materials had little success due to the strong nonpolarity (hydrophobicity) of waxes.

SEM photographs of microcapsules with SBR as a basic wall material are shown in Photo. 3-1 to Photo. 3-5. A particular feature of SBR microcapsule is the fact that there are numerous holes in the wall as shown in Photo. 3-1. Blending with n-paraffin (n-P) and/or beeswax white (Bww), both immiscible with SBR, gives utterly different features having full of small creases. Those holes are all patched up with the waxes as shown in Photo. 3-2 and Photo. 3-3. Photo. 3-4 shows a three component (SBR/n-P/Bww) wall microcapsule, having a similar feature as that of SBR/n-P wall.

PS wall was shown in Photo. 3-5. PS capsules revealed quite smooth surface and thin thickness, however, the wall was fragile against the impact force. Mixing with miscible SBR remarkably erased this brittleness of PS, and yielded quite resilient microcapsules. As shown in Photo. 3-6. PS/SBR capsules gave a smooth

Table 3-2. Characterizations of microcapsules.

MC No.	Diameter $\overline{dpm}$ (μm)	Wall thickness δ (μm)	Drug content (mg/g-MC)	Solvent
105 SBR/n-P	506	--	43.8	Ch
106 SBR/n-P	471	--	44.0	Ch
107 SBR/n-P	489	34.1	37.6	Ch
201 SBR/n-P	476	50.0	129.0	Ch
403 SBR	458	32.1	14.0	Ch
404 SBR	446	25.1	71.0	Ch
602 SBR/n-P/Bww	415	47.5	53.5	Ch
604 SBR/n-P/Bww	458	51.0	48.8	Ch
606 SBR/n-P/Bww	482	54.1	48.2	Ch
704 SBR/PS	163	27.0	52.4	Ch
706 PS	88	14.0	24.0	Ch
1003 B-4	173	11.4	213.3	Ch
1009 B-6	255	16.1	13.7	Ch
1012 B-5	249	17.0	17.0	Ch
1016 E-1	245	15.1	27.2	Ch
1017 E-2	323	21.0	142.6	Ch
1022 B-4	207	13.9	128.7	Dm
1028 P(MMA-co-BA)	244	15.2	38.5	Ch
1030 P(MMA-co-EA)	276	17.7	94.4	Ch
1035 B-6	198	9.3	102.6	Be
1041 B-6	256	16.8	62.5	Be
1043 B-4	178	11.6	96.5	Ch/Be
1045 B-6	213	12.1	107.2	Ch
1050 B-5	200	13.1	96.0	Ch/Be
1052 B-5	209	14.1	130.4	Ch/Be
1055 B-7	318	17.7	84.3	Ch

Ch = chloroform, Dm = metylene chloride, Be = benzene, Ch/Be = mixed solvent.

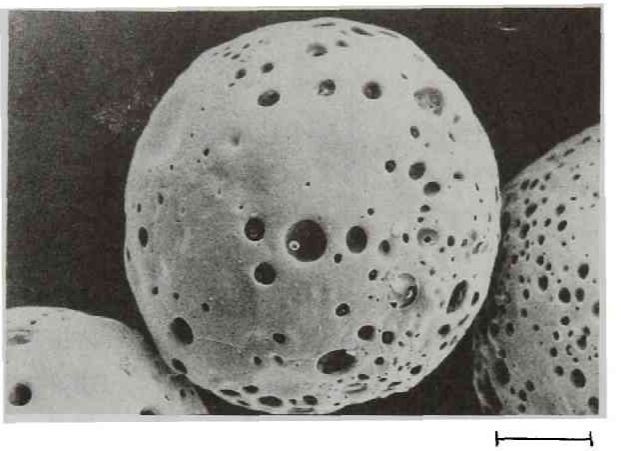

100μm

Photo. 3-1. SBR microcapsule

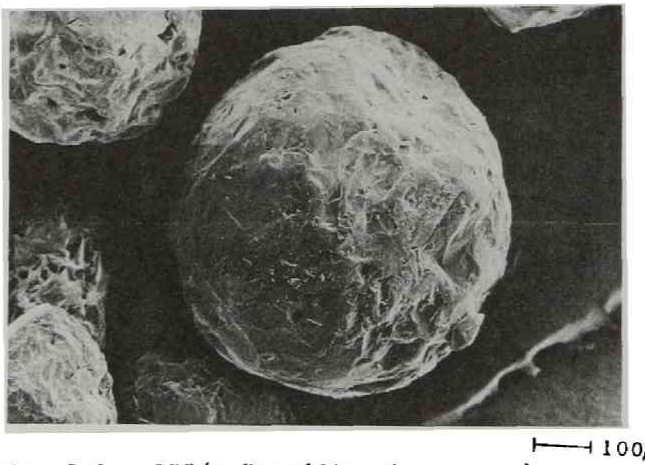

100μm

Photo. 3-2. SBR/n-Paraffin microcapsule

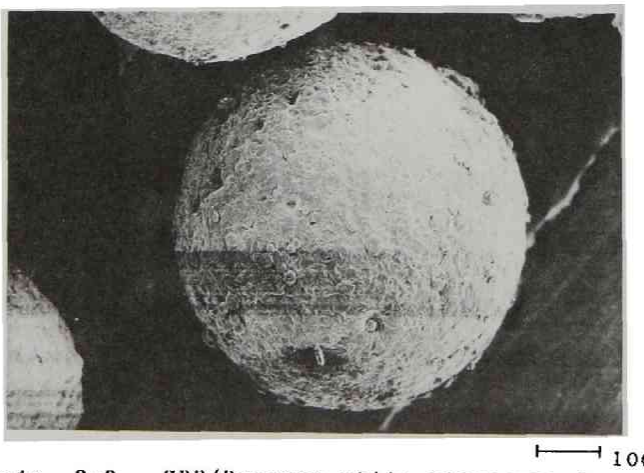

100μm

Photo. 3-3. SBR/Beeswax white microcapsule

Photo. 3-4. SBR/n-Paraffin/Beeswax white microcapsule

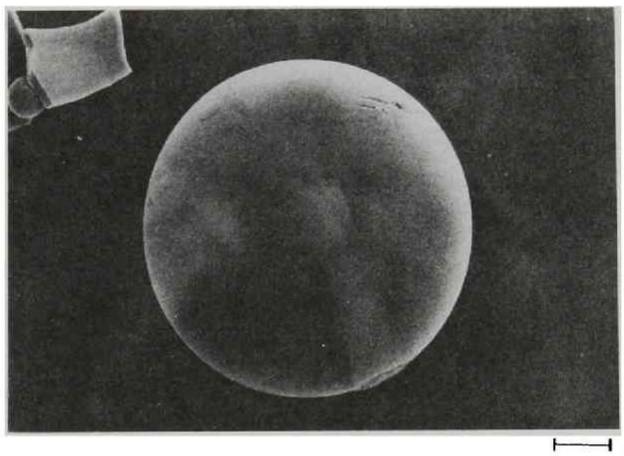

Photo. 3-5. Polystyrene microcapsule

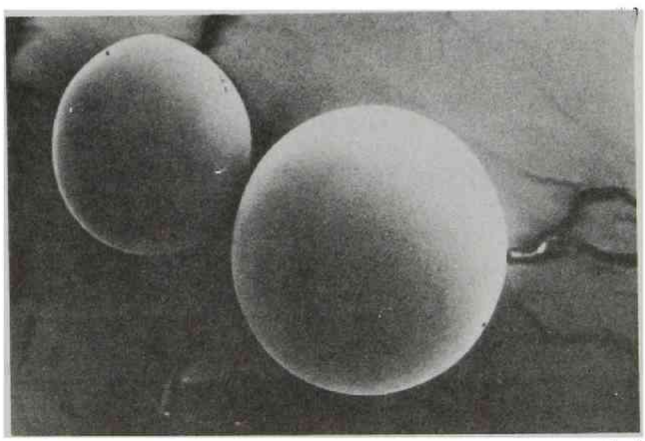

Photo. 3-6. SBR/Polystyrene microcapsule

surface as well as PS capsules.

Synthetic copolymers from styrene as base monomer and acrylic monomers yielded microcapsules with singularly different features depending on particular acrylate copolymerized. n-butyl (B), and ethyl (E), and methyl (M) acrylate were chosen to incorporate different degree of ductility into the stiff PS chains. The glass transition temperature (T_g) of poly-n-butyl acrylate is 219K, almost rubber-like, whilst that of polyethyl acrylate is 248K, and polymethyl acrylate, 283K. Tg of various copolymers shown in Table 3-1 was estimated according to Uematsu[6].

Incorporation of n-butyl acrylate chains (B series in Table 3-1) yielded microcapsules with smooth surface, thin wall and reasonable drug content unless molecular weight of the copolymer was too high. The typical appearance was shown in Photo. 3-7.

General features were nearly same in the cases of ethyl acrylate copolymers (E series), however, either the drug content was low. In several cases there existed sharply bored pin holes on the surface of microcapsules. When methylene chloride, a low-boiling point solvent, was employed, large holes were created on the surface of microcapsules caused by the evaporation of the solvent, an emphasis of very thin wall. One photograph was shown in Photo. 3-8.

Copolymers of methyl acrylate (M series) failed to give smooth-wall microcapsules no matter how conditions of preparation was readjusted. As shown in Photo. 3-9, numerous, sharp pinholes

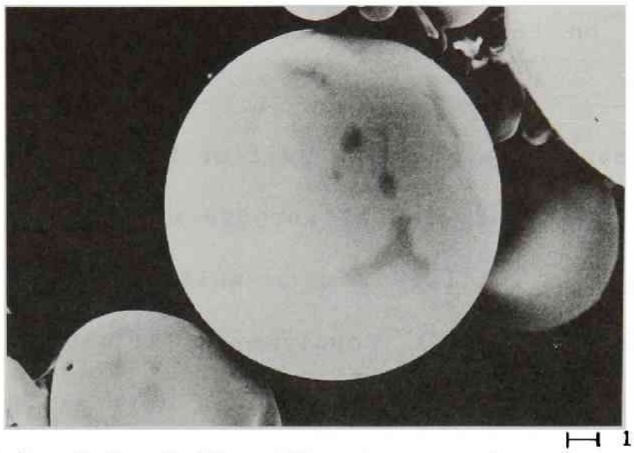

Photo. 3-7. P(ST-co-BA) microcapsule

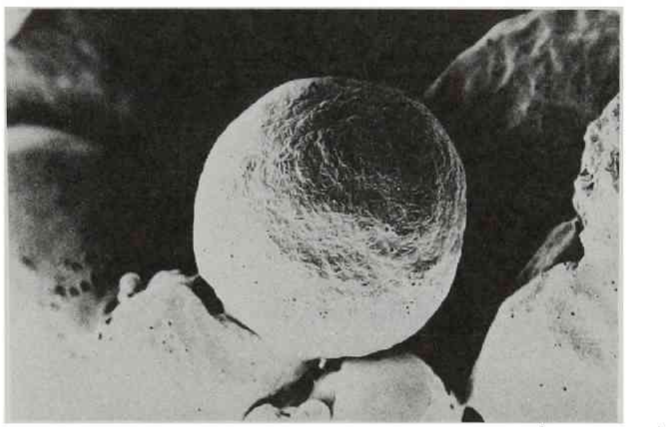

Photo. 3-8. P(ST-co-EA) microcapsule

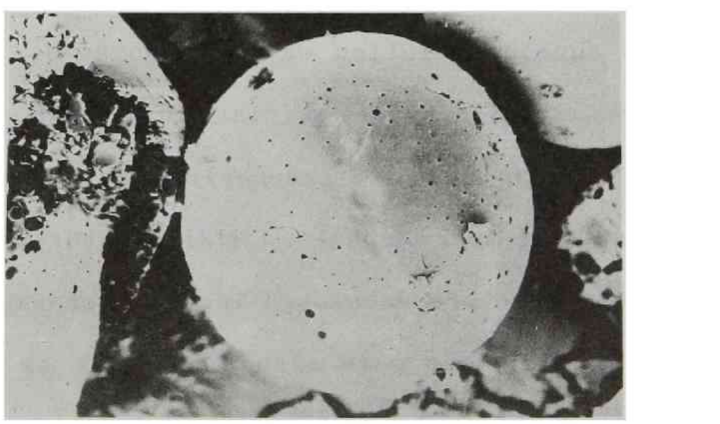

Photo. 3-9. P(ST-co-MA) microcapsule

were observed on the surface, an obvious reason to yield poor drug content.

In this manner, a miscible pair of PS and SBR is recommended for the preparation of general purpose microcapsules, being very tough against the inflicted force whilst retaining appropriate transport through the wall. Copolymer of ST-n-butyl acrylate will provide fine feature of the surface as well as thinner but uniform wall. The drug content is very high. ST-ethyl acrylate copolymer can be a potential wall material, however, more experiences will be necessary to secure the procedure and conditions of preparation.

Conclusion

Hollow sphere microcapsules were prepared with (W/O)/W multiple phase emulsion method. Vitamin B_6 was chosen as a model drug, and the aqueous solution was encapsulated. PS/SBR blends and copolymers of ST-n-butyl acrylate are most recommended as wall materials which provide reasonable drug content as well as physical strength of microcapsules. Mixing natural waxes with SBR yielded fibrous structure developed inside microcapsules. Copolymers of ST-ethyl acrylate were also applicable as wall material, however, the conditions of preparation is limited.

References

1) P.L.Madan, Drug Develop. Indust. Pharm., 4, 289 (1978)

2) M.N.Vrancken and D.A.Claeys, U.S.Patent 3,523,906 (1970)

3) H.Takenaka, Y.Kawashima, Y.Chikamatsu and Y.Ando, Chem. Pharm. Bull., 30, 695 (1982)

4) Y.Nozawa, F.Higashide and T.Kanemoto, J. Appl. Poly. Sci., 20, 3197 (1976)

5) R.Alex and R.Bodmeier, J. Microencapsulation, 7, 347 (1990)

6) I.Uematsu, Kyojugotai no gosei to bussei, Kagaku zokan, 27, 141 (1967)

Chapter 4

Microencapsulation of pheromone-analog by complex coacervation and (S/W)/O multiple phase suspension method

Abstract

2-Ethylhexyl acetate (EHA) that was selected as a insect pheromone-analog due to its similar structure was encapsulated. For control of insect populations, microcapsules should release the core substance at an intended rate for a long-term, and desired goal of effective release was set at least half a year. For this purpose, complex coacervation method and multiple phase suspension method were adopted. At first EHA was impregnated in wax particles, which were then encapsulated employing the complex coacervation of gelatin/gum arabic system. As a second attempt, solid-in-water-in-oil (S/W)/O multiple suspension method was employed to encapsulate multiple numbers of wax particles in hydrated networks of gelatin. The difference of wall structure was revealed with SEM.

Introduction

Pheromone is a new type of insecticide, being very specific and effective in trace amount (ppm or even ppd), and leaves no harmful after-effects to surrounding environment[1,2]. For example nearly 50 pheromones have been identified as to belong to the lepidoptera. Being classified as esters, alcohols, aldehydes and ketones, they have in common a long carbon chain with one or two double bonds. Against the advantages mentioned above, minor deficit is due to expensive cost of synthesis based upon the absolute necessity to incorporate double bonds in the exact location of a carbon chain.

Since pheromone is so expensive and effective in very small amount, controlled release of the drug from microcapsules seems to provide a promising solution to prevent unnecessary waste during the practice. Herbig and Smith[3] has reported the encapsulation of gossyplure (pheromone for the pink bollworm) in a particular asymmetric microporus beads, which were distributed from an airplane. The effective duration of the release was a month utmost forcing the repeated distribution once for every few weeks. For the practical use, the time-scale required to obstruct the mating of target insects should be at least half a year, or hopefully a full year, and has remained unsurmountable for the conventional encapsulation techniques.

In this chapter, the preparations of microcapsules having an effective rate for a long period of time are investigated[4].

Experimental

Reagents

Pheromone syrup and its analog. Pheromone syrup (Z,Z-7,11-hexadecadienyl acetate : Z,E-7,11-hexadecadienyl acetate = 50 : 50) for pink bollworm was donated from Shin-etsu Chemical Co. Ltd., and was encapsulated as served. 2-Ethylhexyl acetate (EHA) was reagent grade and supplied from Tokyo Chemical Co. Ltd.

Wall materials. Gelatin (Wako Pure Chemical Industries) and gum arabic (Kokusan Chemical Co.) were used as the agents of complex coacervation. Beeswax white was used to prepared wax particles impregnated with EHA or pheromone.

Crosslinking agent. 30wt percent aqueous solution of formaldehyde was used to crosslink gelatin chains.

Other reagents. 10wt percent aqueous solution of acetic acid and the same concentration of sodium hydroxide were used to control the pH of solutions. Liquid paraffin was used as a medium of the aqueous suspension (S/W) in oil (O) dispersion.

Preparation of wax microparticles

4.5g of molten beeswax white was mixed with 0.5g of EHA, and then added to 200g of 1wt percent gelatin solution stirred in a

500ml separable flask equipped with a teflon-blade stirrer and four baffle plates. The agitation rate was 250min^{-1}, and the temperature was kept at 343K. After five minutes the ingredient was quenched in an ice water bath, and wax particles were filtered.

Preparation of microcapsules

Complex coacervation method Equal portion (30g) of 5wt percent gelatin and 5wt percent gum arabic aqueous solution was mixed in a 300ml separable flask equipped with a stirrer blade and a thermometer. Wax particles were added, and the temperature was kept at 313K under the agitation. Then 140g of warm water was added, and after pH of the ingredient was adjusted at 4.0 by the drop-by-drop addition of 10wt percent of acetic acid, generation of coacervate droplets was observed. After 30 minutes elapsed, the ingredient was quenched to 278K. 3ml of 30wt percent formaldehyde aqueous solution was added to crosslink the gelatin with pH being adjusted at 9.0, using 10wt percent sodium hydroxide. Crosslinking continued for 2hr, and then the temperature was raised to 313K. Microcapsules were separated by means of centrifuge.

(S/W)/O multiple phase suspension method Wax particles were dispersed in 20g of 20wt percent aqueous solution of gelatin, and then this suspension (S/W) was redispersed in 200g of liquid paraffin. After 30 minutes agitation at 250min^{-1}, (W/O) emulsion composed of 4g of formaldehyde aqueous solution and 50g of liquid

paraffin was added to the (S/W)/O dispersion. Crosslinking reaction was allowed to proceed for 2hr, microcapsules were filtered, and washed with petroleum benzine, ethanol and cold water.

Characterization of microcapsules

General features of the surface and cross-section of the wall were observed with. Average diameters of wax particles and microcapsules were measured from the photographs of optical microscope.

Average wall thickness of microcapsules were calculated from the mathematical formula written below by measuring the amount of gelatin. Elemental analysis (CHN analyzer Model CHN-1A, Shimadzu Co.) was conducted to measure the nitrogen content in microcapsules. Since nitrogen is contained only in gelatin, the amount of gelatin was easily obtained. The correction for the small amount of gum arabic incorporated during the complex coacervation process was done based upon the composition of crosslinked coacervates.

The average wall thickness of microcapsules can be obtained from previous Equation (2-2).

As mentioned later, microcapsules obtained from (S/W)/O suspension method contained multiple numbers of wax particles. Approximate numbers of wax particles in one microcapsule can be estimated from the following equation.

$$N = \frac{\left(\frac{\bar{d}_{pm}}{2} - \delta\right)^3}{\left(\frac{\bar{d}_{pc}}{2}\right)^3} \qquad (4\text{-}1)$$

In this equation, $\bar{d}_{pm}$ is the average diameter of dried microcapsules, and related to that of wet ones (containing moisture soon after the preparation) as follows,

$$\bar{d}_{pm} = \left(\frac{100 - w - m}{100} \right)^{1/3} \bar{d}_{pmw} \qquad (4\text{-}2)$$

where, $\bar{d}_{pmw}$ = average diameter of wet microcapsules, w,m = wt percent of moisture and drug in microcapsules, respectively.

Measurement of drug content

Content of encapsulated EHA was determined by gas chromatograph (GC-163, Hitachi Co. Ltd.) with a flame ionization detector (FID). Stainless steel column (3mm diameter and 3m length, Silicone SE-30 adsorbed on Chromosorb carrier) was used with 463K column temperature and 523K at injection port. n-Dodecyl acetate (Tokyo Kasei Co.) was employed as an internal standard substance, and chloroform as a solvent.

Results and discussion

Wax particles.

Appearance of wax particle, impregnated with pheromone, was observed as shown in Photo. 4-1(a) with SEM, and that of enlarged surface feature in Photo. 4-1(b). No pin-holes or cracks were observed besides the fine creases which characterized the surface of wax materials. The particles distributed between the diameter

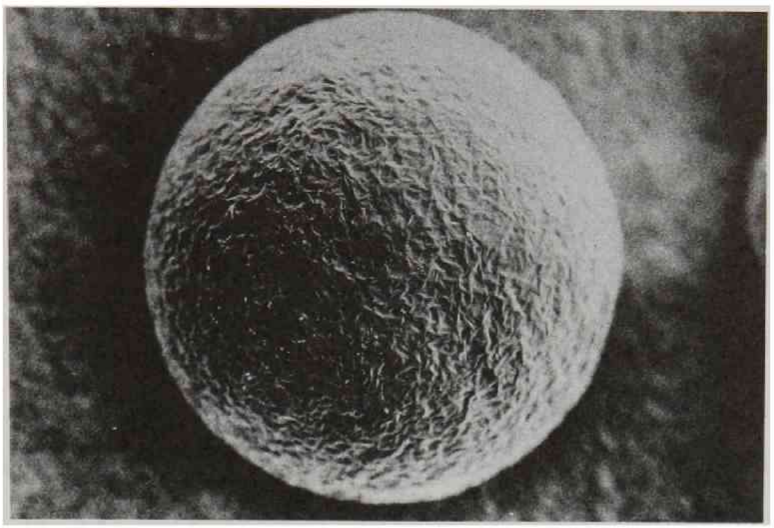

(a) 100μm

(b) 10μm

Photo. 4-1. SEM photograph of wax particle impregnated EHA.

of 40 to 400μm, the average value being around 250μm, and very few agglomerated particles were observed.

EHA content in the particles was around 70mg/g-MC, approximately 80 percent yield based on the feed EHA.

Microcapsules prepared using complex coacervation

Composition of coacervates from gelatin/gum arabic system.

Composition of gelatin in coacervates was 75wt percent, and remained constant regardless the feed ratio. At the present condition, pH = 4.0 and 313K, maximum amount of coacervates was observed at the feed ratio of gelatin/gum arabic = 60/40(wt). This result was slightly different from that of Bungenberg de Jong and Dekker[5,6] whose data showed the maximum at 40wt percent of gelatin.

In the following encapsulation, majority of procedures were carried out with the feed composition of 50/50(wt).

Microencapsulation of wax particles. All the microcapsules were obtained containing only a single core. No doublets or further multiple cores were observed.

Characteristics of prepared microcapsules together with one example of uncapsulated wax particles were listed in Table 4-1. EHA content was sufficient for the present purpose. However, the thickness of the wall was an order of 1μm utmost, leaving the concern that the wall thickness may be too thin. On this context, MC-107 was encapsulated twice to double the wall thickness.

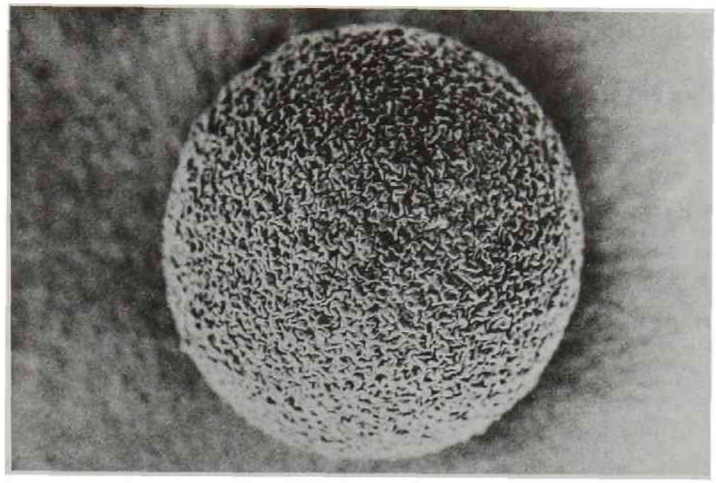

(a)

100μm

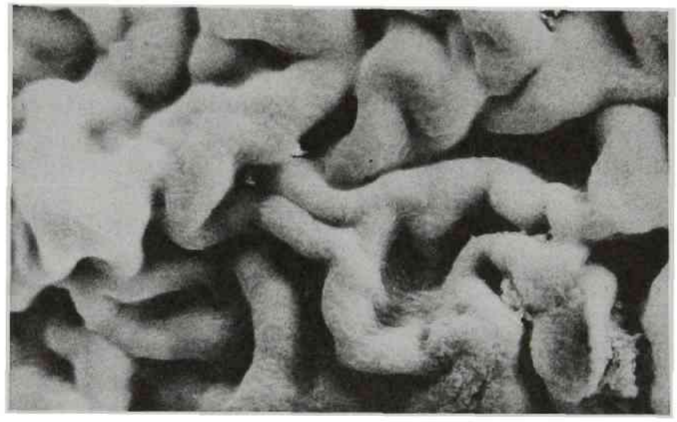

(b)

10μm

Photo. 4-2. SEM photograph of microcapsule prepared using complex coacervation method.

SEM photographs of the general feature of microcapsule and its surface were shown in Photo. 4-2(a) and 4-2(b), respectively. One may feel that there are not so much differences between the features of Photo 4-1(a) and 4-2(a), but the magnified view of Photo 4-2(b) revealed that the uniform and somewhat soft structure of gelatin wall developed on the surface of wax particles.

Microcapsules prepared using (S/W)/O multiple phase suspension

Dimensions and properties of microcapsules obtained from (S/W)/O multiple phase suspension method were listed in Table 4-2. Significant changes one may notice from those microcapsules in Table 4-1 were the size and the high moisture content. Due to the preparation using solid-in-water suspension, microcapsules contained multiple numbers of wax particles ranging from 10 to 70 expressed as N in the column of Table 4-2. Moisture content just after the preparation was understandably high indicating that the gelatin wall is present in swollen state. Based on the weight of completely dried-up microcapsules, content of gelatin became more than 60 percent.

The loaded EHA per gram microcapsule decreased naturally as the content of gelatin increased. From MC-201 to 203, the temperature employed for the preparation of second-stage dispersion, (S/W) into O, was changed from 293 to 313K. As the viscosity of the continuous phase (O) decreased with increasing temperature, the size of (S/W) droplets became smaller, resulting the smaller

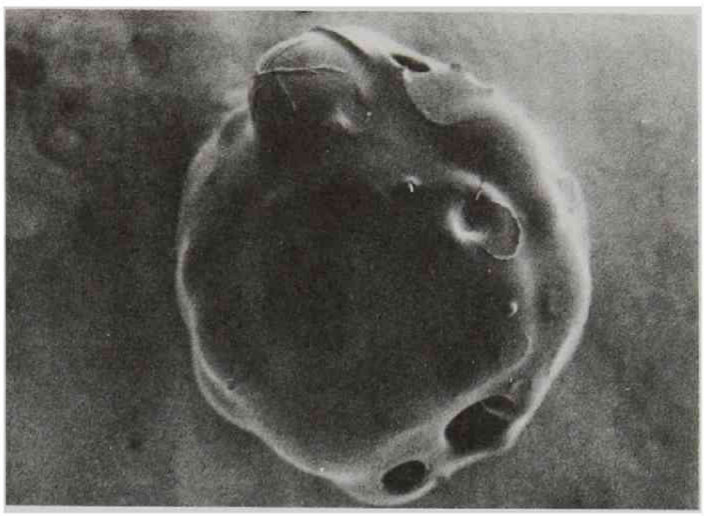

(a) surface of capsule 100μm

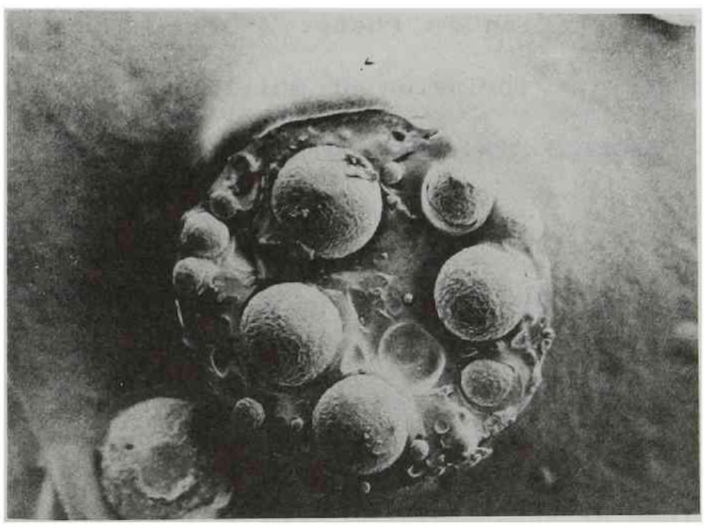

(b) cross-section of capsule 100μm

Photo. 4-3. SEM photograph of multiple-core microcapsule containing real pheromone syrup.

number of wax particles encapsulated. In the preparation of MC-203, the temperature was too high (313K) for the gelatin solution (W) to envelope the wax particles (S). Consequently the operating temperature for the preparation of second-stage dispersion should be kept low to keep the EHA loading within the reasonable range, though the size of microcapsules becomes larger.

In MC-204, charged amount of EHA in the preparation of wax particles was five times more than that of MC-201. Amount of EHA eventually loaded was no more than three times of MC-201.

An appearance of microcapsules containing real pheromone syrup (not listed in Table 4-2) was shown in Photo. 4-3(a), and that of cross-section in Photo. 4-3(b). The surface feature clearly showed the inclusion of multiple numbers of wax particles. From Photo. 4-3(b) one could observe quite tight domain of gelatin wall.

Conclusion

Two kinds of encapsulation method, complex coacervation and (S/W)/O multiple phase suspension method, were investigated with a view to obtaining an effective release rate of pheromone for a long period of time. The multiple suspension method could give the thicker wall, compared with complex coacervation method. In addition, the observation by SEM showed that the structure of

Table 4-1. Characterization of microcapsules prepared with complex coacervation method.

MC No.	Diameter of core (μm) $\bar{d}_{pc}$	EHA (mg/g-MC)	Gelatin (wt%)	Water (wt%)	Thickness (μm) δ	Diameter of MC(μm) $\bar{d}_{pm}$
101	335	66.0	3.0	17.8	1.3	338
102	268	71.9	4.4	15.8	1.5	271
107	256	71.6	8.7	17.9	3.0	262
Wax P.	233	78.1	--	--	--	--

Table 4-2. Characterization of microcapsules prepared with (S/W)/O multiple phase suspension method.

MC No.	Diameter of core $\bar{d}_{pm}$ (μm)	EHA (mg/g-MC)	Gelatin[1)] (wt%)	Water (wt%)	Thickness[2)] δ (μm)	Wet Diameter $\bar{d}_{pmw}$ (μm)	Dry Diameter[2)] $\bar{d}_{pm}$ (μm)	N[2)]
201	302	14.1	58.5	52.6	133	1545	1192	28
202	237	6.9	64.8	59.8	95	987	724	11
203	176	1.5	76.1	68.8	107	914	618	12
204	212	50.0	78.6	62.8	247	1904	1366	70

1)Based on dried capsules. 2)Based on calculations.

capsules differ from one another. These differences in the wall thickness and wall structure will influence the release rate of pheromone. In next part, Chapter 3 will make the difference clearer.

References

1) W.L.Roelofs, J. Chem. Ecol., 4, 685 (1978)

2) R.J.Marks, B.F.Hall, R.Lester, B.F.Nesbitt and R.K.Lambert, Bull. ent. Res., 71, 403 (1981)

3) S.M.Herbig and K.L.Smith, Proceedings of ICOM '90, August 20, Chicago, USA, Vol.1, 592 (1990)

4) S.Omi, N.Umeki, H.Mohri and M.Iso, J. Microencapsulation, 8, 465 (1991)

5) H.G.Bungenberg de Jong and W.A.L.Dekker, Kolloidchem. Beih., 43, 143 (1935)

6) H.G.Bungenberg de Jong and W.A,L.Dekker, Kolloidchem. Beih., 43, 213 (1936)

Part 2

Controlled Release from Microcapsules

Chapter 1

Controlled release of water-soluble substances from microcapsules prepared by nonaqueous coacervation methods

Abstract

Controlled release behavior from microcapsules prepared by nonaqueous coacervation methods was successfully investigated by using encapsulated anhydrous sodium sulphate (ASS) particles. Microcapsules were prepared by PS-cyclohexane binary system and PS-cyclohexane-n-hexane ternary system. In either case, Higuchi model was sufficient to evaluate the release behavior of ASS through the wall as the effective diffusion coefficient estimated from the model was correlated with the operating factor on micro-encapsulation. The values of diffusion coefficients were in order of between 10^{-7} and 10^{-8} cm^2/sec depending on the thickness of PS in the wall.

Introduction

Release behavior of core materials from microcapsules is a mass transport phenomenon involving diffusion of core material molecules through the wall of polymeric membranes. Release model is important to an understanding of how core materials are released from microcapsules. The wall of microcapsule normally acts as a barrier, the resistance of which is remarkably influenced by the wall structure, e.g. the wall thickness, chemical composition and morphology. Studies to model the release behavior have been reported by several workers[1,2]. However, since core materials transport through the wall is a very complex, there still exist many uncertainties and inconsistencies in the available information. Takenaka et al.[3] reported apparent diffusion coefficient of sulfamethoxazole, that was calculated by Higuchi model[4,5], through gelatin-acasia coacervated microcapsule. Senjkovic and Jalsenjak[6] have studied the apparent diffusion coefficient of sodium phenobarbitone from variable size ethylcellulose capsule.

In this chapter, the controlled release of anhydrous sodium sulphate (ASS) from microcapsules produced by nonaqueous coacervation method is mentioned with the correlated results obtained by employing the Higuchi model. These results will provide substantial clues for the practical design of microcapsules on a commercial basis.

Table 4-1. Characterization of microcapsules prepared with complex coacervation method.

MC No.	Diameter of core (μm) $\bar{d}_{pc}$	EHA (mg/g-MC)	Gelatin (wt%)	Water (wt%)	Thickness (μm) δ	Diameter of MC(μm) $\bar{d}_{pm}$
101	335	66.0	3.0	17.8	1.3	338
102	268	71.9	4.4	15.8	1.5	271
107	256	71.6	8.7	17.9	3.0	262
Wax P.	233	78.1	--	--	--	--

Table 4-2. Characterization of microcapsules prepared with (S/W)/O multiple phase suspension method.

MC No.	Diameter of core $\bar{d}_{pm}$ (μm)	EHA (mg/g-MC)	Gelatin[1)] (wt%)	Water (wt%)	Thickness[2)] δ (μm)	Wet Diameter $\bar{d}_{pmw}$ (μm)	Dry Diameter[2)] $\bar{d}_{pm}$ (μm)	N[2)]
201	302	14.1	58.5	52.6	133	1545	1192	28
202	237	6.9	64.8	59.8	95	987	724	11
203	176	1.5	76.1	68.8	107	914	618	12
204	212	50.0	78.6	62.8	247	1904	1366	70

1)Based on dried capsules. 2)Based on calculations.

Experimental

A major part of the microencapsulation procedure was described in Chapter 1 of Part 1.

In PS-cyclohexane binary system, crystals of ASS were encapsulated to investigate the mechanism of controlled release from microcapsules. 1wt percent of solution of PS-5($\bar{M}_w$=50,940) was used in the temperature range 285 to 292K.

1.5g of dried microcapsules containing ASS were added in 1l of distilled water and stirred with a magnetic stirrer. Aliquots of 5.0ml each of aqueous solution was withdrawn at prefixed time intervals through a glass filter, and the concentration of ASS was determined with a UV spectrophotometer. The wavelength selected was 188nm.

For the microcapsules prepared by PS-cyclohexane-n-hexane ternary system, the procedure was essentially regarded as same as in the case of binary system.

Results and Discussion

Release profiles

Binary system. In PS-cyclohexane binary system, controlled release profiles of ASS encapsulated within a PS film and talc shell are shown in Figure 1-1 and 1-2. Curves in the two figures

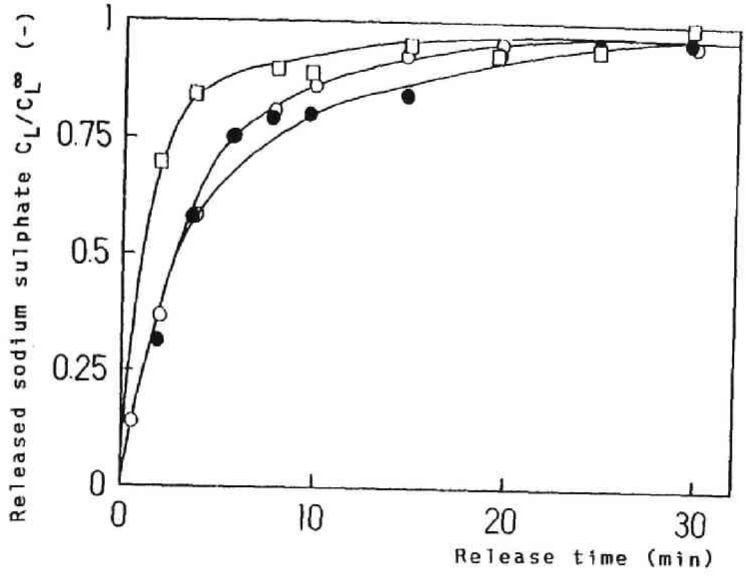

Figure 1-1. Release profile of anhydrous sodium sulphate. Effect of encapsulation temperature: ○, 285K; ●, 286K; □, 287K. Measured at 303K. 1.5g of dried microcapsules was added in 1l distilled water.

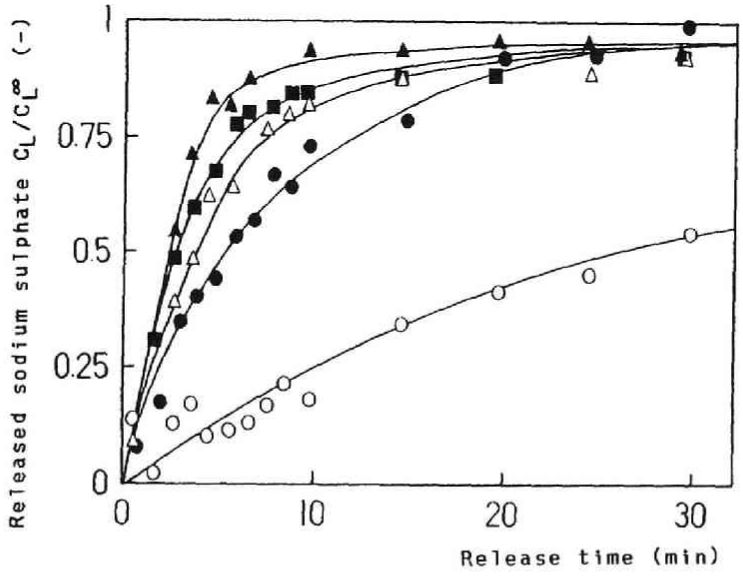

Figure 1-2. Release profile of anhydrous sodium sulphate. Effect of encapsulation temperature: ○, 285K; ●, 286K; ■, 288K; △, 290K; ▲, 292K. Encapsulated twice and measured at 303K. Other conditions were the same as above.

show the effect of encapsulation temperature on the release rate of ASS. The difference in encapsulation temperature was expected to cause different wall thicknesses and average molecular weights of PS in the capsule wall, thus yielding different release rates.

All the microcapsules shown in Figure 1-1 were prepared according to the ordinary procedure described previously in Part 1. However, the release rate was insensitive to the difference in encapsulation temperature, due probably to the thin PS wall. In Figure 1-2, the encapsulation procedure was repeated twice as represented, and this time the effect of encapsulation temperature becomes enhanced, as the release rate is decreased with lowering encapsulation temperature.

As encapsulation temperature is raised, especially over 290K, the release behavior becomes less affected by the encapsulation temperature. This tendency may be explained by the fact that the PS film hardened at the first encapsulation dissolves again during the subsequent processing.

Ternary system. In the case of PS-cyclohexane-n-hexane ternary system, effect of added amount of nonsolvent, n-hexane, to the release profile is shown in Figure 1-3. PS concentration in the original solution was 1wt percent, and encapsulation temperature was 298.2K. The release rate was strongly affected by the amount of n-hexane.

Effect of the encapsulation temperature to the release

profile is shown in Figure 1-4. Microcapsules were prepared with 1wt percent PS solution and by the addition of n-hexane with 0.07 weight ratio to the original solution. The profile revealed a significant dependence on the encapsulation temperature as well as the added amount of n-hexane, for example showing 60min of release time constant in the case of 288.2K.

Correlation of the release

The effective diffusion coefficient of ASS, D_2, was obtained from the well-known Higuchi plot[4,5] and will be discussed as a suitable measure of the mass transport to evaluate the mode of the controlled release.

Assume that each microcapsule is spherical, having uniform structure with the solute included. Key equations for the plot can be written as follows.

$$f(x) = 1 - \alpha + 2(1 - \alpha)x^3 - (3 - 4\alpha)x^2 - \alpha x - \alpha \ln x = B\theta \quad (1\text{-}1)$$

$$B = 6C_s D_2 / C_0 b^2, \quad \alpha = C_s / C_0, \quad x = a'/b \quad (1\text{-}2)$$

$$C_L / C_L^{\infty} = 1 - x^3 \quad (1\text{-}3)$$

where C_L, C_s and C_0 denote the concentrations of the solute in the aqueous phase, in saturated solution, and in microcapsules at time zero, respectively. b and a' denote the mean radius of the microcapsules and that of the penetrating front of the solvent (water). C_L^{∞} denotes the equilibrium concentration of the solute

after the release curve levels off.

Obviously the structure of the microcapsules containing ASS crystals does not belong to the category described above. However, the plots of f(x) against release time shown in Figure 1-5 yield good linear relationships up to the time when nearly all solute molecules are released. This figure was obtained using the samples encapsulated twice in the binary system. The value of D_2 can be easily calculated from the slope of the plot of B against time and shown in Figure 1-6.

In the case of ternary system, Higuchi plots of the experimental values also fairly gave linear relationships, and D_2 were obtained as shown in Figure 1-7. D_2 was a tendency to increase with increasing film thickness of PS. The wall thickness of the binary system was not measured due to the twice repeated encapsulation procedure. In either case, the values were in order of 10^{-7} between $10^{-8}cm^2/sec$, and were similar to the values measured by Senjkovic and Jalsenjak[7], who reported that the effective diffusion coefficient of isoniazid in ethylcellulose wall of microcapsules varied from $0.53x10^{-7}$ to $2.79x10^{-7}cm^2/sec$.

Though Omi[8] has proposed a more strict mass transfer model to deal with the release from spherical microcapsules, the Higuchi model seems to be sufficient to correlate the data presented here. As microcapsules were encapsulated twice in the binary system, direct comparison will be unjustified owing to the difference in the wall structure of microcapsule. However, these

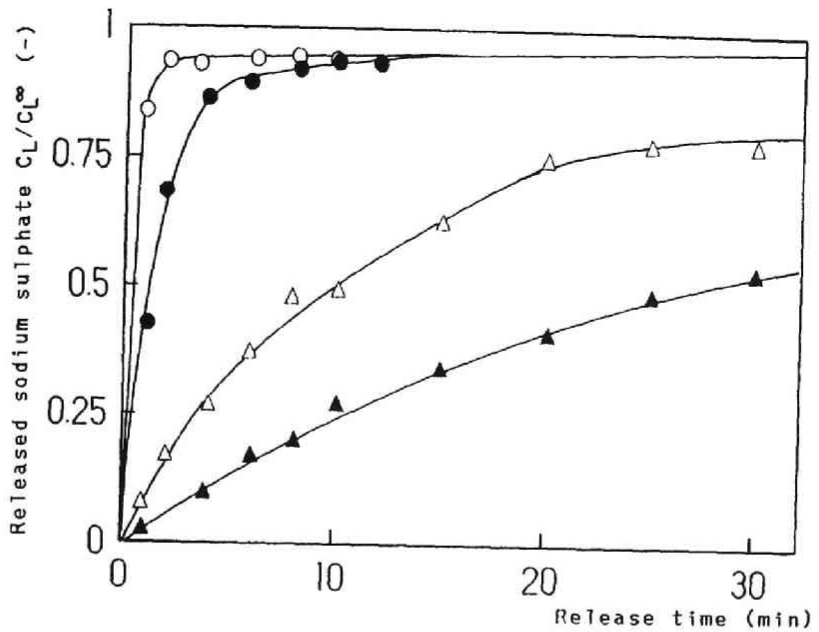

Figure 1-3. Release profile of anhydrous sodium sulphate. Effect of the weight ratio of n-hexane added as a nonsolvent: ○, 0.07; ●, 0.11; △, 0.15; ▲, 0.20. Measured at 303K.

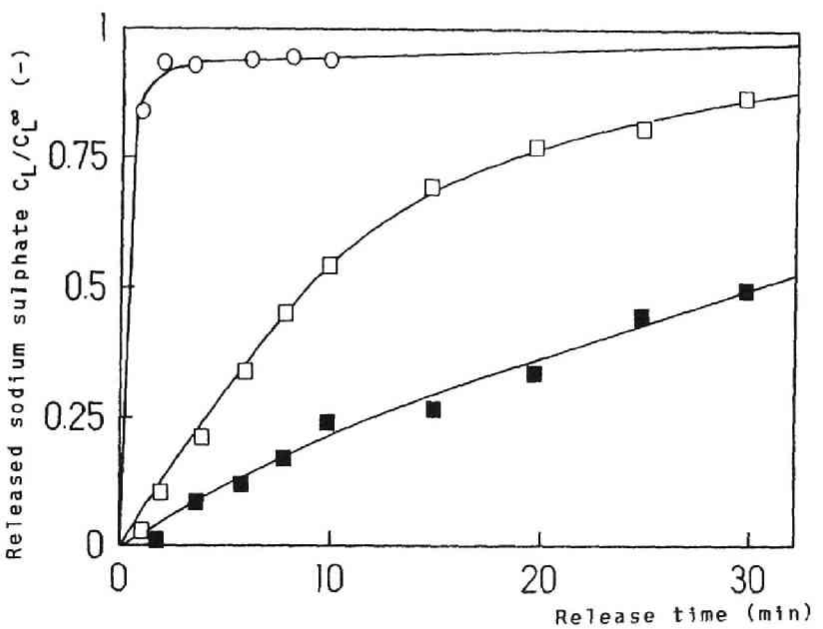

Figure 1-4. Release profile of anhydrous sodium sulphate. Effect of encapsulation temperature: ■, 288K; □, 293K; ○, 298K. Measured at 303K.

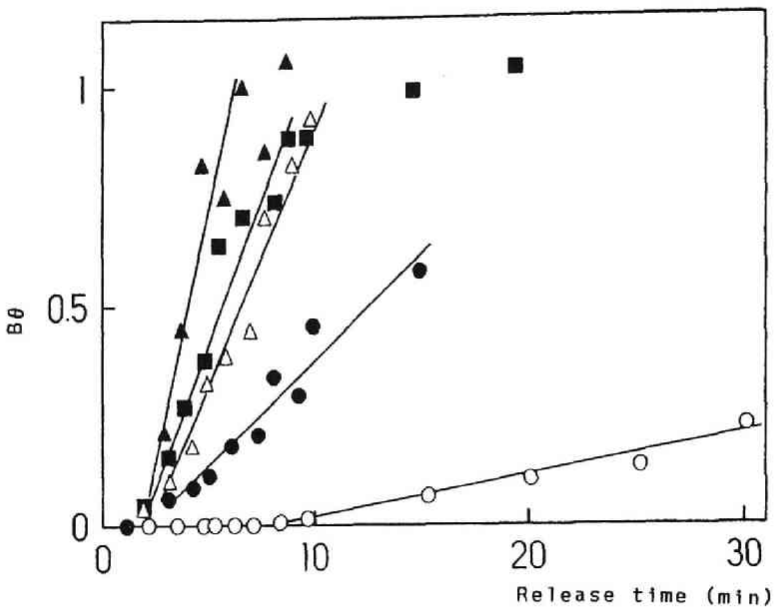

Figure 1-5. Higuchi plot corresponding to the result in figure 1-2. Encapsulation temperature: ○, 285K; ●, 286K; ■, 288K; △, 290K; ▲, 292K. See Equation (1-1) to (1-3) for an explanation of Bθ.

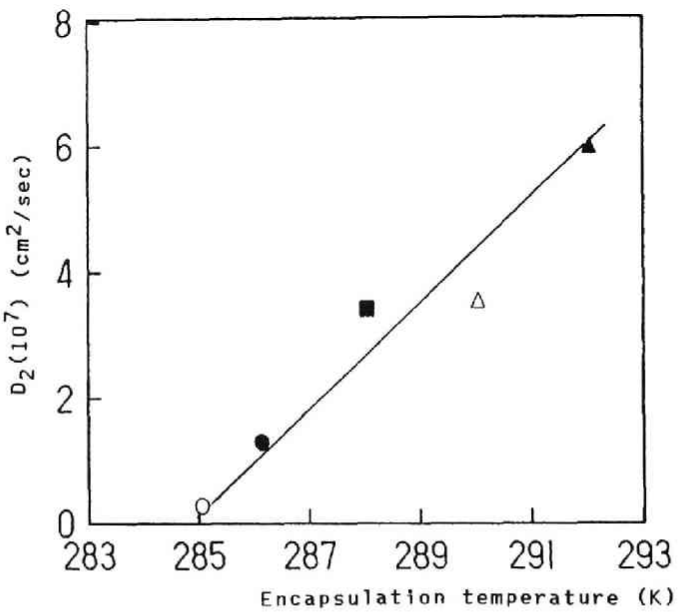

Figure 1-6. Correlation between effective diffusion coefficient and encapsulation temperature. Symbols are the same as figure 1-2 and 1-5.

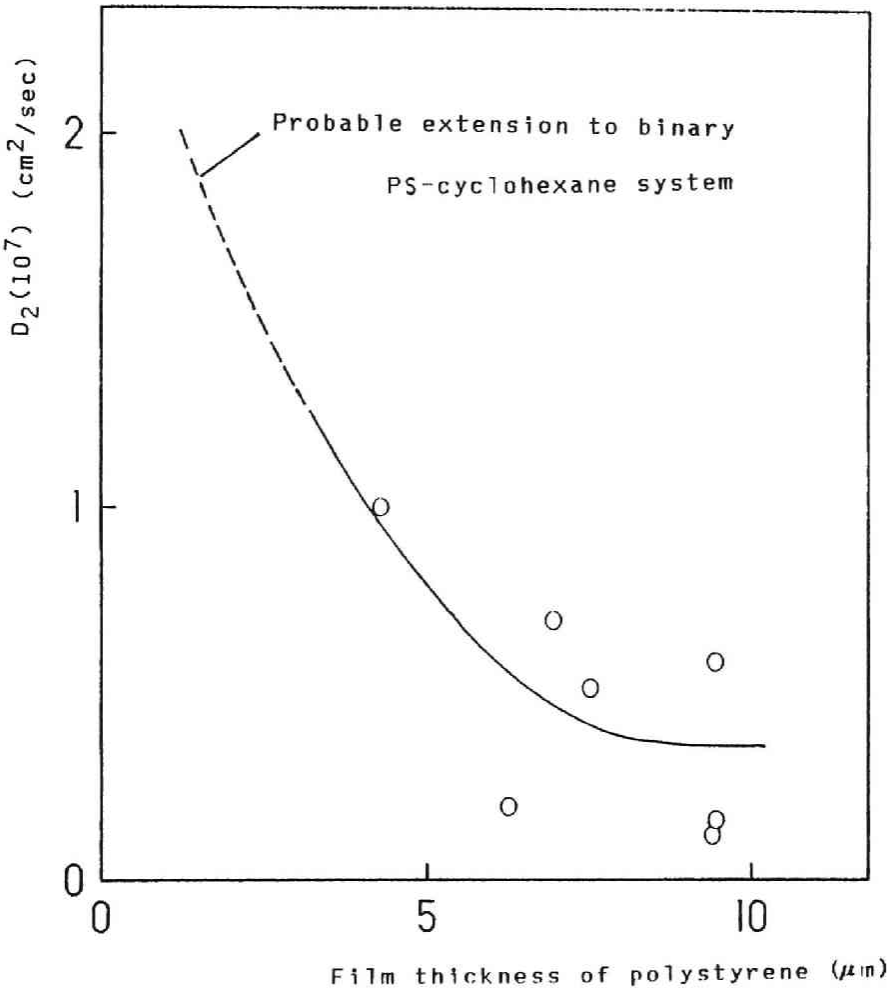

Figure 1-7. Correlation between effective diffusion coefficient and film thickness of polystyrene.

measurements suggest that the thickness and structure of PS film control the release behavior even if there exit considerable layer of talcum shell.

Conclusion

The release behaviors of ASS encapsulated by PS-cyclohexane binary system and PS-cyclohexane-n-hexane ternary system were investigated. Higuchi model revealed adequate to evaluate outcomes of release profile, and value of effective diffusion coefficient was in the range between 10^{-7} to $10^{-8}cm^2/sec$, depending on the wall thickness of microcapsules. Control of the wall thickness was well performed by adjusting the encapsulation temperature in the binary system and more effectively the amount of n-hexane added and encapsulation temperature in the ternary system.

References

1) J.R.Nixon and S.E.Walker, J. Pharm. Pharmacol., 23, 147 (1971)

2) P.L.Madan, J. Pharm. Sci., 70, 430 (1981)

3) H.Takenaka, Y.Kawashima and S.Y.Lin, Chem. Pharm. Bull. 27, 3054 (1979)

4) T.Higuchi, J. Pharm. Sci., 50, 874 (1961)

5) T.Higuchi, J. Pharm. Sci., 52, 1145 (1963)

6) R.Senjkovic and I.Jalsenjak, J. Pharm. Pharmcol. 33, 279 (1981)

7) R.Senjkovic and I.Jalsenjak, Pharm. Acta Helv. 57, 16 (1982)

8) S.Omi, Seiyaku Kojo, 4, 19 (1984)

Chapter 2

Controlled release of water-soluble substances from microcapsules prepared by spray drying method

Abstract

Controlled release of encapsulated nicotinic acid prepared by spray drying method was investigated. To evaluate quickly the contribution of several operational conditions to the release rate, the release behavior was characterized by the half life of the drug release, T_{50}. Capacity coefficient model and Higuchi model were used to explain this release profile. Higuchi model was effective to correlate the release behavior up to 80 percent release. As the amount of n-paraffin increased in the wall material, compared with other operational conditions, T_{50} became drastically longer due to the enhanced agglomeration and its water-repellent nature.

Introduction

Microencapsulation by the spray drying method using nonaqueous solution was reported in some patents[1-3], however the approach to quantifying drug release from the capsules have been not developed. In Chapter 2 of Part 1, microcapsule of the water soluble core substance, nicotinic acid crystal, was prepared using a spray drying tower equipped with a two-fluid nozzle.

In this Chapter, the effects of the operational conditions such as nozzle diameter, gas flow rate of the nozzle, drying temperature, composition and weight of wall material on the release behavior is studied, and an appropriate release model is offered[4].

Experimental

All reagents and analytical procedures are given in Chapter 2 of Part 1.

Apparatus for the measurement of release profile was same as that in Chapter 1. The concentration of nicotinic acid released in water was determined by a UV spectorophotometer (=261nm).

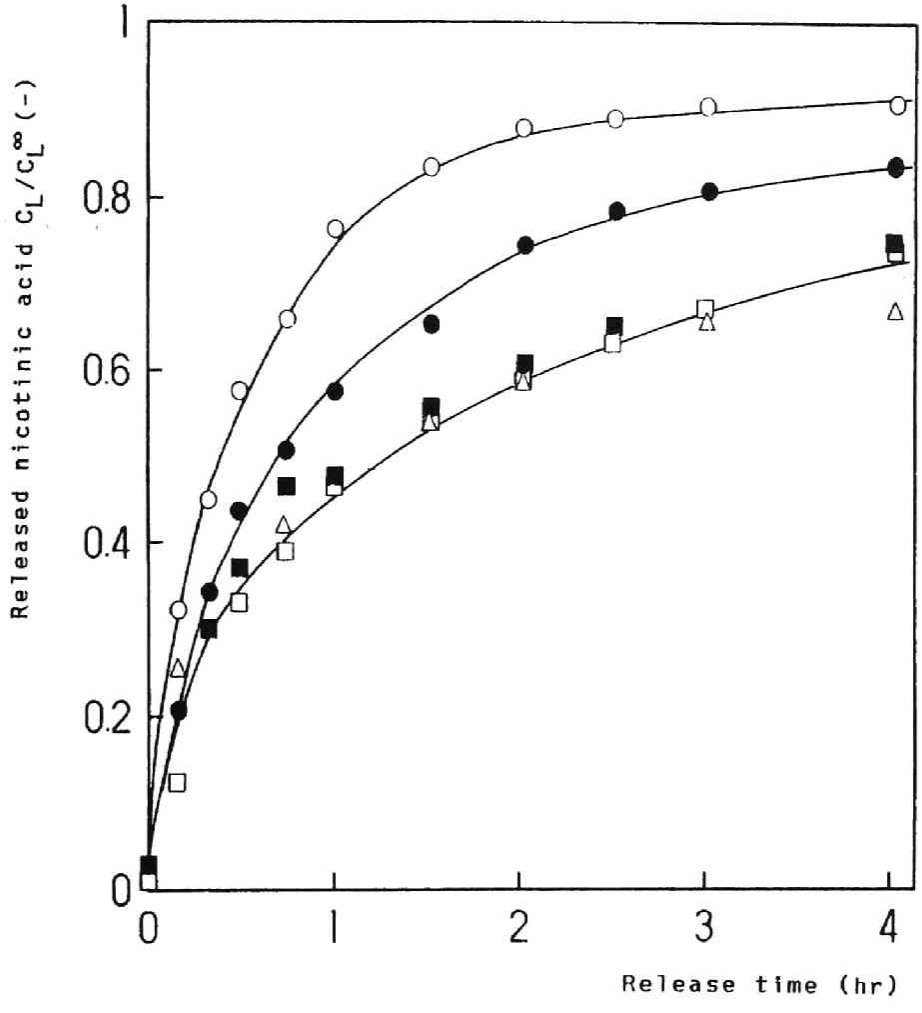

Figure 2-1. Release profile of encapsulated nicotinic acid. Effect of gas flow rate: ○, 13.0l/min; ●, 17.5l/min; □, 20.0l/min; ■, 25.6l/min; △, 30.8l/min. 0.5g of microcapsules were used in 1l water. Measured at 293K.

Results and discussion

Release profiles

A typical example of the release profile was shown in Figure 2-1 when gas flow rate of the two-fluid nozzle was changed. Microcapsules were allowed floating on the surface, and water in the vessel was well-stirred to assure the uniform drug concentration at any instant. Effectiveness of microencapsulation is quite obvious if one notices that untreated nicotinic acid dissolved completely within 5 min.

Half life of the release[5], T_{50}, defined as the time when a half of the encapsulated drug is released, was shown in Figure 2-2, the operational conditions being changed one after another. T_{50} is in fact a most quantitative parameter to evaluate the rate of release when no suitable mass-transfer model is found. As shown in Figure 2-2(a), increasing gas flow rate of the two-fluid nozzle delayed the drug release, but T_{50} remained unchanged as the gas flow rate was over 20l/min. Clear maximum in T_{50} was observed when temperature in the drying chamber or the nozzle diameter was changed as shown in Figure 2-2(b) and (c).

If one compares these tendencies with the calculated wall thickness in Table 2-1 in Part 1, it may be said that the increase of T_{50} dose not necessarily correspond to that of δ. This is due to the negligence of agglomeration between microcapsules or core crystals which will result in the thicker wall as sug-

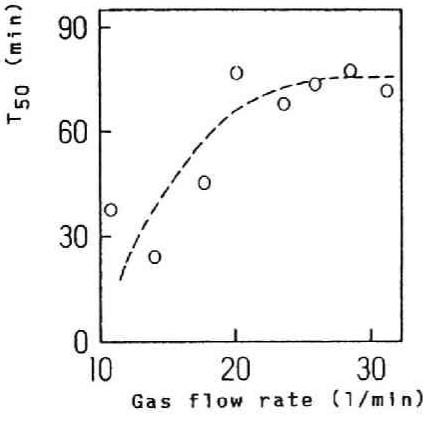

(a) Effect of gas flow rate

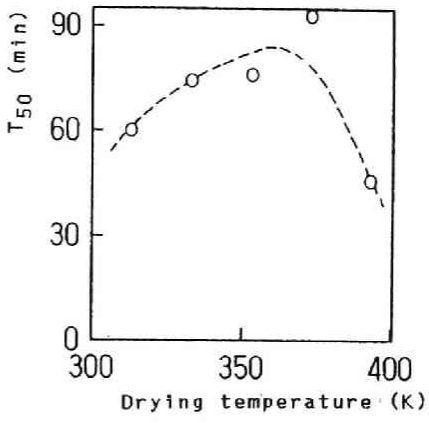

(b) Effect of drying temperature

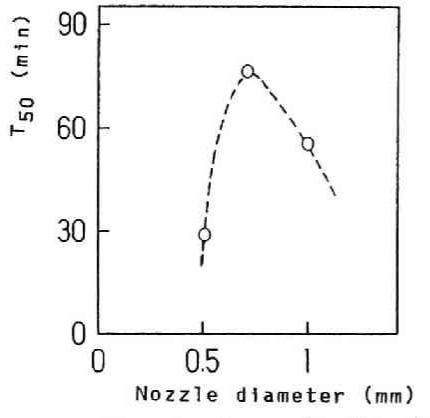

(c) Effect of nozzle diameter

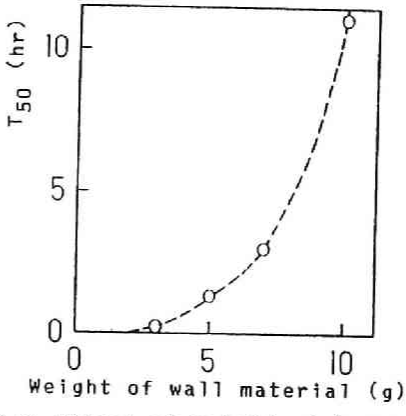

(d) Effect of weighi of beeswax white

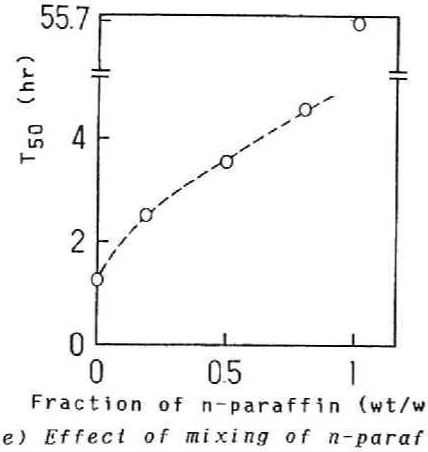

(e) Effect of mixing of n-paraffin

Figure 2-2. Effect of the operational condition on half time of release, T_{50}.

gested in Chapter 2 of Part 1. Since estimation of the wall thickness in the table was done without agglomerated capsules taken in account, the wall thickness may not be enough to correlate the release rate. On the other hand, suppose the value of really represents the average feature of microcapsules, it will mean that the structure of wall depends on the operational conditions employed. It is thought that though the latter in some extent affects the results shown in Figure 2-2(a),(b) and (c), the former will overwhelmingly prevail when the amount of beeswax white increased or mixed wall material was employed as shown in Figure 2-2(d) and (e).

Correlation of the release

The capacity coefficient, K_{La}, model[6] or the Higuchi model[7,8] can be considered to be suited for the correlation of the release profile and to obtain appropriate transport parameters. An integrated formula of K_{La} model can be written as follows.

$$\frac{C_L^{\infty} - C_L}{C_L^{\infty}} = \exp\left(-\frac{K_{La}}{\beta}\theta\right)$$

$$\beta = \frac{4\pi(a/10^4)^3 N}{3V} \qquad (2\text{-}1)$$

where C_L, C_L = concentration of drug released in water, and that at the equilibrium, a = radius of core, N = number of microcapsules added in water, and V = volume of water.

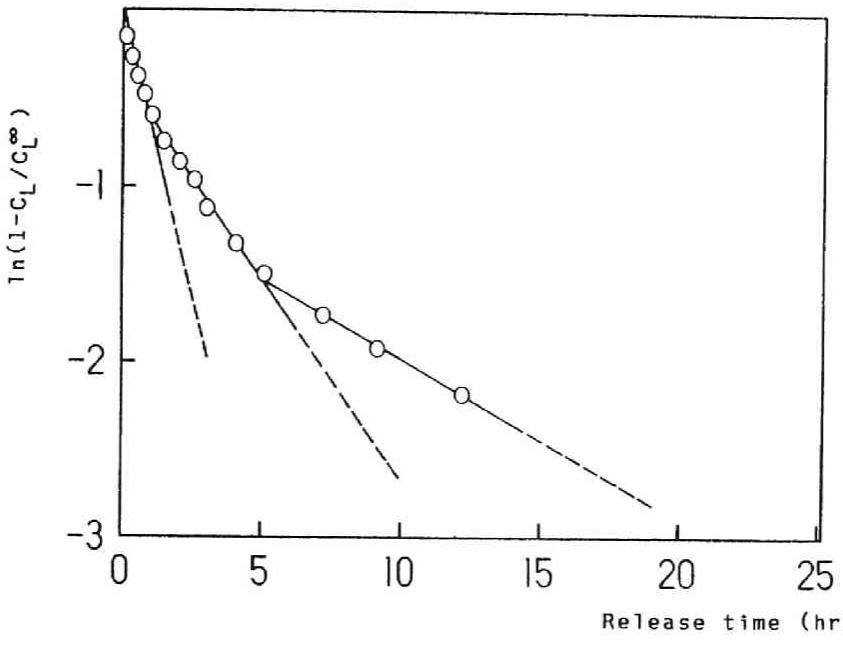

Figure 2-3. Correlation of drug release with the capacity coefficient model. 500mg of microcapsules were used in 1l water. Measured at 293K.

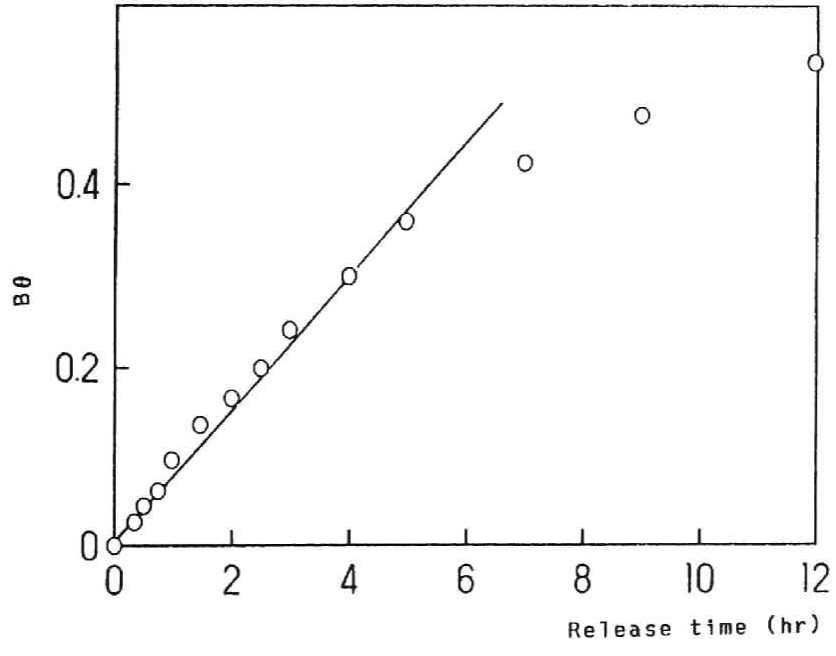

Figure 2-4. Correlation of drug release with the Higuchi model.

The basic equation from Higuchi model was expressed in Chapter 1.

Respective transport parameters for two models, K_{La} and D_2, effective diffusion coefficient of drug, are easily obtained from the slope of straight correlation line.

Examples of the correlation curves were shown in Figure 2-3 and Figure 2-4, respectively. It is evident that the Higuchi model is better than the other in this system as the latter correlation gave no conceivable straight line, while a good straight line was obtained up to 80 percent release. Though it was discussed in the preceding part that $\bar{d}_{pm}$ may not necessarily present the overall feature of microcapsules, D_2 can be estimated if b in Equation (1-1) in Chapter 1 is regarded as $\bar{d}_{pm}/2$. Obtained D_2 was given as a function of gas flow rate of the two-fluid nozzle and temperature in the drying chamber as shown in Figure 2-5.

Obviously, the profiles become those of reciprocal T_{50}. Order of D_2, 10^{-7} to $10^{-8}cm^2/sec$, was in good agreement with that of anhydrous sodium sulfate microcapsules coated with polystyrene in the preceding chapter the wall thickness of which was 5 to 10mm.

Higuchi model gave less encouraged results when it was applied to the correlation of the release profile obtained from the microcapsules with enhanced agglomeration.

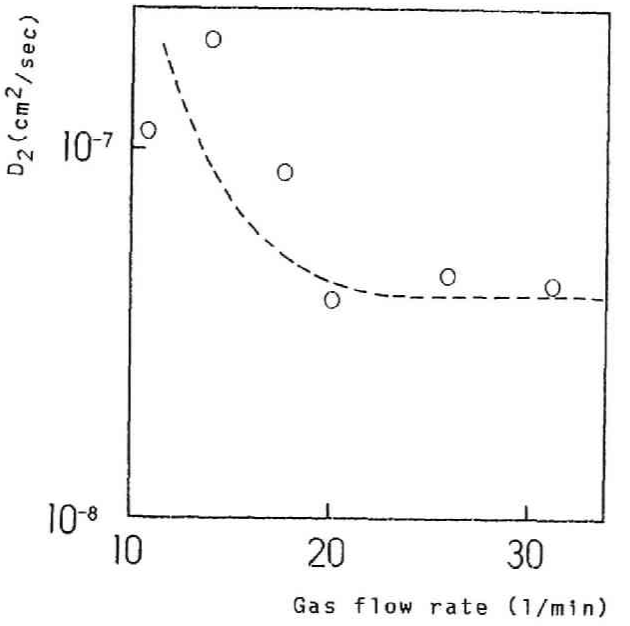

(a) Effect of gas flow rate

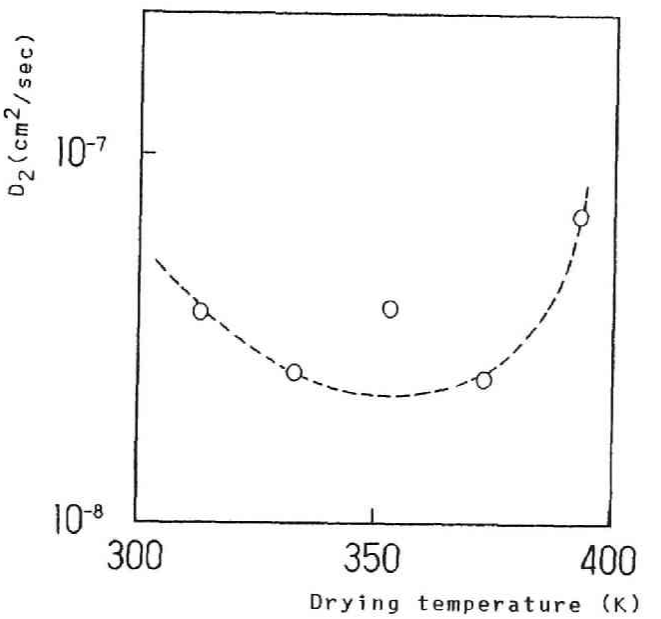

(b) Effect of drying temperature

Figure 2-5. Effective diffusion coefficient obtained from the Higuchi model.

Conclusion

Release behavior of nicotinic acid from microcapsule employing the spray drying method was investigated. In operational conditions, mixing of n-paraffin with beeswax white led to an enhanced agglomeration of microcapsules though apparently the release rate of nicotinic acid decreased drastically. Obviously increase of the wall material against the core favored the slower release, and promoted the agglomeration.

Higuchi model was more effective than the capacity coefficient model to simulate the release profile of nicotinic acid. Diffusion coefficient, 10^{-7} to $10^{-8}cm^2/sec$, was obtained if one assumes that all microcapsules are mono-nucleus.

References

1) M.J.Robinson and E.V.Svedres, U.S.Patent 2,805,977 (1957)

2) A.P.Granatek, B.C.Nunning, N.G.Athanas, R.L.Dana, E.S.Granatek and R.G.Daoust, U.S.Patent 3,549,746 (1970)

3) A.P.Granatek, B.C.Nunning, N.G.Athanas, R.L.Dana, E.S.Granatek and R.G.Daoust, U.S.Patent 3,626,056 (1971)

4) N.Umeki, K.Terauchi, M.Iso and S.Omi, Zairyo Gijutsu 5, 133 (1987)

5) R.W.Baker and H.K.Lonsdale, Controlled Release of Biologically Active Agents (A.C.Tranquary and R.E.Lacey, eds.), Plenum, New York, (1974)

6) S.Omi, Seiyaku Kojo, 4, 603 (1984)

Chapter 3

Controlled release of water-soluble drugs from microcapsules prepared by (W/O)/W multiple phase emulsion method

Abstract

Release behavior of Vitamin B_6 from microcapsules prepared by (W/O)/W multiple phase emulsion method was investigated. Release profile of Vitamin B_6 was successfully simulated by the proposed model using two masstransfer parameters, each of which separately accounts for the initial fast release and the much slower release in the later stage. These transport parameters were correlated with the type of wall materials and the drug content.

Introduction

In previous chapter, the release behaviors of encapsulated water-soluble crystals to the external environment were studied, and the proposed mathematical model could successfully simulate

the measured values[1,2].

In this chapter, microcapsules containing aqueous solution of Vitamin B_6 are prepared by (W/O)/W multiple phase emulsion method that was investigated in Chapter 3 of Part 1, and the release behaviors are measured. PS, copolymers of styrene with acrylates and SBR are employed as wall materials together with natural waxes, n-paraffin (n-P) or beeswax white (Bww), to change the mode of release and rate. Appropriate masstransfer model is proposed to simulate the release behavior. Finally attempts to correlate the model parameters with the type of wall material and the drug content are tried[3].

Experimental

Wall materials, Vitamin B_6 and others are given in Chapter 3 of Part 1. Apparatus for the measurement of release profile was same as that in Chapter 1.

Results and discussion

Model of controlled release

Observed release profiles were curve-fitting with the calculated values, and the transport parameters were determined. In

principle these parameters together with the model equations can be used for the designing of controlled release patterns of particular drugs. Two mathematical models, diffusion model (Model 1) and capacity coefficient model (Model 2), were proposed.

Diffusion model (Model 1)

Consider the diffusion of small molecules through a spherical shell. The Fickean diffusion equation[4] for spheres can be applied for drug release from microcapsules. The solution was given as follows,

$$\frac{C_L^{\infty} - C_L}{C_L^{\infty}} = \exp\left(- \frac{6 D_2}{b^2 - a^2} \theta \right) \qquad (3\text{-}1)$$

where a, b = inner and outer radius of microcapsule, C_L = drug concentration in water, and D_2 = effective diffusion coefficient in the wall. C_L^{∞} denotes the equilibrium concentration of the drug.

In actual experiments, small amount of the drug was always detected in the aqueous phase at time 0. This is due from the drugs left on the surface, or very fast burst effect[5] from some microcapsules with erratic wall. The theoretical solution was modified for practical correlations, introducing the concentration at time 0, C_{L0}.

$$\frac{C_L^{\infty} - C_L}{C_L^{\infty} - C_{L0}} = \exp\left(- \frac{6 D_2}{b^2 - a^2} \theta \right) \qquad (3\text{-}2)$$

Capacity coefficient model (Model 2)

As will be discussed in the later, the release profiles revealed very fast rate in the initial stage, and slowed down significantly in the later stage. Although being more consistent theoretically, Model 1 was hardly successful to simulate the release behaviors. Instead, Model 2 was developed for more practical purposes.

Suppose there exist two types of masstransfer resistances in microcapsules, one being assigned for the initial and faster release rate, and the other for the later and slower rate. Two capacity coefficients, K_{La2} and K_{La1}, were defined as the quantitative measure of the resistances. Schematic diagrams of the concentration profile were shown in Figure 3-1.

K_{La2} is assigned for the release from larger microcapsules with thinner wall, whilst K_{La1}, for smaller ones with thicker wall.

An alternative, probably more complex, model can be drawn; outer shell and inner core model. The outer shell corresponds to the resistance through the wall of microcapsule, whereas the inner core anticipates possible existence of inside structure. The reality to assume the latter structure can be recognized from cross-sectional photographs shown elsewhere[6].

1) Fast release in the initial stage

Considering that the concentration of drug in inner core remains unchanged, the solution of release in this initial stage

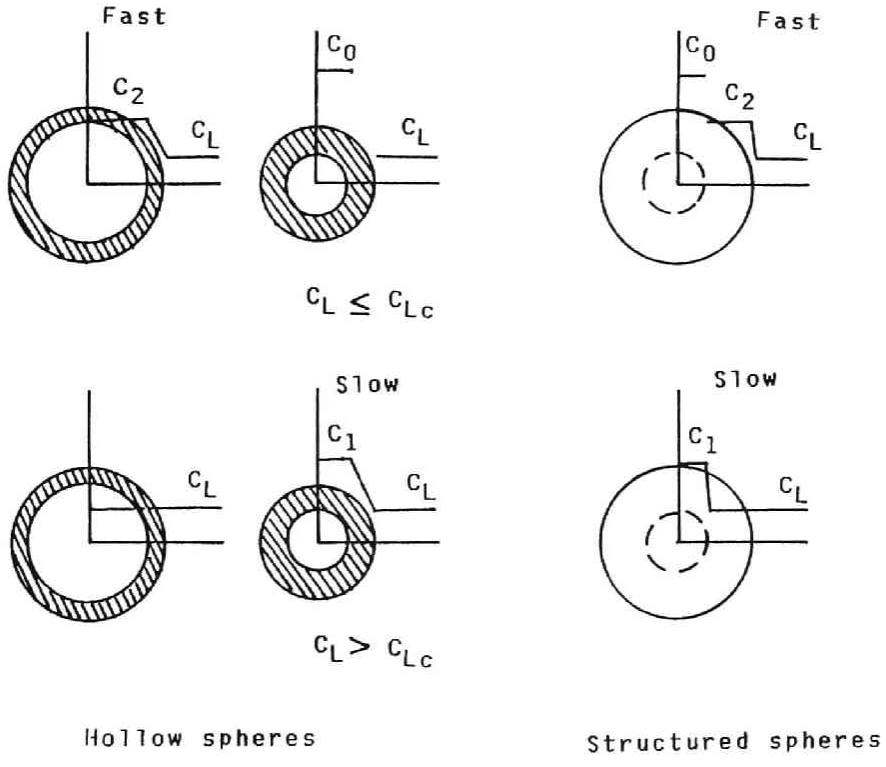

Figure 3-1. Schematic diagram of Model 2.

is easily obtained as follows.

$$\ln\left(\frac{C_{Lc}-C_{L0}}{C_{Lc}-C_{L}}\right) = K_{La2}\,\theta \qquad (3\text{-}3)$$

where C_L, C_{L0}, C_{Lc} = the concentrations of the drug in the aqueous phase at initial stage, at time zero and the critical value of the concentration at the finished time of initial stage.

2) Slow release in the later stage

When the release rate becomes slower, and the release from the inner core of microcapsules becomes dominant, no considerable difference exists between C_2 and C_L. The solution is obtained as follows.

$$\ln\left(\frac{C_L^{\infty}-C_{Lc}}{C_L^{\infty}-C_{L}}\right) = K_{La1}\left(\theta-\theta_c\right) \qquad (3\text{-}4)$$

where C_L^{∞} = the equilibrium concentration of the drug, and θ_c = the finished time of initial stage.

Eventual goal of the data analysis is to determine two transport parameters, K_{La2} and K_{La1}. Correlation with a few example will be shown later.

Release profile of Vitamin B_6

Several release profiles of Vitamin B_6 through the wax-based wall were shown in Figure 3-2, non-dimensional concentration, C_L/C_L^{∞}, being plotted against the elapsed time. As mentioned before, fast release up to the release time of 10hr preceded the

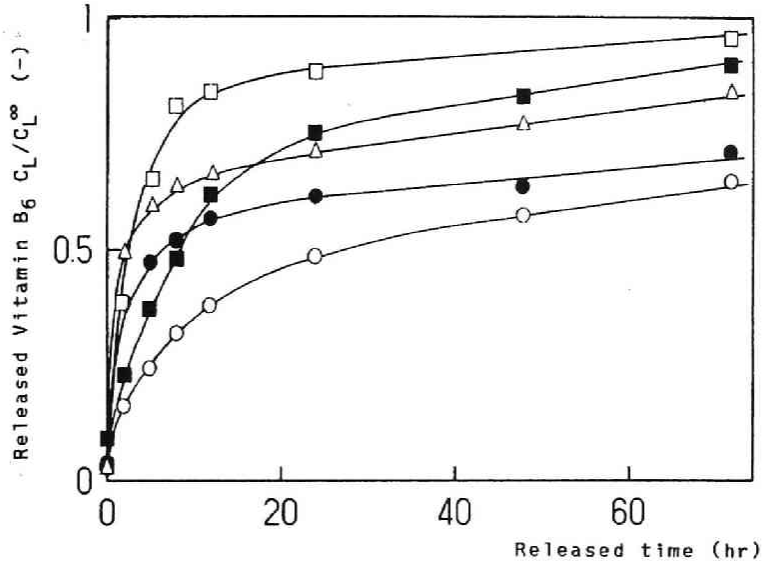

Figure 3-2. Release profile of Vitamin B_6 through the wax-based wall.

□, MC-403; ■, MC-107; ○, MC-602; ●, MC-606; △, MC-604. 1g of microcapsules were used in 1l water. Measured at 293K.

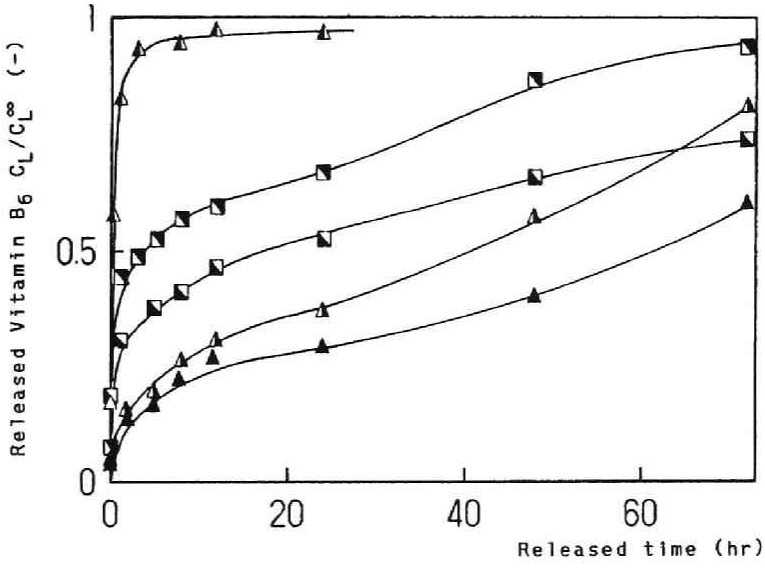

Figure 3-3. Release profile of Vitamin B_6 through the copolymer wall.

B-4(◪, MC-1003; ◪, MC-1043), B-5(◭, MC-1012; ◭, MC-1050; ◭, MC-1052). Experimental conditions were the same as above.

slower release in the later stage. As the wall thickness of these microcapsules were fairly thick (Table 3-2 in Part 1), and the inside structure was somewhat fibrous, the later release took quite a long time to reach the equilibrium of the release.

2) Release through the copolymer wall

Release profiles through copolymer walls were shown in Figure 3-3. Initial release rates were faster than those shown in Figure 3-2 because of the thinner wall thickness. Abnormal release profiles were repeatedly observed for MC-1043, 1050 and 1052, an acceleration of release during the later stage. This may be explained as the bursting of some microcapsules having thinner wall thickness due to the counter diffusion of water from the outside medium to the inside caused by the osmotic pressure. Note in Table 3-2 in Part 1 that all the microcapsules were prepared with the mixed solvent of chloroform-benzene. The viscosity of oil phase became lower by the presence of benzene which is a better solvent for styrene copolymers than chloroform.

The release profile of MC-1050 or 1052 will be desirable for the controlled and sustained release of drugs.

Simulation of release behavior

1) Correlations according to two models.

Take the release profile of MC-602 shown in Figure 3-2 as an example to test the validity of the two models.

If the diffusion model is adequate, then the plot according to Equation (3-1) will yield a straight line, and effective

Table 3-1. Parameters of drug release for Model 1 and Model 2.

MC No.	Model 1	Model 2				
	$D_2 \times 10^{18}$ (cm^2/sec)	K_{la2} (1/hr)	K_{la1} (1/hr)	θ_c (hr)	C_{lc} (mg/L)	ϕ_2
105 SBR/n-P	9.1	0.34	0.0087	9.2	14	0.42
106 SBR/n-P	10	0.40	0.018	8.4	20	0.57
107 SBR/n-P	8.0	0.35	0.021	8.3	18	0.50
201 SBR/n-P	11	0.27	0.026	10.0	80	0.57
403 SBR	13	0.36	0.023	7.5	11	0.79
404 SBR	7.2	0.70	0.025	5.8	34	0.48
602 SBR/n-P/Bww	5.0	0.41	0.01	6.3	15	0.28
604 SBR/n-P/Bww	34	0.81	0.012	6.2	30	0.61
606 SBR/n-P/Bww	25	0.81	0.0070	5.1	23	0.48
704 SBR/PS	2.1	0.81	0.0073	5.3	13	0.33
706 PS	1.3	0.36	0.0090	9.2	15	0.68
1003 B-4	1.4	1.6	0.014	2.4	40	0.34
1009 B-6	36	2.4	--	1.6	14.5	0.98
1012 B-5	22	1.6	0.038	2.7	40	0.93
1016 E-1	20	2.3	0.00071	2.5	19.8	0.91
1017 E-2	16	0.47	0.030	8.4	110	0.87
1022 B-4	4.9	0.76	0.034	4.2	100	0.56
1028 P(MMA-co-BA)	9.7	0.58	0.013	5.8	28	0.80
1030 P(MMA-co-EA)	14	0.54	0.045	7.4	47	0.86
1035 B-6	4.7	0.89	0.015	8.4	36.5	0.88
1041 B-6	11	0.79	0.022	5.5	23	0.74
1043 B-4	3.0	0.91	0.031	3.5	50	0.51
1045 B-6	1.9	0.49	0.017	6.7	18	0.45
1050 B-5	0.53	0.36	0.0099	6.0	7	0.19
1052 B-5	0.68	2.1	0.020	2.1	8	0.16
1055 B-7	32	5.4	0.0098	1.1	45.5	0.96

diffusion coefficient can be calculated from the slope. Natural logarithm of the lefthanded term was plotted against the elapsed time in Figure 3-4. Linearity of the plot held only for the first few points, anticipating that more dominant resistance prevailed in the later stage. Calculated value of the diffusion coefficient was $5.0(10^{-9})cm^2/sec$.

On the other hand, one has to assume the critical values of C_L and release time beforehand to correlate the release profile based on Model 2. This was normally done using the plot shown in Figure 3-4. It was assumed that the first point deviating from the straight line gave C_{Lc} and θ_c in Equations (3-3) and (3-4).

Two plots according to Model 2 were shown in Figure 3-5, indicating excellent agreements. Two transport parameters, K_{La2} and K_{La1}, were easily determined from the slope of respective lines. In some cases readjustment of the critical values improved the fitness of correlation. All the parameters estimated by these correlations were listed in Table 3-1. ϕ_2 is defined as the volume fraction of microcapsules responsible for the fast release, and can be calculated as follows,

$$\phi_2 = \frac{V_2}{V_1 + V_2} = \frac{C_{Lc} - C_{L0}}{\beta C_0} = \frac{C_{Lc} - C_{L0}}{C_L^{\infty} - C_{L0}} \qquad (3\text{-}5)$$

Simulation curves of the release profile of MC-602 was shown in Figure 3-6 to demonstrate the preference of Model 2.

Correlations between transport parameters and drug content

Several experiments were done to estimate the transport

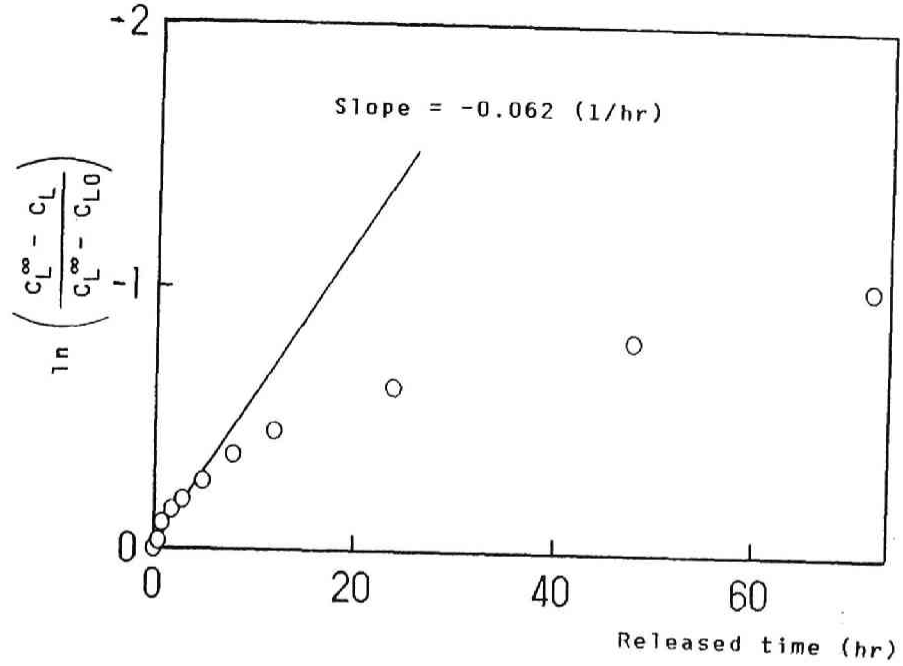

Figure 3-4. Correlation (MC-602) according to Model 1.

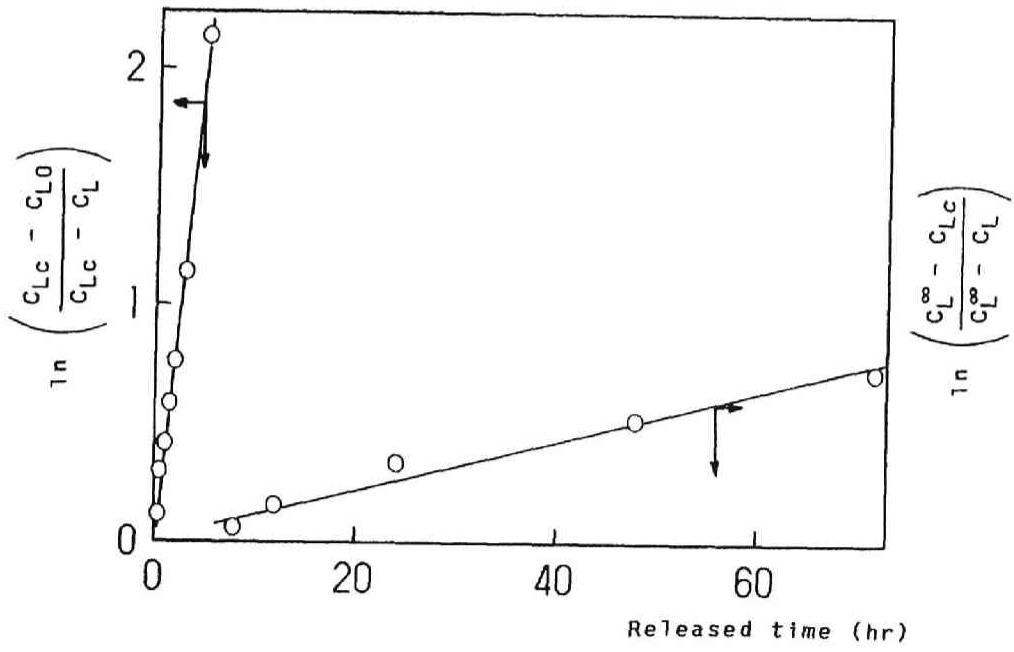

Figure 3-5. Correlation (MC-602) according to Model 2.

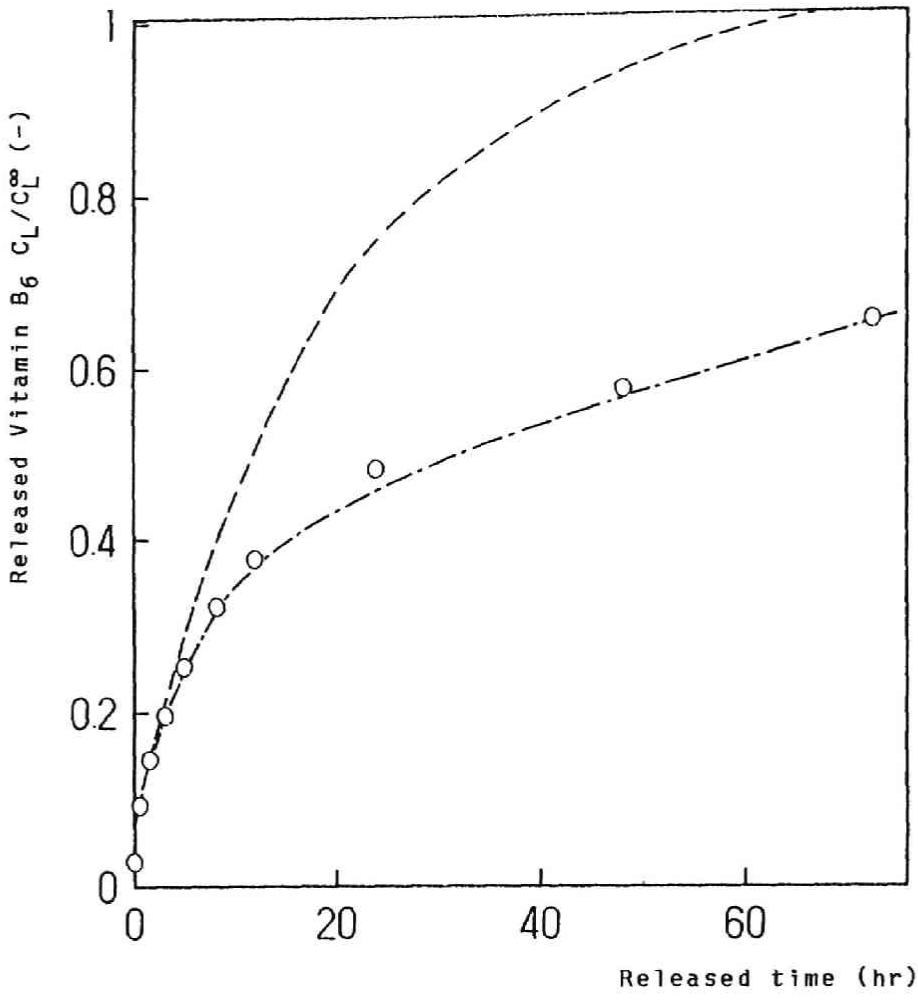

Figure 3-6. Comparisons between two models and observed values (MC-602).
○, observed value; ----, calculated curve by Model 1; -·-·-, calculated curve by Model 2.

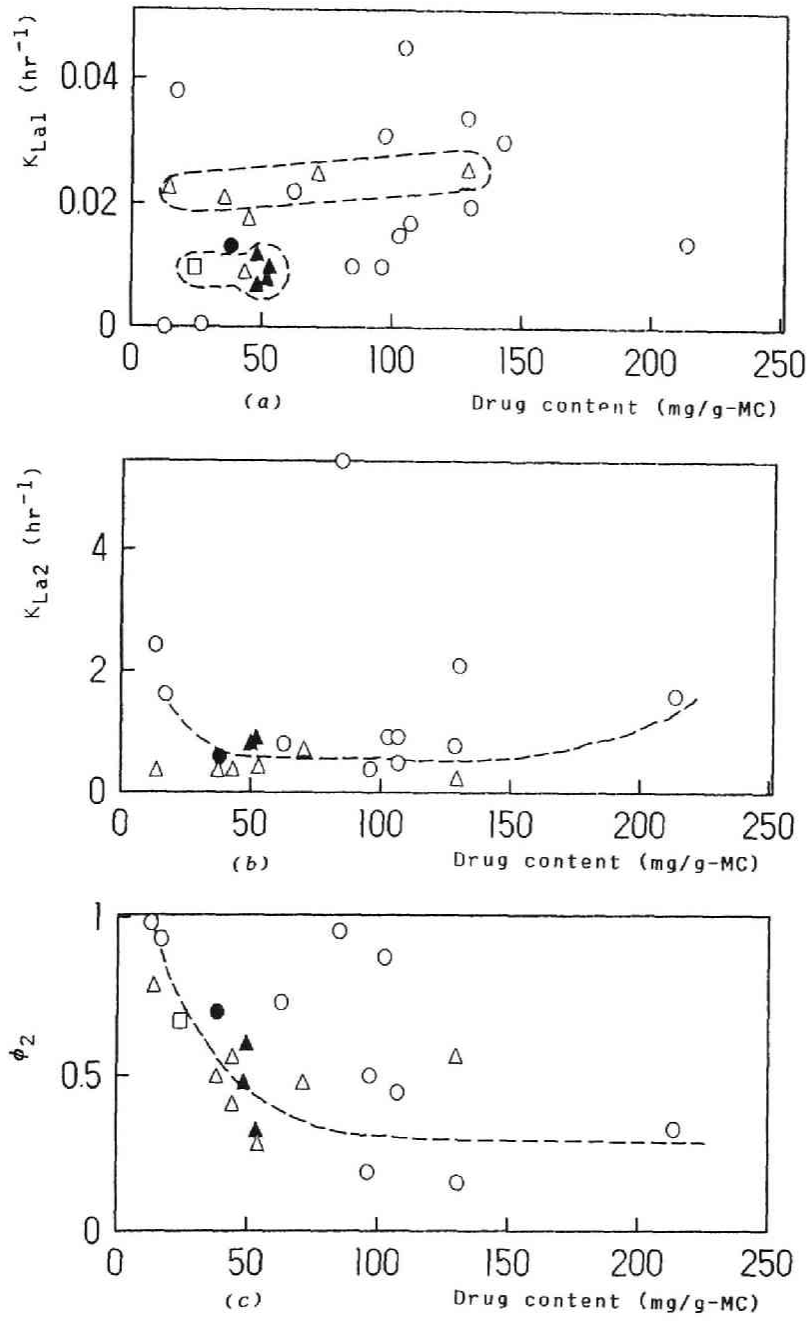

Figure 3-7. Correlations of transport parameters of Model 2 (K_{La1}, K_{La2}, ϕ_2) with drug content in microcapsules. Effect of wall materials (see Table 3-2 in Part 1): △, SBR/n-P or SBR; ▲, SBR/n-P/Bww or SBR/PS; □, PS; ○, B series; ●, P(MMA-co-BA).

parameters of each lot of microcapsules, K_{La2}, K_{La1} and ϕ_2, from the correlation curves and equations. Rather unexpectedly correlations against the drug content yielded most interrelative results as shown in Figure 3-7. Correlation are fairly scattered, in particular K_{La1}, however, classification with wall material will give some clues. For example note encircled groups in Figure 3-7(a). Microcapsules with SBR/n-P/Bww wall have almost constant K_{La1} as well as those with SBR/PS. Those prepared with ST-n-butyl acrylate copolymers (B series) show no specific tendency.

Majority of the K_{La2} data remained constant against the drug content (Figure 3-7(b)), whereas the volume fraction decreased gradually with increasing the drug content and converged to constant level (Figure 3-7(c)). However, the transition point, approximately from 60 to 90mg/g-MC, was obscured due to the scattering data of ST-n-butyl acrylate copolymers.

Conclusion

A particular masstransfer model was proposed to simulate the release profiles of Vitamin B_6. Two capacity coefficients each of which controls the initial (fast) and later (slow) release were easily calculated from the correlation of data. These transport parameters were correlated with the drug content of microcapsules.

References

1) M.Iso, T.Kando and S.Omi, J. Microencapsulation, 2, 275 (1985)

2) N.Umeki, K.Terauchi, M.Iso and S.Omi, Zairyo Gijutsu, 5, 133 (1987)

3) S.Omi, T.Furuno, A.Ikeda and M.Iso, "Drug Targeting and Delivery" ed. A.T.Florence and G.Gregoriadis., in press

4) J.Crank, The mathematics of Diffusion, 2nd ed., Clarendon Press, Oxford, (1975)

5) P.L.Madan, J. Pharm. Sci., 70, 430 (1981)

6) T.Furuno, A.Ikeda, M.Iso, S.Omi and H.Yokota, Zairyo Gijutsu, 5, 141 (1987)

Chapter 4

Controlled release of pheromone-analog from microcapsules prepared by complex coacervation and (S/W)/O multiple phase suspension method

Abstract

Microcapsules containing pheromone-analog, 2-ethylhexyl acetate (EHA), as core substances were prepared by gelatin/gum arabic complex coacervation and (S/W)/O multiple phase suspension method, and the release behaviors into atmosphere were measured. In the case of microcapsules prepared by complex coacervation method, the release period of EHA through the gelatin wall turned out to be too short, only a week at most. On the contrary, though initial release rate of EHA from microcapsules prepared by (S/W)/O multiple phase suspension method was still too high , 60 percent of encapsulated EHA performed a sustained release over six months after imbibed moisture completely evaporated. Two-step mechanism of masstransfer was proposed and the related parameters

in terms of the capacity coefficient and effective diffusion coefficient were estimated.

Introduction

Since pheromone are expensive, effective, volatile, and in some cases labile compounds, controlled release is essential for efficient, economical use in obtaining a sufficient, long duration. For application to an extensive area, hand-applied dispensers[1,2] that is commonly used for monitoring and detection of insect populations. Microcapsules can be sprayed with conventional equipment, and aerial broadcast application is feasible[3].

In Chapter 4 of Part 1, microcapsules containing pheromone and its analog were prepared by gelatin/gum arabic complex coacervation and (S/W)/O multiple suspension method, and the structure of capsules and drug content were investigated. In this chapter, a pheromone-analog, EHA is encapsulated, and the release profile as well as the rate is observed to evaluate effectiveness of the encapsulation method. Some chemical engineering aspects accompanies with the sustained release, in particular, the modeling of masstransfer process and the estimation of related parameters are also discussed[4].

Experimental

All reagents were given in Chapter 4 of Part 1. A schematic diagram of experimental system to measure the release rate of EHA was shown in Figure 4-1. [2] is a particular glass tube, 2.1cm diameter and 17.5cm length. Microcapsules of known weight were extended on a filter paper placed in the tube. Released EHA was mixed with continuous flow of nitrogen, the flow rate being 1ml/sec at room temperature, and was introduced to the [4] gas sampler with a certain time interval for gas chromatograph (GC-163, Hitachi Co. Ltd.) with a FID. Analytical conditions were same as those in Chapter 4 of Part 1. The release rate of EHA was directly obtained from this procedure.

Results and discussion

Release profile of EHA from microcapsules prepared by complex coacervation method (MC-107)

A typical release profile together with the release rate was shown in Figure 4-2. As mentioned before, MC-107 was twice encapsulated, and has maximum wall thickness of 3.0μm. The fraction of EHA was plotted against the elapsed time, and the release rate also plotted in the figure revealed very fast at the early stage. Unexpectedly, in fact disappointedly, 50 percent of total EHA was

released within three days.

Also the release profile of EHA from uncapsulated wax particles was shown in the figure (broken line). Comparison between two curves of the release rate reflected the ineffectiveness of crosslinked gelatin wall for sustained release. Though twice encapsulated, the wall only managed to decrease the maximum release rate to the half of that observed from the uncapsulated wax particles.

Release profiles from other microcapsules in Table 4-1 of Part 1 yielded more or less the same results; rapid initial release and exhaustion within a week, and being hardly capable to achieve the sustained release of months or more.

Release profile of EHA from microcapsules prepared (S/W)/O multiple suspension method

The result of long-run release experiment from microcapsule MC-201 was shown in Figure 4-3. First of all, it should be remained that the comparison with Figure 4-2 shows the time-scale in this figure changed from hour to day, a demonstration of really long-term release. The initial release rate was still high, the maximum rate being $38.3(10^{-3})$mg-EHA/g-MC/hr. However, after ten days elapsed, 60 percent of loaded EHA still remained. The release rate became almost constant, $1.67(10^{-3})$mg-EHA/g-MC/hr. This constant release continued on even after 36 days when the measurement was discontinued. Analysis of EHA revealed that

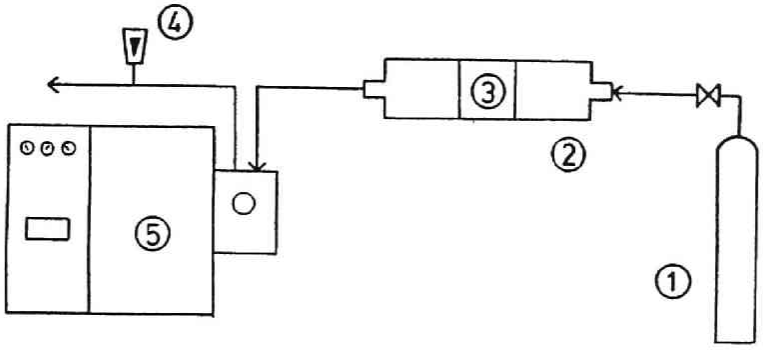

Figure 4-1. Schematic diagram of the system for release experiment.
Key: [1] N_2 cylinder, [2] sample chamber, [3] microcapsules, [4] flow meter, [5] gaschromatgraph.

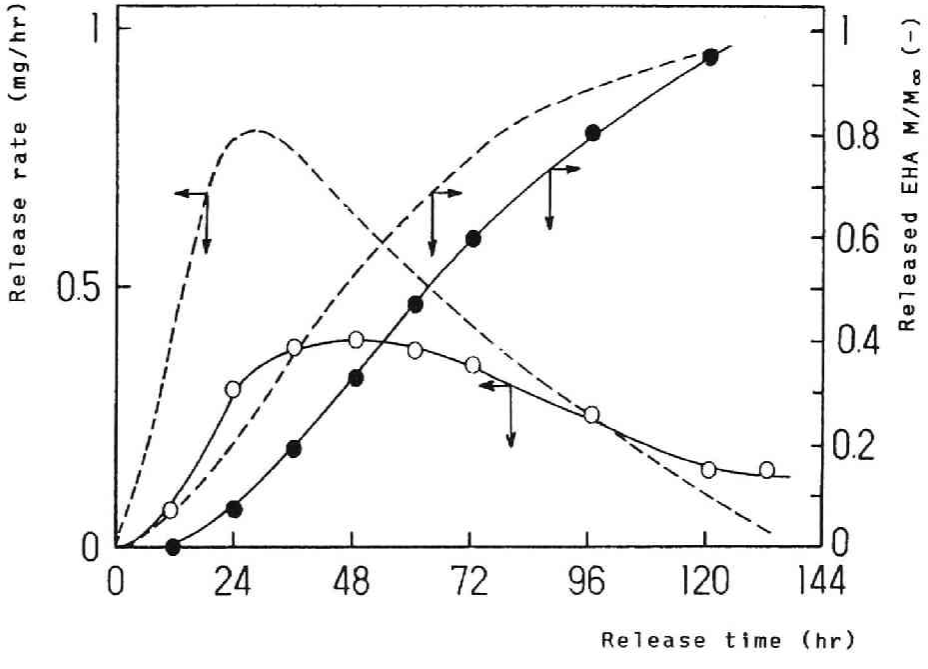

Figure 4-2. Release profile of EHA from MC-107, twice encapsulated by complex coacervation method. ●, released EHA; ○, release rate of EHA; ------, release profile of EHA from unencapsulated wax particles. 0.5g of microcapsules were used.

still 6.8mg of EHA remained in one gram of microcapsules. Supposing that the release continued with the above rate, time-spun of full release will be calculated as 207 days, and 47.4 days for the halflife of release.

Generally higher release rate was observed during daytime than nighttime due to the higher temperature which resulted in higher vapor pressure of EHA as well as the more loose conformation of polymer networks. For example, the vapor pressure of EHA at 293K was reported as 39.8Pa whereas it was 19.0Pa at 283K, roughly a two-fold difference.

The initial fast release is mainly due from the quite high moisture content in microcapsules which swells the gelatin network, and enhances the transport of EHA through the wall. Considerable amount of EHA may have been wasted accompanied with the evaporation of water. Once the evaporation of water settled down, the gelatin networks were dried up, and the tight conformation of the chains prevented the free transport of EHA through the wall.

If one could achieve intensive elimination of the solvent (water in this case), the initial fast release will be suppressed so that the percentage of EHA spent for the latter release will be higher.

Though not shown in detail, when MC-202 was employed, maximum release rate of EHA was measured as 0.1mg-EHA/g-MC/hr, and after ten days reached the constant release mode with the release rate of $1.67(10^{-3})$mg-EHA/g-MC/hr, a coincidence with the result

of MC-201. The total time-spun of release was estimated as 107 days, and the halflife of release as 4 days. As mentioned before, the higher temperature adopted for the preparation of the secondary suspension provided inefficient encapsulation, yielding microcapsules with less EHA content and smaller size.

Masstransfer model and estimation of parameters

A simple two-stage masstransfer model was considered to estimate the values of transport parameters such as the capacity coefficient and diffusion coefficient. As roughly sketched in Figure 4-4, it was assumed that two masstransfer resistances dominate for the transport process of EHA; one is located in the wax particles and the other through the gelatin wall.

If there are no particular adsorption or other accumulation of EHA in gelatin wall, then the release rate for each step can be equated as follows.

$$-r = K_{La1}(C_s - C_1) = K_{La2}(C_1 - C_2) = K_{La}C_s \qquad (4\text{-}1)$$

where, $-r$ = release rate of EHA, K_{La1}, K_{La2}, K_{La} = capacity coefficient for wax particle, gelatin wall, and over all transport, respectively. C_j = concentration of EHA for the location assigned in Figure 4-4. C denotes the concentration in the atmosphere, and can be regarded as 0.

K_{La} can be related to K_{La1} and K_{La2} as follows.

$$\frac{1}{K_{La}} = \frac{1}{K_{La1}} + \frac{1}{K_{La2}} \qquad (4\text{-}2)$$

For the case of masstransfer from sphere, K_{La} is related as a function of the radius of sphere and the diffusion coefficient[5]. Basically non-steady state, Fickian diffusion equation was solved analytically to yield an infinite expansion series of the concentration-time relationship. Further procedures of approximation and application to the analogous masstransfer process as discussed here was given elsewhere[6].

Applying this theory for K_{La1} and K_{La2}, we obtain the following relationships.

$$K_{La1} = \frac{\pi^2 D_1}{a^2} \quad , \quad K_{La2} = \frac{\pi^2 D_2}{b^2} \qquad (4\text{-}3)$$

where, D_1, D_2 = effective diffusion coefficient of wax particle and gelatin wall. a, b = average radius of wax particles and gelatin microcapsules, respectively.

KLa1 was estimated using the release rate of EHA from uncapsulated wax particles shown in Figure 4-2 as broken line. Though K_{La1} remained by no means constant with elapsed time, the estimation was done using the point value at M/M_∞ (fraction of EHA released) = 0.24, where the maximum release rate was attained. The release rate was estimated as 1.6mg-EHA/g-wax particle/hr. Since 76 percent of impregnated EHA (78.1mg-EHA/g-wax particle, see Table 4-1 in Part 1.) still remains in uncapsulated particle, K_{La1} is calculated as follows.

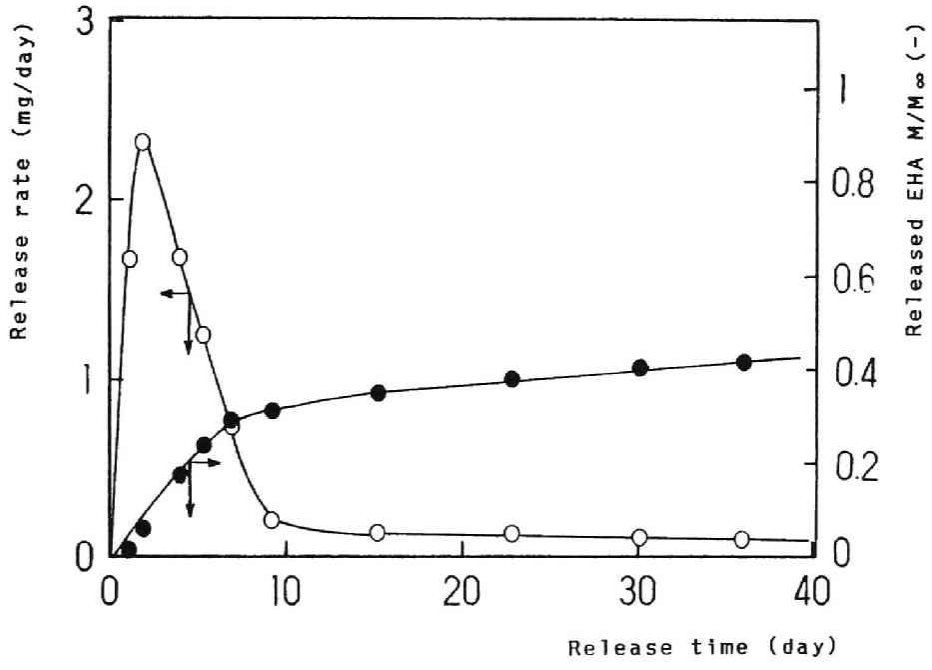

Figure 4-3. Release profile of EHA from MC-201 prepared by (S/W)/O multiple phase suspension method. ●, released EHA; ○, release rate of EHA. 2.5g of microcapsules were used.

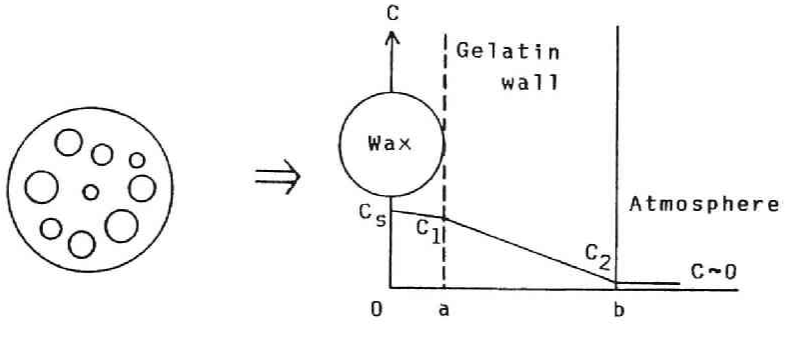

Figure 4-4. Schematic diagram of two-stage transport process.

$$K_{La1} = \frac{1.6/3600}{(78.1)(0.76)} = 7.5(10^{-6})\ sec^{-1} \qquad (4\text{-}4)$$

Using the average diameter of wax particles also shown in Table 4-1 in Part 1, the effective diffusion coefficient in wax was estimated as follows.

$$D_1 = \frac{K_{La1}a^2}{\pi^2} = \frac{(7.5(10^{-6}))(2.33(10^{-2})/2)^2}{(3.14)^2} = 1.0(10^{-10})\ cm^2/sec \qquad (4\text{-}5)$$

On the other hand, K_{La} was estimated using the constant rate of MC 201 observed after 10 days (see Figure 4-3.), the release rate was $1.67(10^{-3})$mg-EHA/g-MC/hr. Since 60 percent of encapsulated EHA (14.1mg-EHA/g-MC, see Table 4-2 in Part 1.) still remained at the time, KLa was estimated as follows.

$$K_{La} = \frac{-r}{C_s} = \frac{1.67(10^{-3})/3600}{(14.1)(0.6)} = 5.5(10^{-8})sec^{-1} \qquad (4\text{-}6)$$

Comparison between the order of K_{La} and K_{La1} flatly revealed that $K_{La2} << K_{La1}$, or $K_{La} = K_{La2}$. The effective diffusion coefficient in gelatin wall was estimated using the dry diameter, $\bar{d}_{pm}$ of MC 201, shown in Table 4-2 as follows.

$$D_2 = \frac{K_{La2}b^2}{\pi^2} = \frac{(5.5(10^{-8}))(0.119/2)^2}{(3.14)^2} = 2.0(10^{-11})\ cm^2/sec \qquad (4\text{-}7)$$

According to the correlation between log(D) and log(molecular weight of penetrant) given by Baker et al[7], the diffusion coefficient in PS is approximately $10^{-12}cm^2/sec$, whereas that of natural rubber is $10^{-7}cm^2/sec$. Comparison with these values revealed that the order of D_2 (crosslinked gelatin) is approximately twenty times higher than the value in PS, whereas D_1 (wax) is approximately two orders higher. On the other hand, D_1 and D_2 were a few orders lower than the value in natural rubber.

Conclusion

The wax particles impregnated with a pheromone-analog, EHA, and encapsulated with gelatin-gum arabic complex coacervation method proved to be insufficient for the sustained release as long as six months, but they are capable for the release of shorter time-spun.

The microcapsules prepared by (S/W)/O multiple suspension method fulfilled the long-term release, though 40 percent of EHA was released in the initial 10 days due the high moisture content. After the complete evaporation of moisture , the release continued with almost constant rate.

As the EHA transfer model yielded the diffusion coefficient in crosslinked gelatin network to be slightly higher order than that in PS, it may be encouraged to replace the present aqueous

suspension with organic recipe provided that an appropriate solvent, good solvent for wall polymer but poor one for the wax, is found. Since it is in general easier to eliminate organic solvent than water, the initial fast release of EHA will be expected to be minimized.

References

1) R.S.Kaae, H.H.Shorey and L.K.Gaston, Science, 179, 487, (1973)

2) T.W.Brooks, Controlled Release Technologies: Methods, Theory and Applications, Vol. 2, CRC Press, Boca Raton, Fla. (1980)

3) S.M.Herbig and K.L.Smith, Proceeding of ICOM '90, August 20, Chicago, USA, Vol. 1, 592 (1990)

4) S.Omi, N.Umeki, H.Mohri and M.Iso, J. Microencapsulation, 8, 465 (1991)

5) R.E.Treybal, Liquid Extraction, Second Edition, McGraw Hill Book Company, INC., p.186 (1963)

6) S.Omi, H.Endo, S.Shibata, M.Iso and H.Kubota, Contemporary Topics in Polymer Science, (ed. W.B.Bailey and T.Tsuruta, Plenum Press, New York and London), 4, 909 (1984)

Part 3

Immobilization of Enzyme by Microcapsules

Chapter 1

Immobilization of enzyme by microencapsulation using (W/O)/W multiple phase emulsion method

Abstract

Microencapsulation of lipase (Pseudomonas fluorescens) was carried out using (W/O)/W multiple phase emulsion method. Polystyrene (PS) and Styrene-Butadiene Rubber (SBR) were utilized as wall materials either separately or in mixture. A particular composition of 2:1 PS/SBR yielded homogeneous and tough wall structure, resilient to the impact and tight confinement of enzyme macromolecules. The appearance and morphology of microcapsule produced were observed with a scanning microscope (SEM) and a transmission microscope (TEM), and its uniqueness of the wall structure was identified.

Introduction

Enzyme catalysis has been utilized with batch reactors, in which enzyme molecules, normally dissolved in the aqueous solution, contact with substrate molecules, and catalyze the reaction. The procedure is rather uneconomical because the spent catalysts are dumped after having being deactivated thermally and separated from the products, even though they still possess enough activity for repeat catalysis.

In order to realize the full advantage of the enzyme, various immobilization techniques have been investigated by which the enzyme is made insoluble in the medium while conserving its activity[1-4]. Microencapsulation by the multiple phase emulsion method has an advantage, being acceptable to a variety of enzymes due to the almost unlimited choice of wall materials. Vrancken et al.[5] patented a microencapsulation method in which an aqueous solution of core material was emulsified into a nonaqueous solution containing wall polymer, followed by emulsification into an external aqueous phase. Takenaka et al.[6] reported that enzymes have been encapsulated within polystyrene membrane by this method. Ogawa et al.[7] produced poly(lactide-glycolide) microcapsules including leuprolide acetate. However, microcapsules are essentially susceptible to mechanical deformation resulting in an eventual fracture because of the thin wall thickness, normally of only a few microns. Unless this disadvantage is countered, they

will not be able to be used in commercial-scale bioreactors, particularly not in those such as fluidized beds and packed column reactors.

In this chapter, one of the prime objectives is to find wall materials with favorable mechanical strength but which retain reasonable diffusion rates for smaller molecules through the wall[8].

Experimental

Reagents

Wall material. PS was prepared using suspension polymerization, for details see Chapter 1 in Part 1. SBR was the same one used in Chapter 3 of Part 1. Properties of the polymer are shown in Table 1-1.

Enzyme. Lipase P (Pseudomonas fluorescences, Amano Pharmaceutical Co. Ltd.), capable of hydrolyzing and position in glycerides, was chosen as the enzyme to be immobilized. It was dissolved in the buffer solution and filtered to remove precipitates prior to use.

Substrate. Triacetin, Triglyceride of acetic acid, was used as a substrate, which releases three moles of acetic acid after undergoing the hydrolysis.

Buffer solution 0.33M solutions of potassium phosphate, monobas-

ic and disodium hydrogen phosphate were mixed, the mixing ratio being adjusted to obtain a solution of the desired pH value.

Protective colloid Polyvinyl alcohol (PVA, $\bar{P}_n$=500, 97 percent mole hydrolyzed, Wako Pure Industries) was used.

Inorganic reagent Analytical grades of sodium carbonate, copper sulphate($5H_2O$), Rochelle salt ($KN_aC_4H_4O_6 \cdot 4H_2O$), and sodium hydroxide were used as analytical reagents.

Microencapsulation

Microcapsules of immobilized enzyme were prepared using the (W/O)/W multiple phase emulsion method[9]. 10wt percent of PS and SBR, either independently or in mixed form, were dissolved in chloroform. In order to prepare the primary W/O emulsion, this solution was homogenized with the phosphate buffer solution (pH7) containing 6.7wt percent of lipase and 2.0wt percent of PVA for 2min under the agitation rate of 5000min^{-1}. The temperature was normally kept at 318K to adjust the viscosity of the emulsion.

Two flasks of different size and shape were used for the preparation of the secondary (W/O)/W emulsion and volatilization of chloroform. A round-bottomed, separable flask of 300ml capacity with four baffle plates was used for the smaller scale preparation. 250ml of buffer solution containing 1wt percent of PVA was supplied in the flask, and the temperature was controlled at 328K under the agitation rate of 250min^{-1}. 40ml of primary emulsion was poured in the flask, and the system was kept under a

slightly reduced pressure to remove chloroform. No damage was inflicted to the encapsulated enzyme under these conditions.

After chloroform was eliminated, the flask was cooled down to 328K, and the microcapsules were recovered by filtration. The leaked amount of the enzyme was measured by analyzing the amount of enzyme in the filtrate, and the efficiency of the immobilization was determined.

A flat-bottomed flask of 1 litre capacity was used for scaled-up productions after the quality of microcapsules was proven to be quite acceptable. The agitation rate was normally set at $350min^{-1}$ without any baffle plates. The proportion of the ingredients was kept the same as that employed in the smaller scale.

Analysis. The amount of the free enzyme was determined to evaluate the immobilization yield by the Lowry method[10]. Photometric analysis was carried out using a UV spectrophotometer at wavelengths of 500 and 750nm, depending on the concentration of enzyme.

The visual features of the surface of the wall, were observed by SEM. After the dried microcapsules were cracked under a stress in liquid nitrogen, the cross-section of the wall was investigated in detail. Therefore, the morphology of the cross-section in which the domains of butadiene in SBR could be stained with O_sO_4 was observed by TEM.

Results and Discussion

Structure of microcapsule

The conditions of preparation and the characteristics of microcapsules were shown in the Table 1-2.

A SEM photograph of microcapsule (MC-2007) prepared with the weight ratio 2:1 PS/SBR is shown in Photo. 1-1(a). This weight ratio was adopted for the experimental evidence that the microcapsule containing Vitamin B_6 solution was obtained with reasonable drug content and a smooth surface[9]. The microcapsules are spherical, the surface feature being quite smooth. Small holes of about 2μm in diameter spotted on the surface are not serious defects because none of these holes bore through the wall as shown in Photo. 1-2(a).

MC-2027 shown in Photo. 1-1(b) was prepared with no SBR in the wall. These capsules had a smooth surface, however, they were extremely fragile, and a number of capsules (approximately 30 percent) had broken in the filtration procedure soon after the preparation. This may be attributed to the brittleness of PS rather than to the thinner wall structure, a major disadvantage compensated only by the blending with SBR.

MC-2028 shown by Photo. 1-1(c) was prepared using SBR only as a wall material. As Chapter 3 in Part 1 showed, there were many holes on the surface, probably formed during the liberation of vaporized solvent. None of these holes, though much larger

Table 1-1. Polymers employed as wall material.

Wall material	Molecular weight		Dispersion index ($\bar{M}_w/\bar{M}_n$)
	Number average ($\bar{M}_n \times 10^{-4}$)	Weight average ($\bar{M}_w \times 10^{-4}$)	
SBR[1)]	7.4	10.74	1.45
PS-11	0.43	1.12	2.61
PS-12	0.32	1.02	3.19
PS-13		21.3	

1)*Solprene T-414*

Table 1-2. Preparation condition and characteristics of the microcapsules.

MC No.	Wall material		Scale	Solvent ($CHCl_3$)	Core material[1)] Lipase/PVA sol.	MC characterization		
	PS (g)	SBR (g)	(ml)	(g)	(g/ml)	Cont.[2)] (%)	$\bar{d}_{pm}$ (μm)	δ (μm)
2007	PS-11 2	SBR 1	250	27	0.5/10	54.0	141.0	14.3
2012	PS-11 10	SBR 5	1000	135	2/30	52.0	78.1	9.80
2019	PS-12 5	SBR 2.5	1000	67.5	2/30	31.0	106.0	3.54
2020	PS-12 15	SBR 7.5	1000	202.5	2/30	34.3	99.2	3.52
2021	PS-12 10	SBR 5	1000	135	2/30	34.0	74.1	5.67
2022	PS-12 10	SBR 5	1000	135	1/30	47.5	81.9	6.17
2023	PS-12 10	SBR 5	1000	135	3/30	47.0	74.9	4.00
2024	PS-13 10	SBR 5	1000	135	2/30	42.4	117.0	9.76
2025	PS-12 5	SBR 10	1000	135	2/30	32.7	99.9	7.19
2026	PS-12 7.5	SBR 7.5	1000	135	2/30	31.4	83.6	4.95
2027	PS-12 15	--	1000	135	2/30	40.8	42.2	--
2028	--	SBR 15	1000	135	2/30	34.5	186.0	28.5

1)*5 and 25 ml of the mixture were used for the smaller and larger scale, respectively.*

2)*Percentage of encapsulated lipase based on the feed.*

than those observed in 2:1 PS/SBR, bored through the entire wall.

The average diameter of microcapsules containing lipase solution becomes smaller as the content of PS in the wall increases.

Photo. 1-2(a) shows the more detail observation of the cross-section under magnification. The wall of microcapsule have the structure consisting of three layers in which the thickness of outer and inner layer are 1μm, respectively. A photograph the cross-section taken with a TEM is show in Photo. 1-2(b). In particular, staining of the residual double-bond in the butadiene unit of SBR chains revealed the unique morphology of the wall. Although the PS/SBR blend system has been regarded as fairly compatible, a separate layer of PS can be clearly observed at the inner and outer surface. A well-blended structure develops between the two layers, and this finely interwoven structure may play a major part in confining the high molecular weight lipase within the capsules, whilst smaller molecules of the substrates diffuse in and out through the wall.

On the basis of this results, subsequent experiments were mainly carried out using the microcapsule of the weight ratio 2:1 PS/SBR.

Reproducibility and activity of encapsulated enzyme

Percentage conversion of triacetin hydrolyzed by the catalysis of encapsulated lipase is shown in Figure 1-1. One gram of wet microcapsules were dispersed in 500ml of the buffer solution

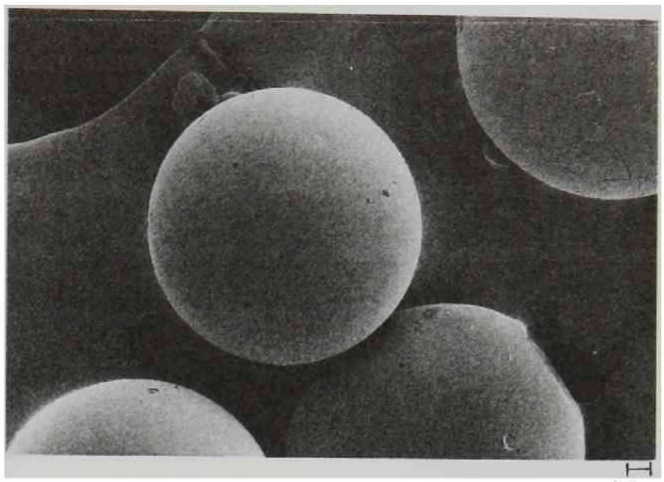

(a)2:1 PS/SBR microcapsule (MC-2021) 10μm

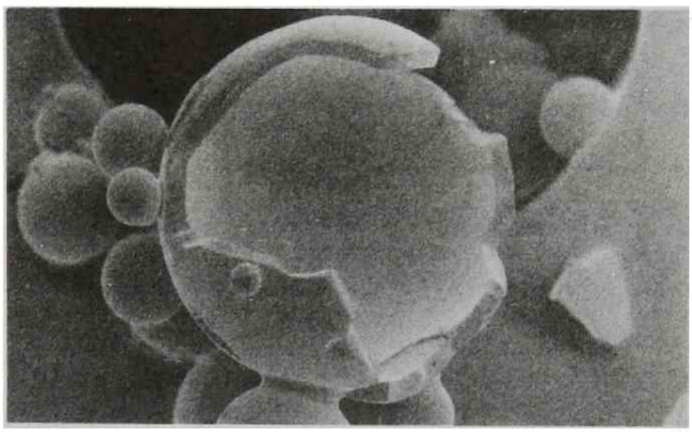

(b)PS microcapsule (MC-2027) 10μm

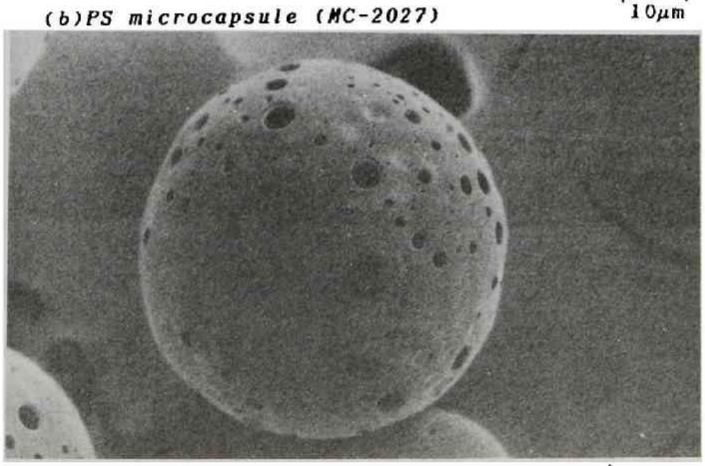

(c)SBR microcapsule (MC-2028) 100μm

Photo. 1-1. SEM photograph of microcapsules containing lipase.

containing 2wt percent of triacetin. The hydrolysis of the substrate actually took place as the released moles of acetic acid increased with the reaction time.

The microcapsules were all recovered after the first hydrolysis, and redispersed in the second batch of the substrate solution. Reproducibility of the second experiment was good, indicating that no leakage enzyme occurred during successive operations, and the hydrolysis proceeded by the diffusion of smaller molecules of the substrate through the wall.

Encapsulated enzyme was extracted after the wall of microcapsules was broken, and the activity per unit weight of the enzyme was measured in order to detect the possible conformational damage which might be inflicted during the encapsulation. It was found that the activity remained unchanged, positive evidence that the conformation of the enzyme was unaffected during the encapsulation.

Molecular size of the permeable substrate

The substrate molecules in the external aqueous phase diffuse into the internal phase through the polymer wall, and are converted by lipase in the microcapsule. It was thought that the diffusion of the substrate through the wall was dependent on its molecular size. In order to investigate the effect of molecular size, the three kinds of PVA having relatively many acetyl residues were used as the substrate. The results of hydrolysis are shown in Table 1-3. The molecular weight of PVA were 1,070, 2,455

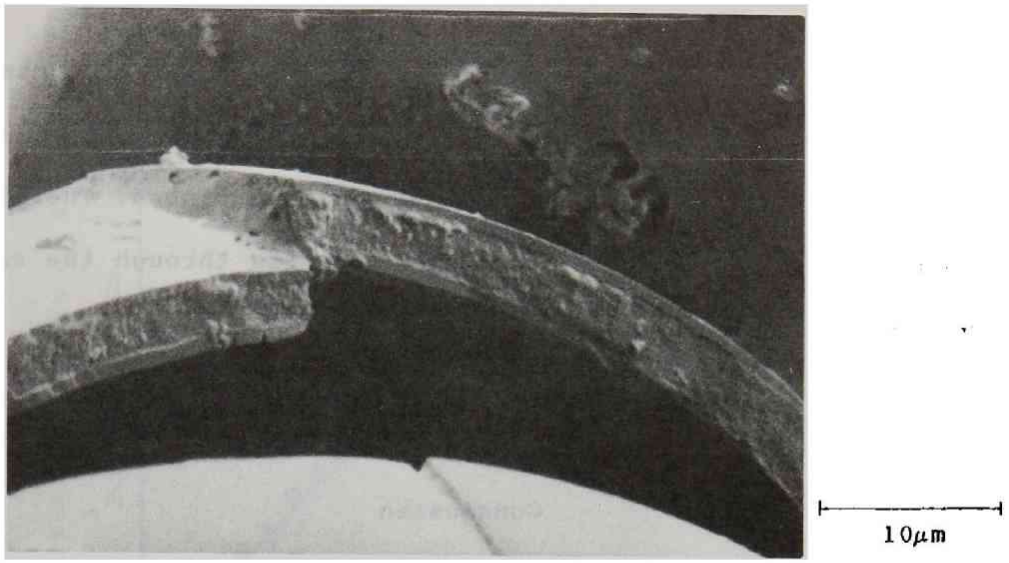

(a)SEM photograph (Layers of polystyrene are clearly visible at the inner and outer surface.).

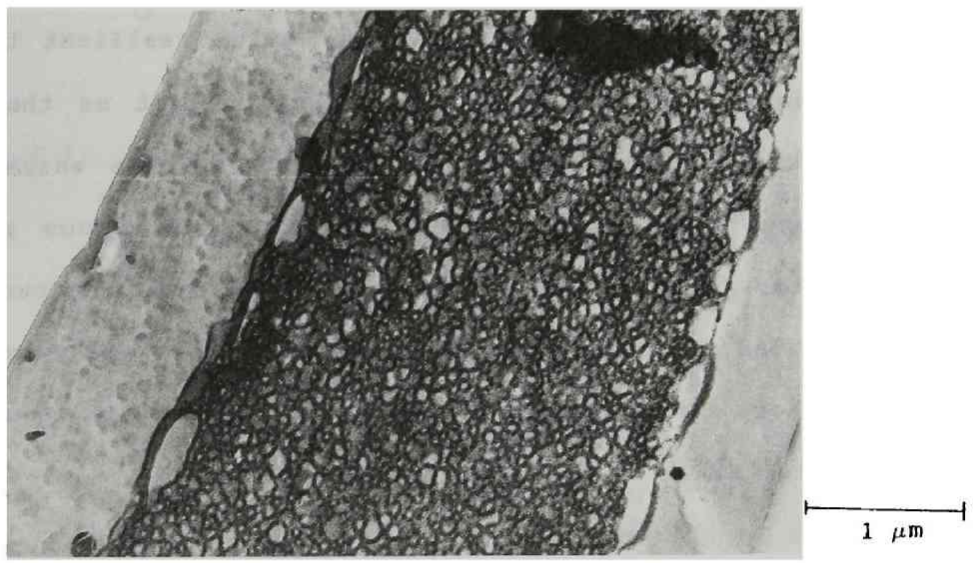

(b)TEM Photograph (The chains of SBR were stained with O_sO_4 and a well-blended domain developed between the layers of PS.).

Photo. 1-2. Cross-section of microcapsule.

and 6,245, respectively. After the reaction the products were analyzed. As shown in Table 1-3, LP-1 having lowest molecular weight was only hydrolyzed with encapsulated lipase. The limitation of molecular size in permeation process through the capsule wall would be between 1,000 to 2,500.

Conclusion

Microcapsules containing lipase were successfully prepared employing the (W/O)/W multiple phase emulsion method. The wall material, a mixture of PS and SBR, was quite resilient to the impacting force, and withstood such a dead weight as that inflicted in the packed condition. No leakage of the enzyme was detected even after the repeated use in a continuous packed column reactor for a few months. The packed column reactor will be investigated in next chapter. Encapsulated enzyme recovered 100 percent of its activity even though the ambient temperature was raised to 328K.

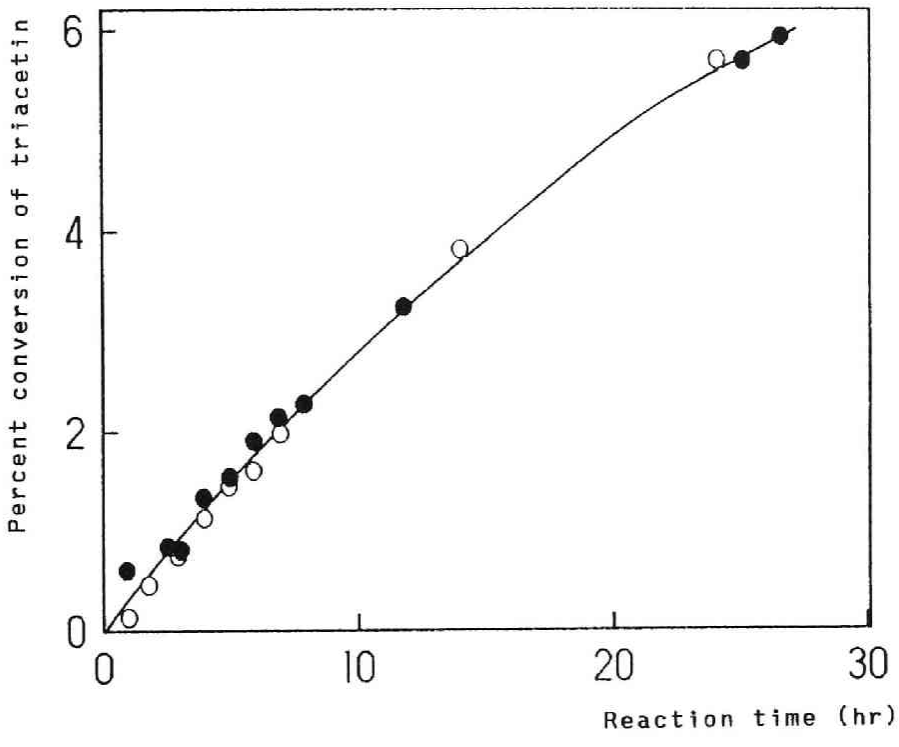

Figure 1-1. Repeated use of lipase microcapsule to the hydrolysis of triacetin. At 310K, 1g of microcapsule MC-2007 was dispersed in 500ml of 2wt percent triacetin solution. ○, Fresh MC; ●, Recycled MC.

Table 1-3. Reactivity of PVA having different molecular weight.

PVA No.[1)]	Degree of polymerization	Degree of saponification (mol. %)	Average molecular weight	Reactivity for hydrolysis
LP-1	22	88.9	1070	Yes
LP-2	50	87.9	2455	No
LP-3	127	87.7	6245	No

References

1) Z.Bohak and N.Sharon, Biotechnological Applications of Proteins and Enzymes, Academic Press (1977)

2) K.Mosbach, Methods in Enzymology, Academic Press (1976)

3) A.D.McLaren and L.Packer, Advs. in Enzymology, 34, 245 (1970)

4) E.Katchalski, I.Silman and R.Goldman, Advs. in Enzymology, 34, 445 (1971)

5) M.N.Vrancken and D.A.Claeys, U.S.Patent 3,523,906 (1970)

6) H.Takenaka, Y.Kawashima, Y.Chikamatsu and Y.Ando, Chem. Pharm. Bull., 30, 695 (1982)

7) Y.Ogawa, M.Yamamoto, H.Okada, T.Yashiki and T.Shimamoto, Chem. Pharm. Bull., 36, 2095 (1988)

8) M.Iso, T.Shirahase, S.Hanamura, S.Urushiyama and S.Omi, J. Microcapsulation, 6, 165 (1989)

9) T.Furuno, A.Ikeda, M.Iso, S.Omi and H.Yokota, Zairyo Gijutsu, 5, 141 (1987)

10) O.H.Lowry, N.J.Rosebrough, A.L.Farr and R.J.Randall, J. Biol. Chem., 193, 265 (1951)

Chapter 2

Application of microencapsulated enzyme in a batch reactor and mathematical approach

Abstract

Performance of microencapsulated enzyme was evaluated employing the hydrolysis of triacetin as a model substrate of the immobilized enzyme catalysis in a batch system. A mathematical model was developed to simulate the behavior of hydrolysis, which was derived under the assumption that the diffusion of molecules (substrate and products) through the wall of microcapsules plays a dominant role to the reaction rate. Inhibition of the reaction by the decreasing pH due to the production of acetic acid was also taken into account. The calculated values agreed quite well with the observed data

Introduction

Immobilization of enzyme for the purpose of repeated utilization has been a major issue for chemical engineers who are extensively engaged in the R&D of commercial scale bioreactors. Atkinson[1] has mentioned in his well-known article that cell-free enzymes, being both water-soluble and relatively unstable, are therefore difficult to recover from the products for reuse, and for these reasons operations using cell-free enzymes tend to be of an ancillary nature rather than a major processing stage. However, he already foresaw potential usefulness of the encapsulated enzyme, and even proposed a few mathematical modelings to predict the overall rate of the catalysis.

In previous chapter, microencapsulation of lipase employing (W/O)/W multiple phase emulsion method, with 2:1 PS/SBR mixture being used as a wall material, was proposed. This chapter intends to investigate the performance of encapsulated enzyme in a batch reactor, and introduces a reasonable mathematical model for understanding the mechanism of enzyme catalysis immobilized in microcapsules[2].

Experimental

Reagents and microencapsulation

All regents and lipase P are given in the previous chapter.

A major part of the microencapsulation procedure was described in the previous chapter. In order to compare the microcapsules having the different concentration of lipase, three kinds of internal enzyme concentration, 3.3, 6.7 and 10wt percent, were prepared.

Hydrolysis of triacetin

Catalysis of the encapsulated enzyme was investigated employing the hydrolysis of triacetin in a stirred vessel. One gram of the microcapsules were used in 500g of the buffer solution (pH = 7) containing 2wt percent of triacetin. A magnetic stirrer was used for agitation, and the temperature was kept at 310K. Samples were withdrawn using a special pipette equipped with a glass filter at the tip to prevent the suction of microcapsules.

Results and discussion

Mathematical simulation of the reaction catalyzed by encapsulated enzyme

The following assumptions were made to derive a mathematical model of the reaction catalyzed by the encapsulated enzyme: (1)Microcapsules are spherical shells, and are uniform in size. (2)Reaction kinetics of the substrate obey the Michaelis-Menten mechanism. (3)Resistance of mass-transfer depends overwhelmingly on the diffusion of substrate molecules through the wall of the

microcapsule.

The hydrolysis of triacetin catalyzed by free lipase dissolved in the buffer solution correlated well with the Michaelis-Menten equation, the Lineweaver-Burke plot gave two kinetic parameters, k_2 = 0.0051sec^{-1} and K_m = 205.8g/l. The second assumption is reasonable since the activity of the enzyme molecule found to be unaffected during the encapsulation as shown in preceding chapter, and it is present as a free molecule in the buffer solution even in the encapsulated state.

The Michaelis-Menten equation is written as follows.

$$-r_s = \frac{k_2 C_E C_1}{K_m + C_1} = \frac{k_2 C_E}{K_m} \frac{C_1}{1 + C_1/K_m} \qquad (2\text{-}1)$$

where, $-r_s$ = reaction rate of substrate, C_E and C_1 = concentration of enzyme and substrate in the microcapsule compartment, K_m = Michaelis constant of enzyme, and k_2 = rate constant.

The third assumption gives a schematic concentration profile of substrate as shown in Figure 2-1.

Provided that there is no accumulation of substrate in the wall, the equation of mass-balance will yield,

$$(-r_s) \frac{3}{4} \pi a^3 N = 4 \pi r^2 N D_2 \frac{dC_2}{dr} = -V \frac{dC_L}{d\theta} \qquad (2\text{-}2)$$

where C_2 and C_L = concentration of substrate in the wall and in

the aqueous phase, N = number of microcapsules in the system, D_2 = effective diffusion coefficient of substrate in the wall, V = volume of the aqueous phase, a = inner radius of microcapsule, r=coordinate of the radial direction, and θ = reaction time.

Strictly speaking, at the initial stage of the catalysis the diffusion equation derived for non-steady state should be applied instead of Equation (2-2). However, as the rigorous solution provided by Crank[3] clearly indicates, the concentration profile is established rather rapidly, in a matter of a few minutes at most. Numerical solutions, obtained from Equation (2-2) and shown in the later figures, quickly offset the discrepancy in the early stage.

Let us introduce the following non-dimensional parameters.

$$\gamma = b/a \qquad x = r/b \qquad \beta = \frac{4}{3}\pi b^3 N/V \tag{2-3}$$

where b:outer radius of microcapsule.

Initial and boundary conditions can be written,

$$\text{I.C.} \qquad \theta = 0 \ ; \quad C_L = C_{s0} \tag{2-4}$$

$$\text{B.C.} \qquad r = a \ (X = 1/\gamma); \quad C_2 = C_1 \tag{2-5}$$

$$r = b \ (x = 1); \quad C_2 = C_L \tag{2-6}$$

Equation (2) can be solved using the conditions given above.

$$\frac{C_1}{\dfrac{1 + C_1/K_m}{k_2C_E/K_m}} = \frac{C_L - C_1}{\dfrac{\gamma - 1}{3D_2\gamma^3/b^2}} = \frac{C_L}{\dfrac{1 + C_1/K_m}{k_2C_E/K_m} + \dfrac{\gamma - 1}{3D_2\gamma^3/b^2}} = -\frac{\gamma^3}{\beta}\frac{dC_L}{d\theta} \qquad (2\text{-}7)$$

The Thiele modulus, originally introduced to estimate the effectiveness factor of inorganic catalyst, was modified so as to fit the enzyme catalysis as follows.

$$\phi_H' = \sqrt{\frac{\gamma - 1}{3\gamma^3}}\,\phi_H \qquad \phi_H = b\sqrt{\frac{k_2C_E}{K_mD_2}} \qquad (2\text{-}8)$$

By substituting these parameters into Equation (2-7), C_1 can be expressed as a function of C_L.

$$C_1/K_m = \frac{1}{2}\left(p + \sqrt{p^2 + 4q} \right) \qquad (2\text{-}9)$$

where, $p = C_L/K_m - 1 - \phi_H'^2$, $q = C_L/K_m$.

The latter part of Equation (2-7) can be rewritten as follows,

$$\frac{dC_L}{d\theta} = -\frac{(k_2C_E/K_m)\,\beta\,C_L/\gamma^3}{1 + C_1/K_m + \phi_H'^2} \qquad (2\text{-}10)$$

Equation (2-9) and (2-10) were numerically solved using those parameters which indicate the characteristics of microcapsules such as the average diameter, wall thickness and diffusion coefficient. Conversion of the substrate and the amount of released acetic acid were simulated as time-dependent variables. Calculated result and comparison with observed data.

Microcapsule MC-2012, with a diameter of 78μm and wall thickness of 9.8μm was used for the particular experiments to test the availability of the reaction model.

The rate constant and the Michaelis constant, as mentioned before, were measured as 0.0051sec^{-1}, and 205.8g/l, respectively.

Numerical correlation of observed data with varied diffusion coefficient is shown in Figure 2-2, indicating 4.1(10^{-10})cm^2/sec as the best fit.

The effect of the wall thickness on the reaction rate is shown in Figure 2-3. As is clearly shown the reaction proceeded faster as the wall thickness reduced.

Effect of substrate concentration

Amount of acetic acid released was plotted against the reaction time in Figure 2-4 as the substrate concentration was changed. Agreement between the observed and calculated values was generally fair except for those at the higher release of acetic acid corresponding to the higher supply of the substrate. Deactivation of enzyme may have occurred due to the decrease of pH by the release of acetic acid.

Rate constant as a function of pH

As mentioned in the above section, it is desirable to investigate the effect of pH on the enzyme catalysis on quantitative basis. The change of pH in the buffer solution, originally ad-

justed at pH = 7, was measured by adding small amounts of acetic acid intermittently. The observed curve is shown in Figure 2-5 as a function of the concentration of acetic acid. The theoretical curve from the dissociation constant of the acid was also shown in the figure, indicating the effect of the buffer solution to offset lowing pH. For the convenience of computation, the curve was empirically expressed in two equations as follows.

$$3 \leqslant pH \leqslant 6.2 \quad ; \quad pH = -\log[H^+] = -1425C^2 - 46.45C + 7 \qquad (2\text{-}11)$$

$$6.2 \leqslant pH \leqslant 7 \quad ; \quad pH = 0.03828/[C + 1.01(10^{-3})] + 3.358 \qquad (2\text{-}12)$$

where C=concentration of acetic acid in mol/l.

The extent of deactivation of free lipase was measured under the adjusted value of pH. The relative value of the rate constant defined as k_{pH}/k_7 was expressed as a function of pH as follows.

$$\log(k_{pH}/k_7) = 0.204pH - 1.428 \qquad (2\text{-}13)$$

k_7 is $0.0051sec^{-1}$ as mentioned previously.

Effect of enzyme concentration in microcapsules

Microcapsules of MC-2022, MC-2021 and MC-2023 were prepared varying the concentration of enzyme in the W phase of the primary emulsion. Conditions are shown in Table 1-2 in Chapter 1.

As the enzyme content increases, the average diameter and the wall thickness become smaller because lipase itself functions

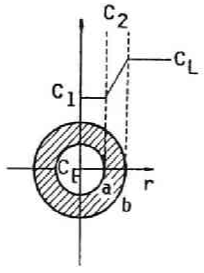

Figure 2-1. Schematic concentration profile of substrate in mass transfer model.

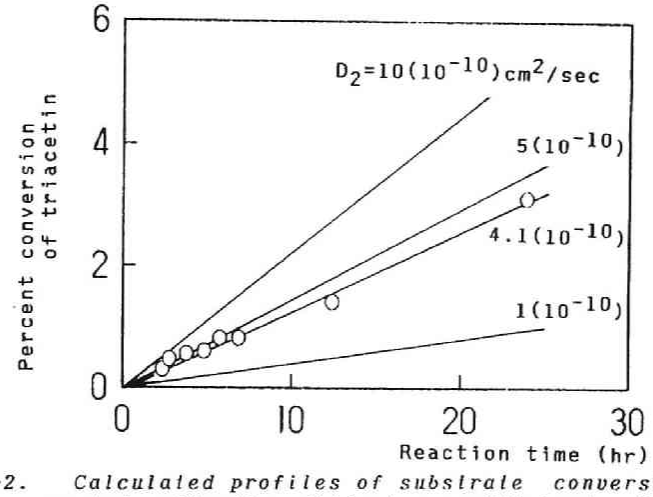

Figure 2-2. Calculated profiles of substrate conversion with varied effective diffusion coefficient. Comparison with the observed data at 310K. 2b = 78.1 μm, δ = 9.8μm, N^{-1} = 3.61(10^5), K_m = 205.8g/l and k_2 = 0.0051sec^{-1}.

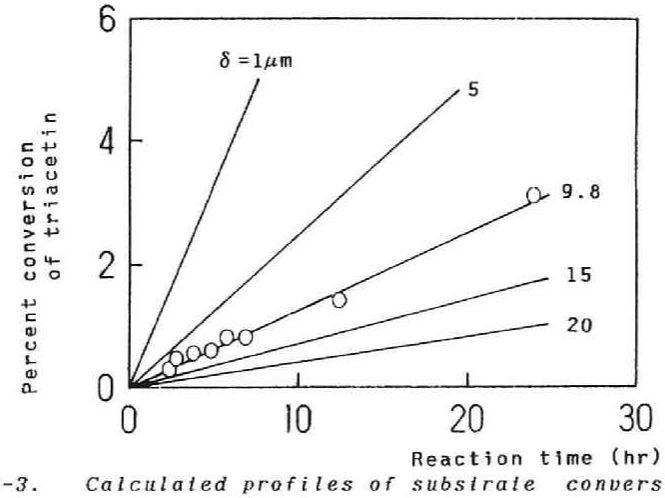

Figure 2-3. Calculated profiles of substrate conversion with varied wall thickness of microcapsules. Comparison with the observed data at 310K.
D_2 = 4.1(10^{-10})cm^2/sec.

as a surface active agent, and reduces the diameter of droplets in the W/O emulsion. No appreciable change was observed in the surface.

Results of the catalysis employing these microcapsules are shown in Figure 2-6 with the calculated curves. The different rate of the reaction was clearly due to the varied amount of encapsulated enzyme. Two calculated curves were shown for each experiment (broken lines being without consideration of the effect of pH, and solid ones calculated using equations (2-11) and (2-12)).

The simulation was carried out under the presumption that the effective diffusion coefficient may change depending on the wall thickness. Those values which gave a best fit to the observed points are shown in Table 2-1. Though the difference is quite small, the diffusion coefficient decreased slightly with increasing wall thickness. The simulation with the correction of pH inhibition during the catalysis predicted well the degrading reaction rate at the higher conversion of the substrate.

Effect of PS/SBR ratio in the capsule wall to the performance of catalysis

Microcapsules of different PS/SBR ratios in the wall were used to compare the performance of the catalysis. The result was shown in Figure 2-7 together with calculated curves. The rate of hydrolysis of triacetin became higher as the fraction of styrene

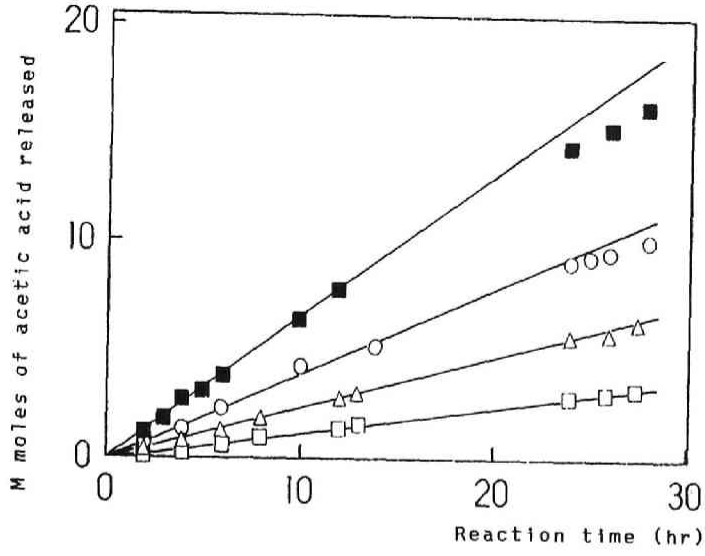

Figure 2-4. Amount of acetic acid released with varied substrate feed. Concentration of triacetin: □, 0.5%; △, 1%; ○, 2%; ■, 3%; ——, calculated curve. Microcapsule MC-2012 was used at 310K. 2g of microcapsules were dispersed in 200ml of triacetin solution.

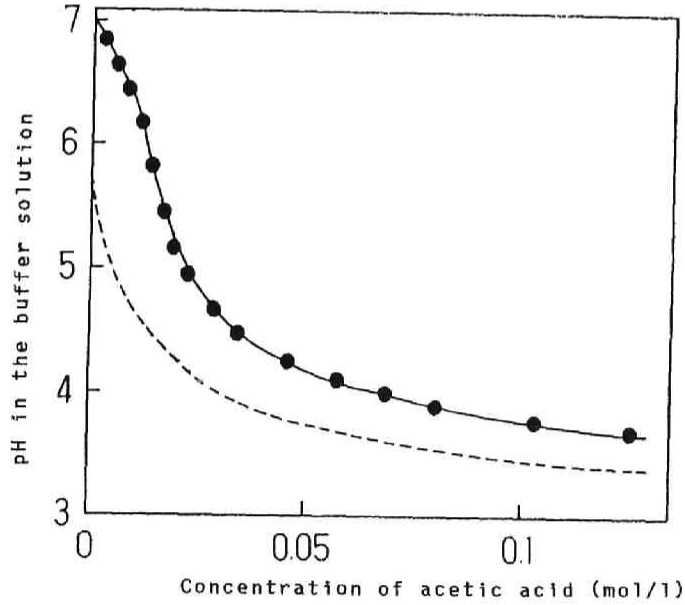

Figure 2-5. Shift of pH in buffer solution against the concentration of acetic acid. ●, observed point, – – – –, calculated from the dissociation constant of acetic acid.

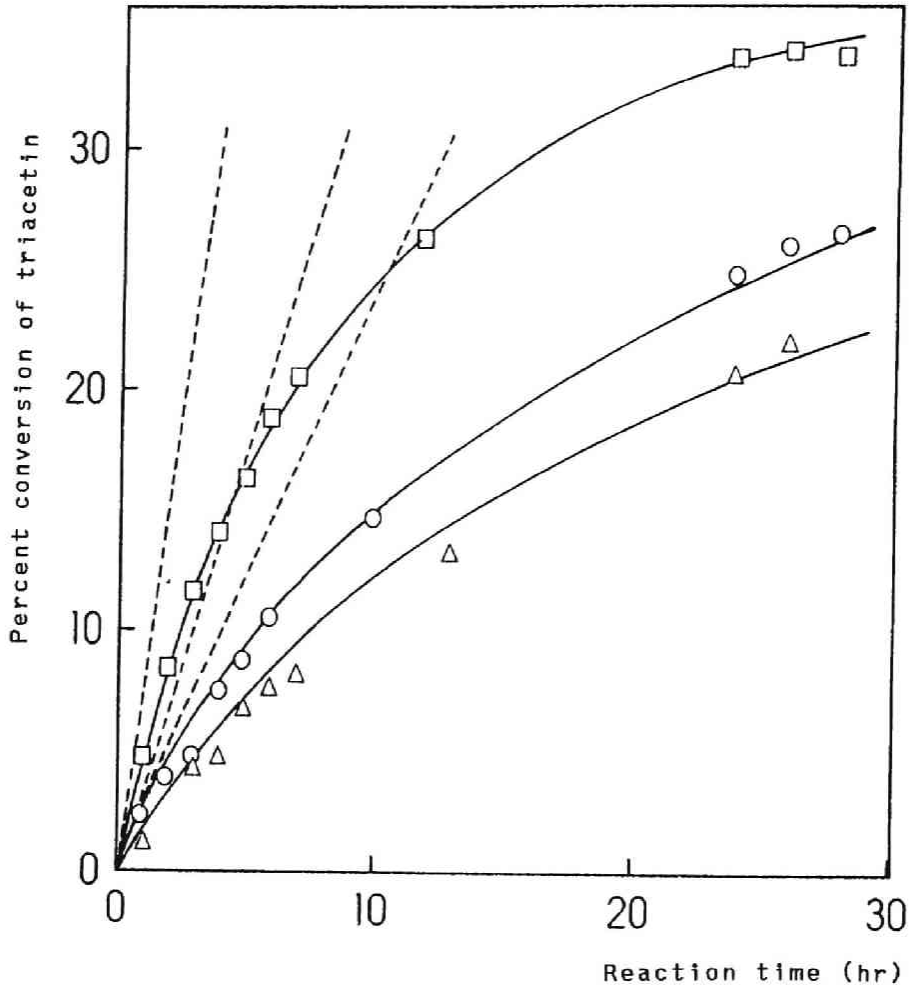

Figure 2-6. Effect of enzyme concentration on the rate of substrate conversion at 310K. Enzyme concentration: △, 33g/l; ○, 67g/l; □, 100g/l. Other conditions are same as in figure 2-4 except the choice of microcapsule. -----, calculated curve without the correction for pH inhibition. ———, calculated curve with the correction for pH inhibition.

Table 2-1. Effective diffusion coefficient of microcapsules

MC No.	Wall material				δ (μm)	$D_2 \times 10^{18}$ (cm^2/sec)
	PS(g)		SBR(g)			
2012	PS-11	10	SBR	5	9.80	4.1
2021	PS-12	10	SBR	5	5.67	5.2
2022	PS-12	10	SBR	5	6.17	4.6
2023	PS-12	10	SBR	5	4.00	6.0
2025	PS-12	5	SBR	10	7.19	5.3
2026	PS-12	7.5	SBR	7.5	4.95	5.3
2028	--		SBR	15	28.5	32.0

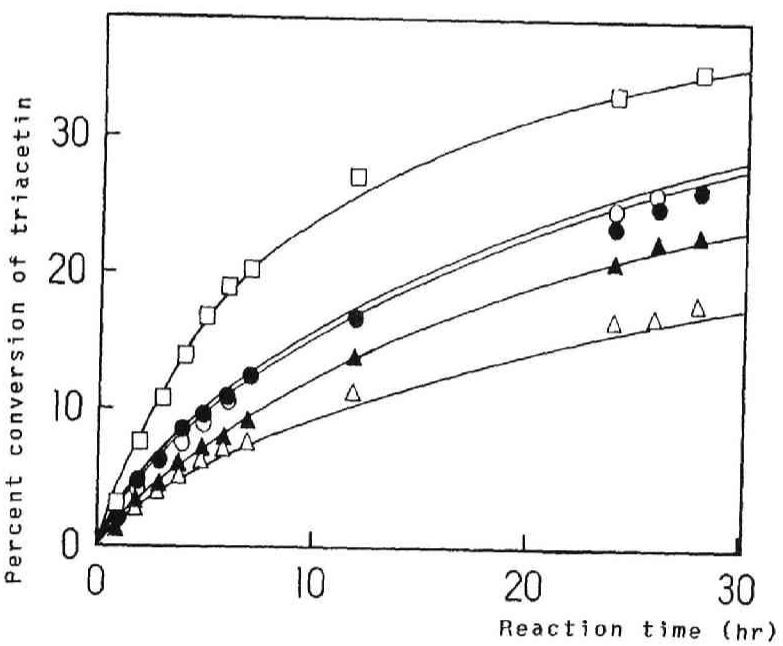

Figure 2-7. Effect of composition of wall materials on the performance of microcapsules. Composition of SBR: □, 0%; ○, 33%; ●, 50%; ▲, 67%; △, 100%. ———, calculated curve with the correction for pH inhibition. Reaction temperature was 310K.

in the wall increased. Since the effective diffusion coefficients are nearly same, the reaction rate seemed to be governed by the size and wall thickness of microcapsules.

It may be worthwhile to describe that the numerical trial to correlate the data taken MC-2028 (100 percent SBR wall) succeeded only when the value of effective diffusion coefficient was assumed to be almost five times as large as those assigned for other microcapsules of blended wall. The particular wall structure of MC-2028 may lead to easier transport of smaller molecules.

Conclusion

Microcapsules of lipase employing a (W/O)/W multiple phase emulsion method was used efficient, recoverable catalysts. Catalysis of the encapsulated enzyme was investigated, and the hydrolysis of triacetin was successfully simulated by the reaction model based upon the Michaelis-Menten mechanism. Other factors affecting the mechanism such as the mass-transfer resistance of the substrate molecules through the wall and the decrease in pH due to the formation of acetic acid were also taken into consideration. No leakage of the enzyme was detected after repeated usage and storage over the duration of a few months.

References

1) B.Atkinson, Biochemical Reactor, Pion, London (1974)

2) M.Iso, T.Shirahase, S.Hanamura, S.Urushiyama and S.Omi, J. Microencapsulation, 6, 165 (1989)

3) J.Crank, The mathematics of Diffusion, 2nd ed., Clarendon Press, Oxford, p.99 (1975)

Chapter 3

Application of microencapsulated enzyme as a continuous packed column reactor

Abstract

The microencapsulated lipase were applied to the continuous tubular reactor system, essentially a packed column reactor, and longevity and mechanical strength of the microcapsules were fully demonstrated.

The reaction model derived for a well-stirred batch reactor in the preceding chapter was also applicable to simulate the behavior in the packed column reactor as it was proved that there is no mass transfer resistance between the reactant stream and the surface of microcapsules. The observed data agreed quite well with the calculated values. Similarity of the behaviors of catalysis observed between two reactor systems was thoroughly confirmed.

Introduction

Generally speaking, the structure of microcapsules has a tendency to be too fragile to cope with the mechanical shear or vigorous agitation in a practical fermenter or a reaction vessel[1]. However, lipase-containing microcapsules prepared in the previous chapter exhibited excellent endurance to the mechanical shear force created in a stirred vessel. The encapsulated lipase retained its activity for the hydrolysis of triacetin as a model substrate under repeated usage[2].

This chapter intends to demonstrate further potentials of the microcapsules by applying them to a packed column reactor in which they are exposed to a continuous flow of the buffer solution including triacetin under various operating temperatures and pH. It is also shown that the similar operational equation and a particular rate equation derived for a batch reactor can be applied to the packed column reactor[3].

Experimental

Reagents and enzyme

All reagents and lipase P were given in Chapter 1.

Procedure of continuous catalysis in a packed column reactor

Microcapsules were packed in a 13mm ID glass column equipped with a water jacket. The reaction temperature was controlled by recirculating the water in and out of a thermostat. The substrate solution was supplied from a feed tank, the flow rate being adjusted by changing the height of the tank. The effluent solution was taken as a sample in a certain time interval, and the changes of the substrate concentration and pH were examined with bed height and flow rate of the substrate solution being changed.

Results and discussion

Effect of the reaction temperature and mean residence time on the substrate conversion

Continuous operations were carried out with 2wt percent triacetin solution as the substrate. Microcapsules of MC-2012 were packed in a column at the height of 17cm. Relations between the mean residence time and substrate conversion are shown in Figure 3-1 with varied reaction temperatures. In this temperature range the substrate conversion became higher as the reaction temperature rose at the fixed residence time. No noticeable deactivation of the catalysis was observed even at the highest reaction temperature.

As the substrate conversion became higher, however, the reaction rate was depressed due to the inhibition by decrease of

pH in the downstream of the column. This deactivation was believed to be temporal because activity of the enzyme was promptly recovered after the environmental pH was readjusted to the optimal level with a continuous supply of the buffer solution for 1hr, and the column was allowed to stand overnight.

In order to demonstrate full recovery of the enzyme activity, one particular experiment, shown as an open circle in the figure, was done on the day after the operation at 323K followed by the treatment mentioned above. The substrate conversion precisely fell upon the correlated curve at 310K, a clear evidence that the activity of the enzyme was fully recovered.

Basic equations for the operation of packed column reactor

The observed behaviors in Figure 3-1 anticipated that the flow in the packed column reactor can be regarded as an ideal plug-flow. One may find in any textbook of chemical reaction engineering[4] that the residence time in the plug-flow reactor is replaceable with the reaction time in the batch operation. This concept may be easily derived from material balance in small section of the plug-flow reactor.

From the schematic diagram shown in Figure 3-2, one can derive the following material balance equation.

$$F_v\left[\left(C_L - dC_L\right) - C_L\right] = -r_s\, dV_r \qquad (3\text{-}1)$$

where, F_v = flow rate of the reaction mixture, C_L = concentration

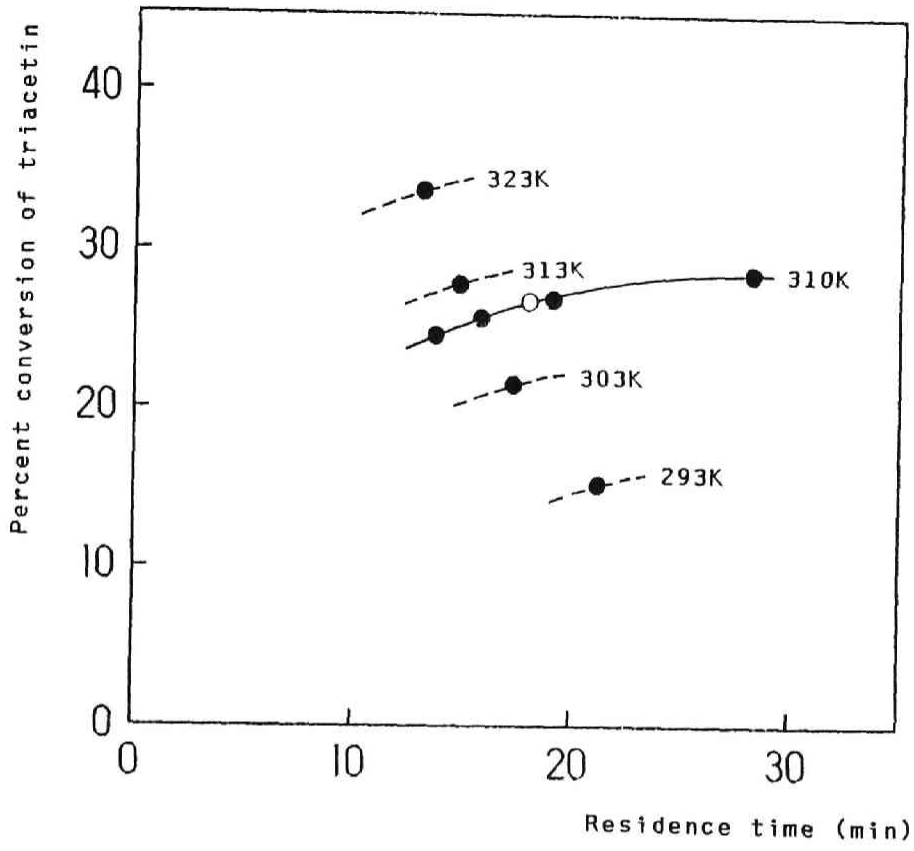

Figure 3-1. General performance of packed column reactor. Substrate conversion versus residence time. Reaction temperature is shown in the figure.

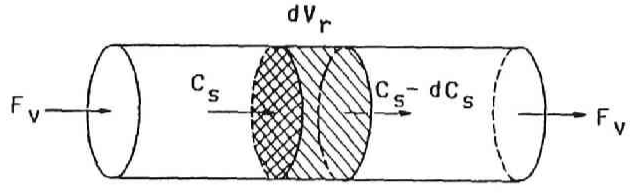

Figure 3-2. Illustration of small section of plug-flow reactor.

of the substrate in the holdup solution, V_r = volume of the holdup solution in the reactor, and r_S = reaction rate of the substrate.

Dividing each side of Equation (3-1) with F_v, and a readjustment will yield,

$$- dC_L = - r_s \, d(V_r/F_v) \tag{3-2}$$

V_r/F_v has a dimension of time, and can be expressed as follows.

$$\theta = V_r/F_v \tag{3-3}$$

Substitution to Equation (3-2) will yield the following equation normally derived for the batch operation.

$$- dC_L/d\theta = - r_s \tag{3-4}$$

Equation (3-4) means that V_r/F_v for the plug-flow reactor is equivalent to the reaction time for the batch operation, and the basic equation of operation is essentially same.

Equation (3-4) may be applied to the reaction system catalyzed by enzyme immobilized in microcapsules provided that there is no appreciable mass transfer resistance between the reactant stream and microcapsules. Let us assume that this condition is satisfied in the present packed column reactor, and derive the essential equations at first. Experimental evaluation of this particular resistance will be shown later.

For the case of enzyme catalysis by immobilized enzyme in

microcapsules, the reaction rate, r_S, was given in the preceding chapter.

Evaluation of mass transfer resistance between the reactant stream and microcapsules

Since it is well-known that the extent of mass transfer resistance between the fluid stream and particles is governed by the velocity of stream, experimental evaluation can be done by undergoing the catalysis with varied flow rate and height of the packed column. If the mass transfer resistance is of considerable intensity, a significant change will appear in the performance of the catalysis depending on the flow rate. On the other hand, if the resistance is negligible, the outcome of the catalysis will be solely correlated with the residence time of fluid in the reactor.

According to this well-established concept, hydrolysis of triacetin was carried out by changing the flow rate and the bed height. Microcapsule MC-2012 was used at 310K. The substrate conversion was correlated with the residence time in Figure 3-3. No significant dependence on the flow rate of the substrate solution was detected as the observed data taken with different column height fell upon one line, a positive evidence that Equation (3-4) can be used as an operational equation for the packed column reactor.

Effect of enzyme concentration in microcapsules

As has been done in the batch reactor of Chapter 2, microcapsules with different enzyme contents, MC-2022, MC-2021 and MC-2023, were packed in the reactor, and the catalysis was carried out. The result was shown in Figure 3-4 together with the calculated curves obtained from the numerical integration of Equation (4). Same values of effective diffusion coefficient as those employed in the calculation of batch operation were adopted. Agreement with the observed data was quite satisfactory.

Effect of PS/SBR ratio in the capsule wall to the performance of catalysis

The catalysis employing the microcapsules of different PS/SBR ratio was investigated. Microcapsule MC-2027 having only PS was too fragile to be packed in the column, so it was not tried in this continuous operation. The result was shown in Figure 3-5 together to the calculated curves. The calculated curves were drawn by using the values of the efficient diffusion coefficient obtained in Chapter 2. The rate of hydrolysis of triacetin became higher as the fraction of styrene in the wall increased, as well as the batch reactor.

Effect of molecular weight of polystyrene

Effect of PS molecular weight on the general feature of microcapsules was investigated with PS-13 having higher molecular

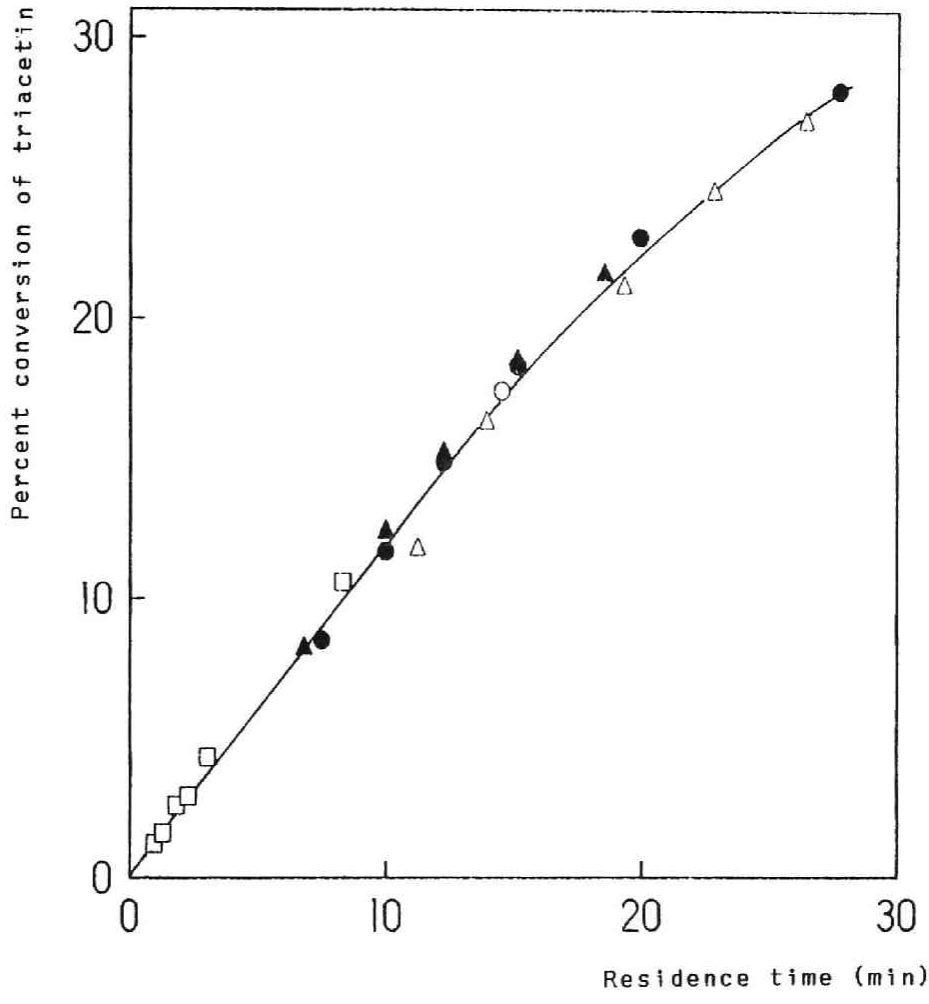

Figure 3-3. Evaluation of mass transfer resistance between the reactant stream and microcapsules. Substrate conversion versus residence time with column height and flow rate being changed. Reaction temperature was 310K. Column height: ○, 17cm; ●, 14cm; △, 10.5cm; ▲, 6.5cm; □, 3.6cm.

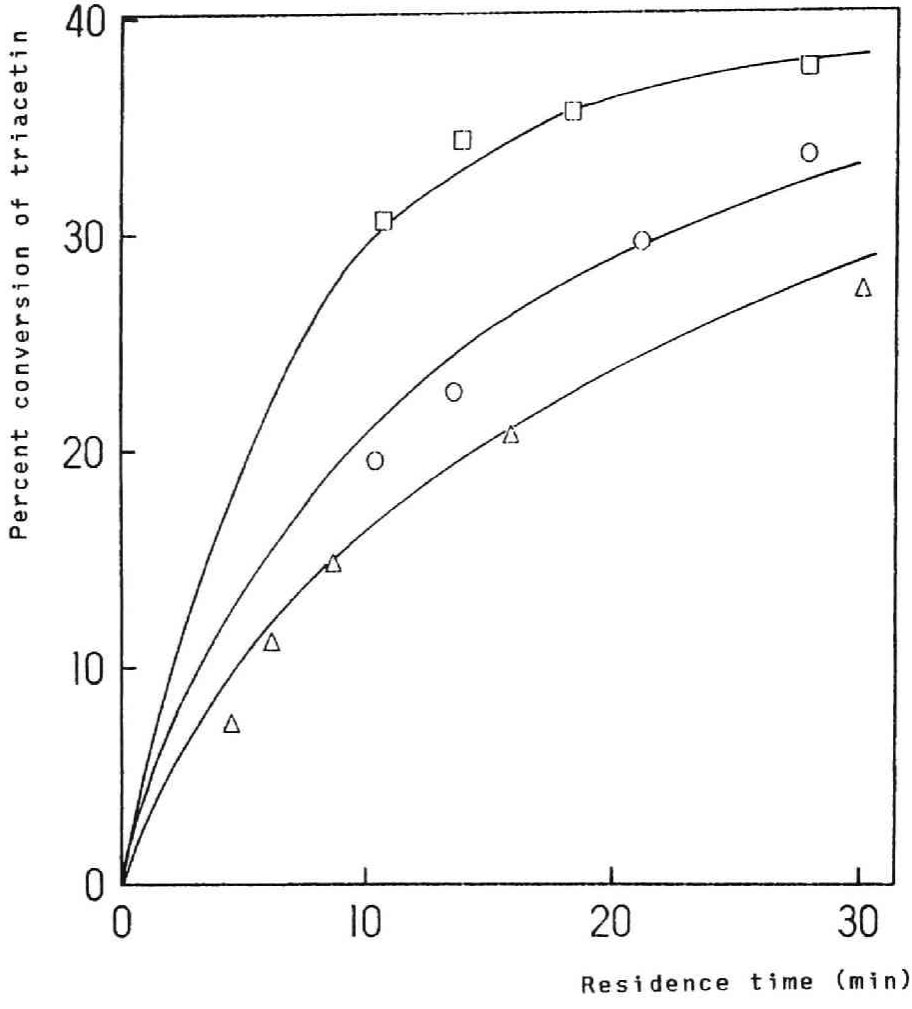

Figure 3-4. Effect of enzyme concentration on the substrate conversion. Enzyme concentration: △, 33g/l; ○, 67g/l; □, 100g/l. ——, calculated curve. Reaction temperature was 310K.

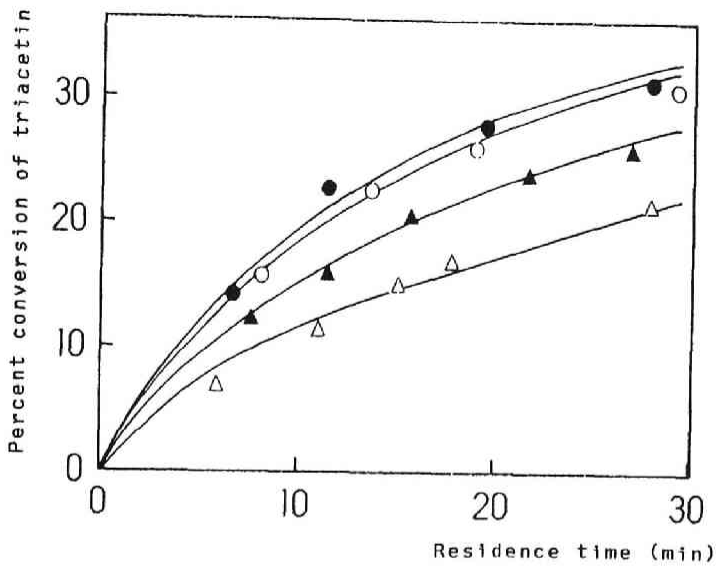

Figure 3-5. Effect of composition of wall materials on the performance of microcapsules. Composition of SBR: ○, 33%; ●, 50%; ▲, 67%; △, 100%. ——, calculated curve. Reaction temperature was 310K.

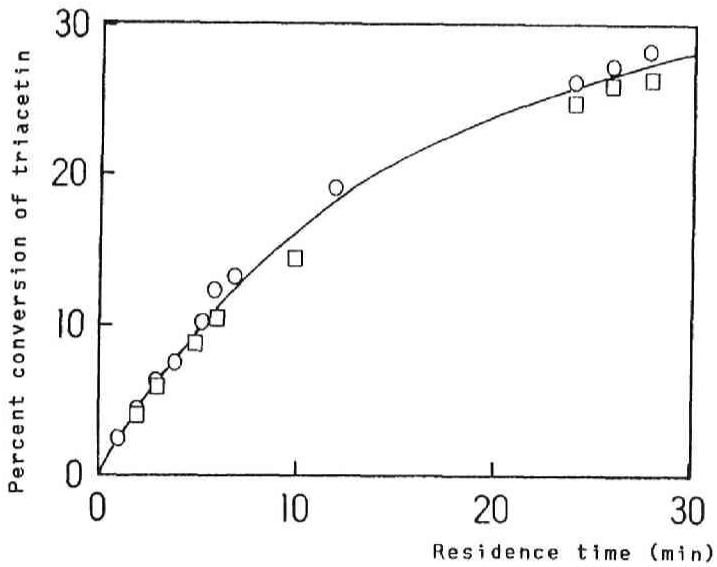

Figure 3-6. Effect of PS molecular weight on the performance of microcapsules. Substrate conversion versus residence time. Reaction temperature was 310K. Weight average molecular weight of PS: ○, 10200 (PS-12); □, 213000 (PS-13).

weight. PS-13 was synthesized by thermally-initiated bulk polymerization at 403K, and the weight average molecular weight was 213,000. Microcapsule MC-2024 was prepared, and the catalysis was carried out to compare the reaction rate with that observed with MC-2021. Since the similarity between operations of the batch and the packed column continuous reactor was well established, only the farmer was done. The substrate conversion was correlated to the reaction time Figure 3-6. Apparently no appreciable change was observed from the conversion curve.

According to the data listed in Table 1-2, MC-2024 is larger in size and thicker in wall thickness than MC-2021, however, these deficits are compensated by larger percentage of the enzyme encapsulated and probably by larger value of the effective diffusion coefficient. Larger molecular weight will certainly favor the effective encapsulation of enzyme because higher viscosity of oil phase in W/O emulsion resists the break-up of W/O droplets when they are suspended in the secondary emulsion.

It can be said to summarize the result that the blending of PS and SBR are flexible enough to change PS molecular weight over wide range.

Conclusion

Feasibility of the lipase microcapsules with tough PS/SBR

wall was successfully established in the continuous catalysis employing a particular packed column reactor. The hydrolysis of triacetin was selected as a model catalysis.

The enzyme immobilized in microcapsules retained its full activity during the continuous operation extending over 2 months. Temporal deactivation due to the accumulation of acetic acid in the reactant stream was completely recovered by a simple treatment, i.e. the column was washed by the continuous flow of the buffer solution for 1hr and then allowed to stand overnight.

References

1) T.Kondo, Saishin Maikurokapuseruka Gijutsu (T.Kondo ed.) Sohgo Gijutsu Center, p.295 (1987)

2) M.Iso, T.Shirahase, S.Hanamura, S.Urushiyama and S.Omi, J. Microencapsulation, 6, 165 (1989)

3) M.Iso, T.Shirahase, S.Hanamura, S.Urushiyama and S.Omi, J. Microencapsulation, 6, 285 (1989)

4) O.Levenspiel, Chemical Reaction Engineering, John Wiley, New York (1972)

Chapter 4

Application of encapsulated enzyme dispersed in a continuous stirred tank reactor

Abstract

An application of encapsulated lipase to the hydrolysis of triacetin was carried out with a continuous stirred tank reactor (CSTR), in which the encapsulated enzyme was dispersed. An automatic control device to control pH of the reaction mixture at a desired level was designed and installed in the reactor system. Conversion of triacetin at the steady state operation with pH controlled became significantly higher than that without pH control. A particular kinetic model proposed in Chapter 2 was applicable to simulate the behavior of CSTR system as in the case of packed column reactor.

Introduction

In Chapter 1 and 2, microencapsulation of lipase solution was prepared employing the (W/O)/W multiple phase emulsion method, and a kinetic model was derived. Simulation of the experimental results employing a batch rector agreed well with the observed values[1]. In Chapter 3, continuous operation was conducted with a packed column reactor to investigate the long-term endurance of microcapsules[2]. The wall of the capsules was quite resilient to the static and mechanical forces due to the reinforcement of hard PS with elastic SBR, and passed the longevity test continued for several months. The kinetic model also quite effectively simulated the experimental results.

One major setback of the packed column operation for this catalysis is that the activity of lipase gradually decreases due to the released acetic acid accumulating towards the downstream of the column. While not impossible it is impractical to inject alkaline solution alongside the column to neutralize the acid. Instead, the use of a CSTR train may be a more reasonable choice since the alkaline injection and pH adjustment can be done for only a small additional cost.

Based on this, this Chapter deals with the operation of a single CSTR which includes the introduction of a simple device for pH adjustment[3]. Extension of this single CSTR to a multiple train system will be easily accomplished.

Experimental

Reagent and enzyme

The lipase and all reagents used were described in Chapter 1.

Microcapsules

Two kinds of microcapsules, MC-Ⅰ and MC-Ⅱ, were prepared by the (W/O)/W multiple phase emulsion method described in previous chapter. The average dimension and properties are listed in Table 4-1.

New analytical method to measure the amount of acetic acid

The neutral titration adopted in previous chapters to measure the amount of acetic acid released is no longer valid when the pH in the reaction mixture is controlled. Instead thin-layer chromatography(TLC) was employed to measure the conversion of triacetin. An Iatroscan TLC-FID Analyzer (TH-10, Diatron Co. Ltd.) was used with the mixture of n-hexane, ethylether, and acetic acid as a developing solvent. The composition in weight ratio was 45:30:1.

Apparatus

A schematic diagram of the experimental apparatus with the pH control device is shown in Figure 4-1. A round-bottomed, glass separable flask of 500ml capacity [5] was employed as reactor immersed in the thermostat controlled at 310K [10]. Continuous

supply and withdrawal of the reaction mixture were performed with a dual-tubing pump [3] and [4] driven by a single motor [2]. The hold volume of the reactor was kept constant by this method. A coarse glass filter [7] was placed at the tip of the sampling tube to prevent microcapsules from mixing with the sampled solution. Mean residence time of the reaction mixture was adjusted by changing the speed of the shaft drive.

Microcapsules were dispersed in the reaction mixture before beginning the operation. Flow rate of the exit solution, conversion of the substrate and the change of pH were measured at a certain time interval. To prevent the agglomeration of microcapsules during the long-hour operation 0.1wt percent PVA was added to the reaction mixture. The pH in the reaction mixture was controlled by using a pH-sensitive electrode [11] to monitor the pH level which activated the relay whenever it decreased to a value of 6.8. Alkaline solution stored in the hypodermic syringe [13] was injected into the reactor until the pH level recovered to 6.9. With this mechanism, pH in the reactor is maintained at 7.0, thus preventing inactivation of the lipase.

Results and discussion

Basic equation for the operation of single CSTR

A well-known mass-balance equation[4)] derived for the opera-

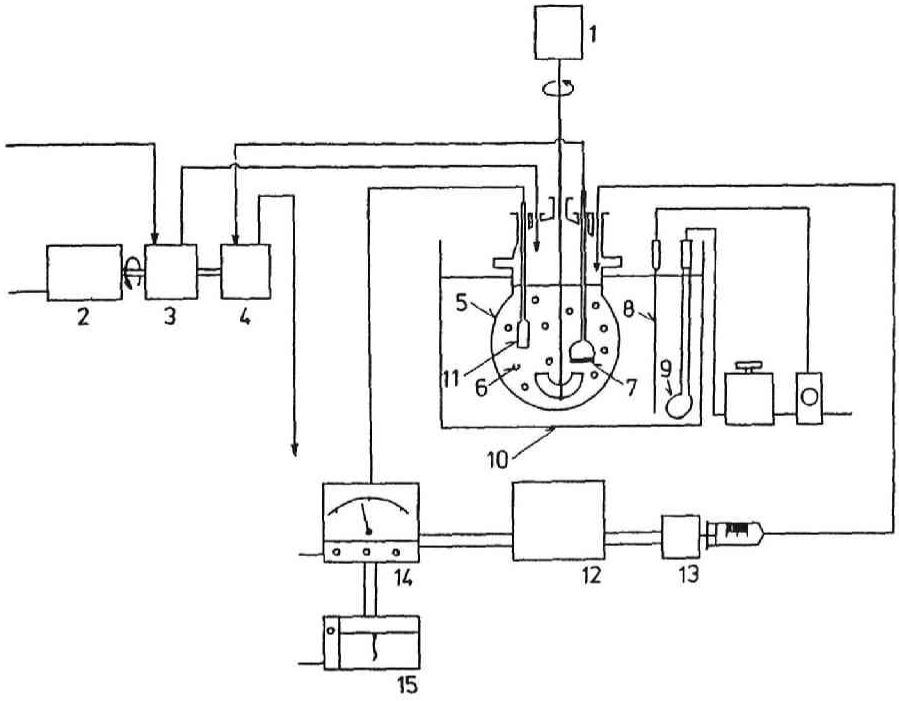

Figure 4-1. Schematic diagram of experimental apparatus.
Key: [1] motor for stirring, [2] motor for driving tubing pump, [3] tubing elements for feed stream, [4] tubing elements for exit stream, [5] reactor, [6] microcapsules, [7] glass filter, [8] thermocouple, [9] heater, [10] thermostat, [11] pH electrode, [12] pH control circuit, [13] syringe to inject alkaline solution, [14] pH meter, [15] recorder.

Table 4-1. Properties of microcapsules and parameters employed for simulation.

MC No.	Lipase cont. (%)	$\bar{d}_{pm}$ (μm)	δ (μm)	$D_2 \times 10^{10}$ (cm^2/sec)
I	39.2	119	4.1	6.0
II	25.4	105	5.6	6.0

tion of single CSTR can be applied to this enzyme-substrate system, assuming a state of perfect mixing. Considering the unsteady state during the initial period of operation, the mass-balance equation for the substrate can be written as follows:

$$\frac{dC_S}{d\theta} = \frac{C_{S0} - C_S}{V_r/F_v} + r_S \qquad (4\text{-}1)$$

where θ = operation time, C_S,C_{S0} = concentration of substrate in the reactor and in the feed-stream, respectively, V_r = hold volume in the reactor, r_S = reaction rate of substrate, and F_v = volumetric flow rate of the reaction mixture.

If the steady state is attained, the derivative in the left-hand side of equation (4-1) becomes 0, and the equation is reduced to algebraical form. The initial condition may be written as follows,

$$\theta = 0, \quad C_S = C_{S0} \qquad (4\text{-}2)$$

The reaction rate of the substrate r_S was derived in Chapter 2. Equation (4-1) can be rewritten as follows after the steady state is attained,

$$\frac{C_S - C_{S0}}{\bar{\theta}} = r_S \qquad \bar{\theta} = \frac{V_r}{F_v} \qquad (4\text{-}3)$$

where, $\bar{\theta}$ = mean residence time of the reaction mixture.

For a given set of C_{S0} and $\bar{\theta}$, C_S in the steady state operation can be obtained from Equation (4-3).

Continuous hydrolysis with a CSTR

Profiles of the substrate conversion and pH with elapsed operation time are shown in Figure 4-2. The mean residence time is 60min. 1wt percent of triacetin in the buffered solution was continuously supplied to the reactor holding 30g of microcapsules (MC-I). No attempt to control the pH was made in this experiment. The steady state was well-established after 3hr of operation, measured values of the substrate conversion and pH remained constant thereafter. The solid line in the figure indicates the calculated values employing the numerical parameters listed in Table 4-1. Agreement with the observed values was quite good, a solid confirmation that the kinetic model derived in Chapter 2 can be extended to the operation of CSTR.

Stable dispersion of the microcapsules was maintained during the operation, and neither the outward diffusion of lipase molecules nor distortion or breakage of the capsules was observed.

The fact that the pH level in the steady state operation stayed constant (approximately at 5.7), even without pH control, is due to the low concentration of acetic acid released. If the operation is carried out with a longer residence time or higher substrate concentration in the feed-stream, concentration of the released acid will become higher than that observed in Figure 4-2. According to the information[5] given by Amano Pharmaceutical Co. Ltd., the activity of lipase is permanently lost when it is

exposed to a pH level of less than 4.0. This implies clear preference to employ pH control, otherwise the steady state may be never established because of the continued inactivation of lipase during the unsteady state operation after the start-up.

A result of the operation with pH controlled at 7.0 is shown in Figure 4-3. Due to the low content of lipase encapsulated in MC-II, the steady state conversion is lower than shown in Figure 4-2 despite employing the same operational conditions of 1wt percent triacetin solution and 60min of the mean residence time. The steady state was established after 4hr of the operation, a little later than observed in Figure 4-2. The two calculated lines in Figure 4-3 (solid for controlled pH and broken for uncontrolled) indicate that the steady state conversion of triacetin became higher with pH controlled at 7.0. No inhibitory effect was observed by the injection of alkaline solution.

Relationship between the steady state conversion and the mean residence time

The calculated relationship between the steady state conversion of triacetin and the mean residence time was shown with a parameter $\delta = b - a$, wall thickness of the microcapsule; Figure 4-4(a) shows the relationship without pH control, and Figure 4-4(b), with controlled pH. Experimental data obtained with $\bar{\theta} = 30$, 60 and 90min were plotted in each figure as well as the calculated line employing the values listed in Table 4-1.

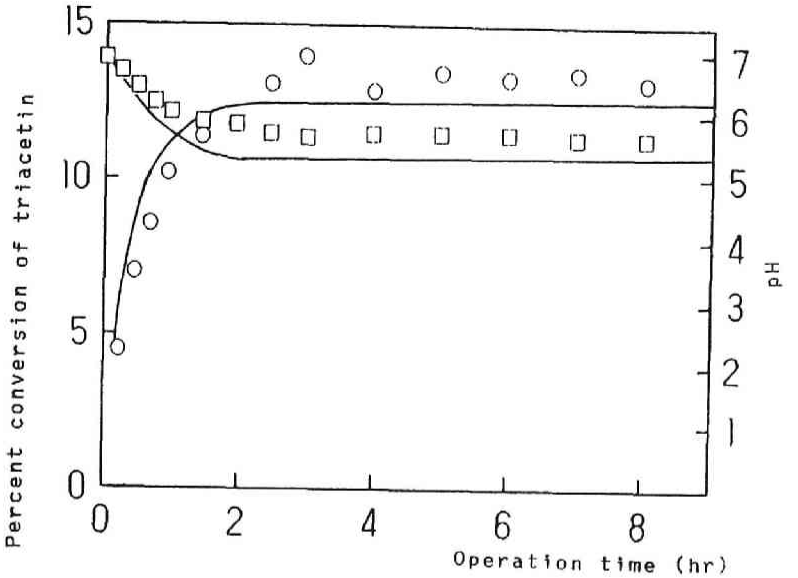

Figure 4-2. Profiles of substrate conversion and pH with elapsed operation time. ○, substrate conversion; □, pH; ——, calculated curve. Without pH control. $\bar{\theta}$ = 60min, 1wt percent triacetin in the feed stream. MC-I was used.

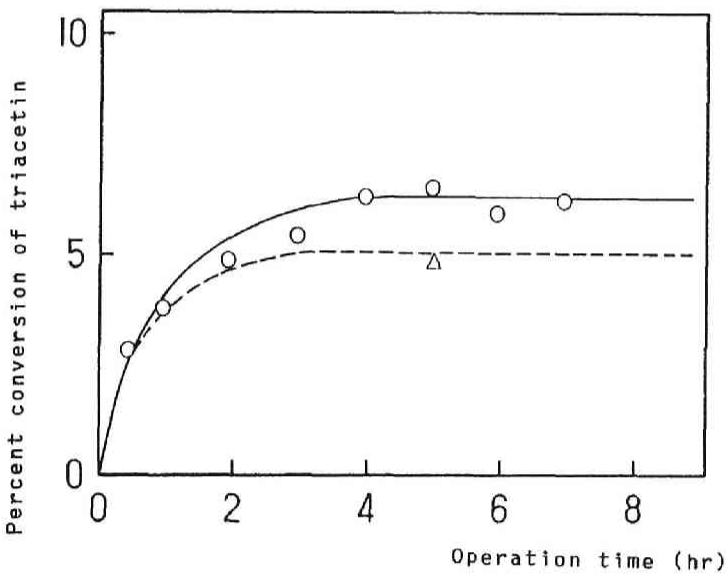

Figure 4-3. Profile of substrate conversion with elapsed operation time. Conditions are the same as for figure 4-2 except that MC-II was used. ○, ——, observed and calculated values with controlled pH at 7; △, ----, observed and calculated values without pH control.

It will be easily understood from the comparison of two figures that the increase of the substrate conversion with longer mean residence time is gradually suppressed in Figure 4-4(a), due to the increased concentration of released acid. No such limit is observed in Figure 4-4(b), another demonstration of the advantage of pH control.

Conclusion

The hydrolysis of triacetin catalyzed by encapsulated lipase was carried out employing a continuous stirred tank reactor (CSTR). An automatic control device of pH in the reaction mixture was introduced into the reactor system, and resulted in stable operation and increased reaction rate. One may attribute the advantage of employing stirred tank reactors over packed column ones to the fact that pH control can be done with less sophistication.

Commercial feasibility of microcapsules for the enzyme catalysis with substrates, small enough to permeate through the wall, was established by these fundamental investigations.

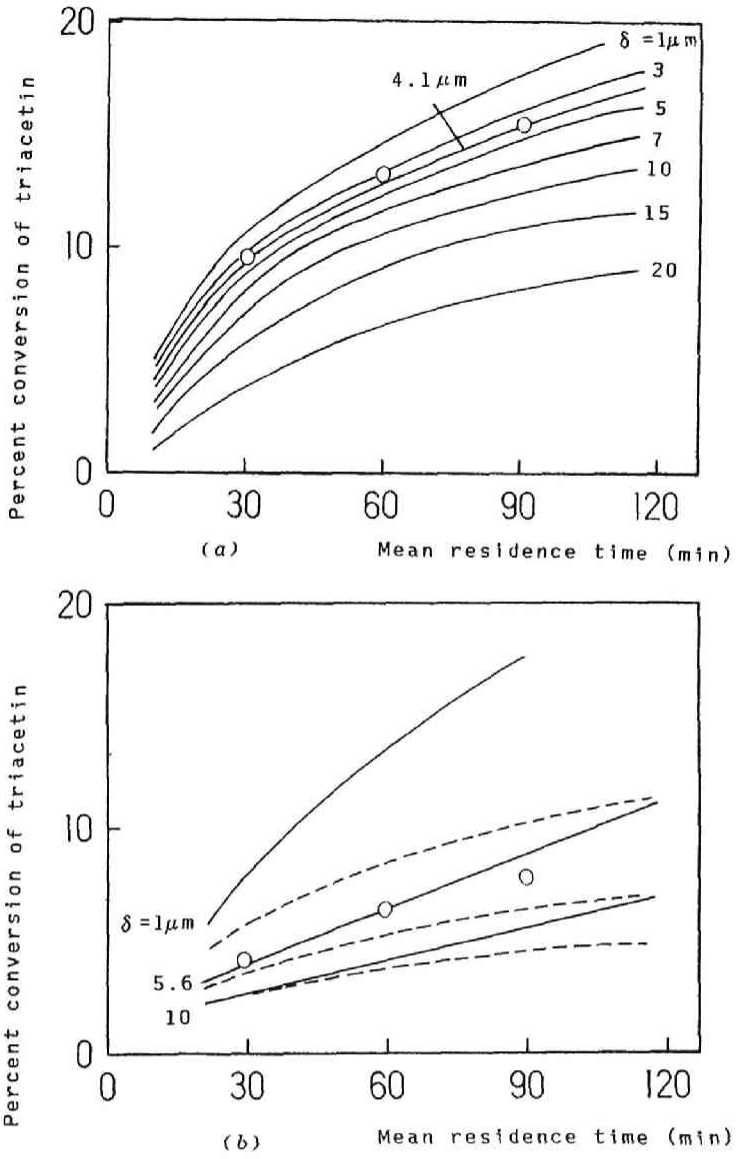

Figure 4-4. Relationship between substrate conversion and mean residence time.
(a)Without pH control: wall thickness(δ) was taken as a parameter; 1wt percent triacetin in the feed stream; MC-I was used; ○, observed value; ——— , calculated curve. (b)With pH control: conditions are the same as in (a) except that MC-II was used; ———, calculated curve controlled pH at 7; – – – – , calculated curve without pH control.

References

1) M.Iso, T.Shirahase, S.Hanamura, S.Urushiyama and S.Omi, J. Microencapsulation, 6, 165 (1989)

2) M.Iso, T.Shirahase, S.Hanamura, S.Urushiyama and S.Omi, J. Microencapsulation, 6, 285 (1989)

3) M.Iso, H.Masumoto, S.Urushiyama and S.Omi, J. Microencapsulation, 7, 167 (1990)

4) O.Levenspiel, Chemical Reaction Engineering, John Wiley, New York (1972)

5) Amano Pharmaceutical Co. Ltd., Lipase (Amano), unpublished document (1987)

Conclusions

Preparation of microcapsules, controlled release of core substances and application to immobilization of enzyme were discussed in each parts. The results obtained are summarized as follows, respectively.

Preparation of Microcapsules.

Several kinds of microencapsulation, coacervation method, spray drying method, (W/O)/W multiple emulsion method and (S/W)/O multiple suspension method were carried out. Anhydrous sodium sulfate, Vitamin B_6 and nicotinic acid were selected as typical water-soluble core substances depending on the encapsulation method. Since these methods have their individual advantages and disadvantages, an adequate method should be chosen considering on the state of core substances and the usage of encapsulated products. Characteristics of microcapsules obtained, e.g., relative difficulty of preparation, wall thickness and dimension of capsules, are summarized in Table 1-1. Half-life of the release of core substances from microcapsules are roughly estimated and also given in this table.

Controlled Release from Microcapsules.

To understand the release behavior of core substance from microcapsules, Higuchi model, capacity coefficient model (K_{La} model) and diffusion model for hollow sphere were proposed in

Part 2. Release of core substances from capsules is needless to say a mass transport phenomenon of the core molecules diffusing through the wall that acts as a barrier. In principle, Fickean diffusional equation can be employed for the correlation of release data to estimate transport parameters. However, the transport of core substance through the wall of microcapsule is by no means straightforward very complex. As described previously, this is due to the great diversity in physical form of microcapsules with respect to shape, size, combination of core substance and wall material.

In the case of multiple emulsion method, microcapsules had relatively well-defined structure, e.g., the appearance of surface, the thickness of wall and the wall structure, therefore, an analytical solution of the diffusion equation for hollow sphere can be applied to correlate the release behavior of core substances. However, more empirical treatment was necessary for the behavior observed in the later part of release.

Capacity coefficient model (K_{La} model) was available when the definition of the interface through which the transport takes place was difficult. The capacity coefficient, K_{La}, is defined as a proportional constant multiplied to the driving force of the overall mass-transfer, in this case, the concentration gradient across the interface.

In microcapsules prepared by (S/W)/O multiple phase suspension method, the interfacial area of diffusion was not exactly

Table 1-1. Characteristics of microcapsules prepared in this work.

Preparation methods	Core Substances	Wall Materials	Relative Difficulty	Wall Thickness	Diameter	Half-life of release
Coacervation Method	·Solids ·Low volatile liquids ·liquids impregnated into solid	·Water-soluble polymers ·Oil-soluble polymers	Easy	0.1~10 μm	1~100 μm	min~hr
Spray drying Method	·Solids	·Water-soluble polymers ·Oil-soluble polymers ·Waxes	Difficult	1~20 μm	10~200 μm	min~hr
(W/O)/W Multiple Phase Emulsion Method	·Liquids ·Slurries	·Oil-soluble polymers ·Waxes	Easy	1~10 μm	10~200 μm	hr~day
(S/W)/O Multiple Phase Suspension Method	·Solid	·Water-soluble polymers	Easy	10~300 μm	0.5~2mm	day~year

determined, inviting the capacity coefficient model as an efficient alternative. It should be born in mind that the capacity coefficient can be related to the diffusion coefficient, D_2, if the structure of microcapsules is identified so as to allow the theoretical treatment. For example, K_{La} is related to the diffusion coefficient of spherical solid particle as expressed by Equation (4-3) in Chapter 4 of Part 2.

On the other hand, microencapsulation of solid particles by coacervation or spray drying method yielded microcapsules having multinucleous clusters of irregular shape. Release behavior from the surface of such a granular-type cluster was assumed to be analogous to that from the spherical matrix of uniform network. Therefore, it was possible to express the release behavior by the Higuchi model in which a mathematical solution has been obtained from the Fickean diffusional equation by assuming core substances dispersed in a homogeneously in the matrix.

Immobilization of Enzyme by Microcapsules.

In this work, the wall material (PS/SBR) having mechanical durability was obtained, and the microencapsulation of lipase was carried out using (W/O)/W multiple emulsion method. Employing the microencapsulated enzyme, several types of reactors, e.g., batch stirred tank reactor, packed column reactor and continuous stirred tank reactor (CSTR), were investigated. By immobilization, the enzyme can be easily recovered for recycle, and contin-

uous production becomes possible.

In Chapter 2 of Part 3, the hydrolysis of short-chain lipid using microencapsulated lipase was carried out in a batch stirred tank reactor, and the modeling analysis of the reaction was tried. A mathematical model of this reaction system was successfully developed by introducing the concept of catalyst effectiveness factor. As has been the days of employing free enzymes, batch stirred tank reactors can not exert a full advantages of the encapsulated enzyme because of their intermittent operation in practical industrial processes.

Therefore, the attention was then shifted to the continuous system, and an operation in a packed column reactor was conducted to investigate the long-term endurance of microcapsules. The wall of the microcapsules was quite resilient to the static load in the packed column, and passed the longevity test which continued for several months. The kinetic model quite effectively simulated the experimental results.

The setback of the packed column operation is that the acid product from the hydrolysis may lead to the reduction of the enzyme activity towards the downstream of the column. As the activity of lipase decreased with an decrease of pH in the downstream, though not being impossible, it was impractical to inject alkaline solution alongside the column to adjust pH in the reaction mixture. These problems may be overcome by increasing the flow rate, but it will reduce the substrate conversion, and

require unnecessarily large scale. A potential advantage of packed column reactors, low costs of construction, operation and maintenance, can be fully enjoyed only when the catalysis reveals no such serious problems mentioned above.

CSTR consists of a series of stirred tanks,each equipped with a substrate inlet and product outlet, and can overcome the problems encountered in the packed column reactor. The use of a CSTR train may be a more reasonable choice since pH adjustment can be done for a small additional cost.

A single CSTR equipped with an automatic pH controlling system was used to offset the acid formation in the reactor. The operation was quite successful, no pH drop being observed. The same kinetic model was applicable to simulate the reaction behavior.

This microencapsulated enzyme using PS/SBR as mixed wall material can be practically extended to the large-scale industrial processes because it has mechanical durability superior to those reported in past research works. It can be said that the general design concepts for the bioreactor systems involving microcapsules were established by this work.

As a summary, two major issues concerned with the practical usage of microcapsules in commercial scale were investigated in this thesis.

In Part 2, controlled release of core substances from microcapsules was investigated together with the practice of several

encapsulation methods which yielded microcapsules of different characters. Emphasis of the investigation was focussed on the derivation of mathematical models useful to correlate the release data. Quantitative analysis was possible based on the Fickean diffusion model, and the capacity coefficient model.

Understanding the release behavior of core substances through the microcapsule wall encouraged conducting the assignments in Part 3.

In Part 3, enzyme catalysis by microencapsulated enzyme was investigated. A mathematical model of this particular catalysis was derived introducing the catalyst effectiveness factor to the ordinary kinetics of free enzyme catalysis. An advantage of the continuous operation corresponding to the longevity of encapsulated enzyme was demonstrated in the operations of the packed column, and a single CSTR, an advantage of automatic pH control being shown in the latter operation.

To conclude this thesis, the author sincerely wishes that these investigations will provide some fundamental directions in the future research and application of microcapsules.

List of Publications

List of Publications

1)Fundamental study of microencapsulation procedure utilizing coacervation induced from polystyrene-cyclohexane-n-hexane system.

M.Iso, I.Suzuki and S.Omi, Zairyo Gijutsu 3, 287-293 (1985)

-- Chapter 1 in Part 1, Chapter 1 in Part 2

2)A fundamental study of the microencapsulation procedure utilizing coacervation in a polystyrene-cyclohexane solution.

M.Iso, T.Kando and S.Omi, J. Microencapsulation, 2, 275-287 (1985)

-- Chapter 1 in Part 1, Chapter 1 in Part 2

3)Microencapsulation of nicotinic acid employing a spray drying tower.

N.Umeki, K.Terauchi, M.Iso and S.Omi, Zairyo Gijutsu 5, 133-140 (1987)

-- Chapter 2 in Part 1, Chapter 2 in Part 2

4)On the microencapsulation of Vitamin B_6 aqueous solution employing (W/O)/W two-phase emulsion technique.

T.Furuno, A.Ikeda, M.Iso and S.Omi, Zairyo Gijutsu 5, 141-148 (1987)

-- Chapter 3 in Part 1

5)Controlled release of water-soluble drugs from hollow spheres: Experiments and model analysis.
S.Omi, T.Furuno, A.Ikeda and M.Iso, "Drug Targeting and Delivery" ed. A.T.Florence and G.Gregoriadis in press
-- Chapter 3 in Part 2

6)Microencapsulation of pheromone-analogue and measurement of the sustained release.
S.Omi, N.Umeki, H.Mohri and M.Iso, J.Microencapsulation, 8, 465-478 (1991)
-- Chapter 4 in Part 1, Chapter 4 in Part 2

7)Immobilization of enzyme by microencapsulation and application of the encapsulated enzyme in the catalysis.
M.Iso, T.Shirahase, S.Hanamura, S.Urushiyama and S.Omi, J. Microencapsulation, 6, 165-176 (1989)
-- Chapter 1 in Part 3, Chapter 2 in Part 3

8)Application of encapsulated enzyme as a continuous packed-bed reactor.
M.Iso, T.Shirahase, S.Hanamura, S.Urushiyama and S.Omi, J. Microencapsulation, 6, 285-299 (1989)
-- Chapter 3 in Part 3

9)Application of encapsulated enzyme dispersed in a continuous stirred tank reactor.
M.Iso, H.Masumoto, S.Urushiyama and S.Omi, J. Microencapsulation, 7, 167-177 (1990)
-- Chapter 4 in Part 3

Acknowledgements

The author takes this opportunity to express his deep gratitude to Prof. Takeo Shimizu, Prof. Isao Morishima and to Prof. Yukio Imanishi for their many helpful suggestions relating to this thesis.

The author is grateful to Prof. Shinzo Omi for his invaluable guidance. His many helpful suggestions and discussions have always supported the author throughout this work.

Particular thanks are due to many students of Omi Laboratory for their cooperation in laborious experiments and helpful advice.

The author wish to express their appreciation to Amano Pharmaceutical Co., Ltd. for having supplied the enzyme Lipase P and to Shin-etsu Chemical Co., Ltd. for donation of the pheromone syrup. Acknowledgements are also conveyed to Mr. A.Toyoda and Mr. H. Takano of the Research and Development Center in Nippon Zeon Co., Ltd., who provided TEM photographs of the microcapsules.

Finally, the author would like to give his greatest thanks to his parents for their encouragement.

Mamoru Iso